Combination therapy targeting both innate and adaptive immunity improves survival in a preclinical model of ovarian cancer

Dissertation

der Mathematisch-Naturwissenschaftlichen Fakultät

der Eberhard Karls Universität Tübingen

zur Erlangung des Grades eines

Doktors der Naturwissenschaften

(Dr. rer. nat.)

vorgelegt von

M.Sc. Christina Hartl

aus Mainburg

Tübingen

2019

Gedruckt mit Genehmigung der Mathematisch-Naturwissenschaftlichen Fakultät der Eberhard Karls Universität Tübingen.

Tag der mündlichen Qualifikation: 17.05.2019

Dekan: Prof. Dr. Wolfgang Rosenstiel

1. Berichterstatter: Prof. Dr. Stefan Stevanovic

2. Berichterstatter: Dr. Michael Goldberg

Acknowledgments

This PhD also gave me the opportunity to meet some truly wonderful people and an opportunity to forge life-long friendships. **Lina**, **Patrick**, **Leon**, **Kevin**, **Eddy**, **Archis**, and **Adam** - thanks for many good memories and making every holiday party legendary. A special mention to my fellow German and partner in crime **Steffie**. I am so glad to call you my friend.

My deepest gratitude goes to **Chris** for his continued support and for always believing in me. You are the best thing I could have hoped to find in Boston.

Nicht zuletzt vielen Dank an meine Familie, besonders meine **Eltern**, die mich immer unterstützt haben und ohne deren Rückhalt diese Arbeit wohl nicht zustande gekommen wäre.

Abstract

Despite major advancements in immunotherapy among a number of solid tumors, response rates among ovarian cancer patients remain modest. Standard treatment for ovarian cancer is still surgery followed by taxane- and platinum-based chemotherapy. Thus, there is an urgent need to develop novel treatment options for clinical translation.

Our approach was to analyze the effects of standard chemotherapy in the tumor microenvironment of mice harboring orthotopic, syngeneic ID8-Vegf-Defb29 ovarian tumors in order to mechanistically determine a complementary immunotherapy combination. Specifically, we interrogated the molecular and cellular consequences of chemotherapy by analyzing gene expression and flow cytometry data.

These data show that there is an immunosuppressive shift in the myeloid compartment, with increased expression of IL-10 and ARG1, but no activation of $CD3^+$ T cells shortly after chemotherapy treatment. Chemotherapy together with various single immunotherapies was not able to increase survival in this model. We therefore selected immunotherapy combinations that target both the innate and adaptive arms of the immune system. Survival studies revealed that standard chemotherapy was complemented most effectively by a combination of anti-IL-10, 2'3'-cGAMP, and anti-PD-L1. Immunotherapy dramatically decreased the immunosuppressive myeloid population while chemotherapy effectively activated dendritic cells. Together, combination treatment increased the number of activated T and dendritic cells as well as expression of cytotoxic factors. It was also determined that the immunotherapy had to be administered concurrently with the chemotherapy to reverse the acute immunosuppression caused by chemotherapy. Mechanistic studies revealed that antitumor immunity in this context was driven by $CD4^+$ T cells, which acquired a highly activated phenotype. Our data suggest that these $CD4^+$ T cells can kill cancer cells directly via granzyme B-mediated cytotoxicity. Further analysis of human samples revealed that there is also downregulation of immune function after treatment with chemotherapy. Finally, we showed that this combination therapy is also effective at delaying tumor growth substantially in an aggressive model of lung cancer, which is also treated clinically with taxane- and platinum-based chemotherapy.

This work highlights the importance of $CD4^+$ T cells in tumor immunology. Furthermore, the data support the initiation of clinical trials in ovarian cancer that target both innate and adaptive immunity, with a focus on optimizing dosing schedules.

Zusammenfassung

Die Erfolgsquote von Immuntherapien in Eierstockkrebs bleibt trotz bedeutender Forschungserfolge auf diesem Feld gering. Die derzeitige Standardtherapie bei einer Eierstockkrebsdiagnose ist weiterhin eine radikale Operation und unterstützende Behandlung mit taxan- und platinhaltigen Chemotherapien. Die Entwicklung von neuartigen Behandlungsmethoden für Patienten mit Eistockkrebs ist daher dringend nötig.

Das Ziel unseres Projekts war den Effekt von Chemotherapie auf das Tumorgewebe in einem Maus-Modell zu untersuchen und darauf basierend eine ergänzende Immuntherapie-Kombination zu ermitteln. Dafür verwendeten wir Mäuse denen isogene ID8-Vegf-Defb29 Eierstockkrebszellen injiziert wurden und analysieren mittels Genexpressionsanalyse und Durchflusszytometrie welche Auswirkungen Chemotherapie auf molekularer und zellulärer Ebene hat.

Unsere Ergebnisse zeigen, dass in diesem Maus-Modell kurz nach der Behandlung Zellen der unspezifischen Immunantwort Prozesse, die gegen den Tumor gerichtet sind unterdrücken, und vermehrt die immunsuppressiven Proteine IL-10 und ARG1 absondern. Im Gegenzug gibt es keine Aktivierung von CD3$^+$ T-Zellen. Einzelne Immuntherapien in Kombination mit Chemotherapie konnten das Tumorwachstum nicht verlangsamen. Bei der Wahl der Immuntherapien setzten wir daher auf Behandlungen die sowohl auf die unspezifische als auch die adaptive Immunabwehr abzielen. In den nachfolgenden Experimenten konnten wir ermitteln, dass die Kombination von anti-IL-10, 2'3'-cGAMP, und anti-PD-L1 mit Chemotherapie am wirksamsten war um das Tumorwachstum in Mäusen zu verlangsamen. Die Immuntherapien verhinderte die immunsuppressive Wirkung der angeborenen Immunantwort, während die Chemotherapie dendritische Zellen entscheidend aktivierte. Zusammen führte die Kombination von Immuntherapien und Chemotherapie zu einem Anstieg an aktivierten T-Zellen und dendritischen Zellen im Tumorgewebe, sowie der erhöhten Expression von cytotoxischen Proteinen. Desweitern konnten wir feststellen, dass die Immuntherapie und Chemotherapie zeitgleich verabreicht werden müssen um Immunsuppression zu verhindern. Weitere mechanistische Studien ergaben, dass in diesem Maus-Modell Tumorzellen hauptsächlich von aktivierten CD4$^+$ T-Zellen zerstört werden. Wahrscheinlich geschieht dies durch zytotoxische Granzyme, die von den CD4$^+$ T-Zellen ausgeschüttet werden und die gebundenen Krebszellen direkt töten. Untersuchungen von klinischen Proben ergaben überdies, dass auch in Eierstockkrebspatienten das Immunsystem durch Chemotherapie stark gehemmt

wird. Die Kombinationstherapie wurde anschließend auf ein aggressives Lungenkrebs-Modell ausgeweitet. Lungenkarzinome werden ebenfalls mit taxan- und platinhaltigen Chemotherapien behandelt und Immuntherapie und Chemotherapie zusammen zeigte auch hier eine drastische Verlangsamung des Tumorwachstums.

Unsere Ergebnisse unterstreichen die entscheidende Rolle von CD4$^+$ T-Zellen in der Krebsimmuntherapie. Desweitern liefert das Projekt wichtige Hinweise um zukünftige klinische Studien für Frauen mit Eierstockkrebs zu veranlassen. Neue Therapien sollten sowohl die unspezifische als auch adaptive Immunabwehr miteinbeziehen und ein Augenmerk auf die Optimierung des Behandlungsplan legen.

Table of contents

1. Introduction

1.1. Pathogenesis and standard treatment of ovarian cancers

Epithelial ovarian carcinoma is the most lethal gynecological cancer, with about 295,414 new cases of ovarian cancer in 2018 and 184,799 deaths worldwide[1]. Survival rates vary depending on the stage of diagnosis, but average around 44% and have only increased marginally in the last 40 years[2]. Despite major efforts invested in studying new cytotoxic and targeted agents, ovarian cancer remains the most lethal gynecologic malignancy in developed countries[3]. Ovarian cancers can be classified into three subtypes: (i) epithelial tumors, which begin in the thin layer of tissue that covers the outside of the ovaries or the fallopian tube; (ii) germ cell tumors, which develop in the egg-producing cells; and (iii) stromal cell tumors, which begin in the ovarian tissue that contains hormone-producing cells[4]. Epithelia tumors makes up about 90% of ovarian cancers cases and of those 75% are high-grade serous ovarian carcinomas (HGSOC). These are highly aggressive which generally, have no specific symptoms in the early stages[5,2]. As a consequence, the majority of women are diagnosed at an advanced stage when metastasis have already spread throughout the peritoneal cavity. Standard-of-care treatment remains surgery and a combination of taxane- and platinum-based chemotherapy, most often paclitaxel and carboplatin[6].

Most often chemotherapy is delivered intravenously, even though intraperitoneal administration results in a 20–30% improvement in survival times for advanced-stage epithelial disease. However, due to toxic side effects, delivery issues, and complications intraperitoneal chemotherapy has not been universally accepted[7].

Even though 80% of patients respond to first-line chemotherapy, the success of cytotoxic chemotherapy is generally short-lived[8]. Due to the heterogeneous nature of cancer cell populations almost invariably cell clones develop drug-resistance. These resistant cells cease to respond to chemotherapy and ultimately lead to disease relapse, as seen in about 75% of ovarian cancer patients[9]. Treatment options for recurrence are limited and include other chemotherapy drugs or targeted therapies (such as PARP inhibitors), which are only effective in a certain patient population[10]. These second-line interventions can improve survival and quality of life but are not curative[7].

1.2. Immunotherapy in ovarian cancer

In contrast to chemotherapy, immunotherapy offers an effective alternative strategy that can achieve durable benefits by leveraging the patient's immune system to recognize and eliminate cancer cells. The immune system is able to invoke an adaptive memory response, which is highly coordinated and able to traffic appropriate cells to the site of disease. Unlike chemotherapy, the immune response is highly specific and able to adapt to an evolving heterozygous cancer cell population, which can enable surveillance and elimination of recurring disease even after completion of treatment. Evidence presented over the last decade has shown that ovarian cancer is an immunogenic tumor that can be recognized by the host immune system[11]. Indeed, the first proof that the presence of intratumoral T cells correlates with improved clinical outcome was demonstrated in advanced ovarian cancer[12]. Also, antigen-specific antibodies and tumor-reactive T cells have been isolated from ovarian cancer patients[13]. Unfortunately, responses to immune checkpoint blockade to date remain modest in this patient population.

The first published data of checkpoint blockade in ovarian cancer patients used the anti-PD-L1 antibody BMS-936559 and showed a partial response rate of only 6% and a stable disease rate of 18% with the highest dose tested[14]. In a later study the best overall response rate was 15% with the anti-PD-1 antibody nivolumab[15]. The most recent studies found that the anti-PD-L1 antibody avelumab demonstrated an objective response rate in 9.6% of advanced ovarian cancer patients[16] and overall response rate for Merck's anti-PD-1 antibody pembrolizumab was 11.5% in metastatic ovarian cancer patients[17]. Immune evasion by ovarian tumors often renders antitumor responses incomplete and prevents striking results as reported for melanoma, NSCLC, and bladder cancer[18].

Current work is therefore focusing on combining the effects of immunotherapy with standard-of-care chemotherapy. Conventional chemotherapy can stimulate the immune system in four ways: (i) enhance the immunovisibility of cancer cells by upregulation of MHC class I; (ii) generate antigenic debris in the context of danger signals, thereby producing an *in situ* vaccine, which increases activation of immune effector cells; (iii) exert antitumor immunomodulation on effector cells; and (iv) deplete immunosuppressive factors or cell populations that are present in the tumor microenvironment (e.g. myeloid derived suppressor cells, regulator T cells, M2-like macrophages) [19]; (Fig. I).

In ovarian cancer it was shown that standard-of-care paclitaxel specifically upregulates MHC class I expression and increases antigen-processing[20,21], but also suppresses NK and T cells and
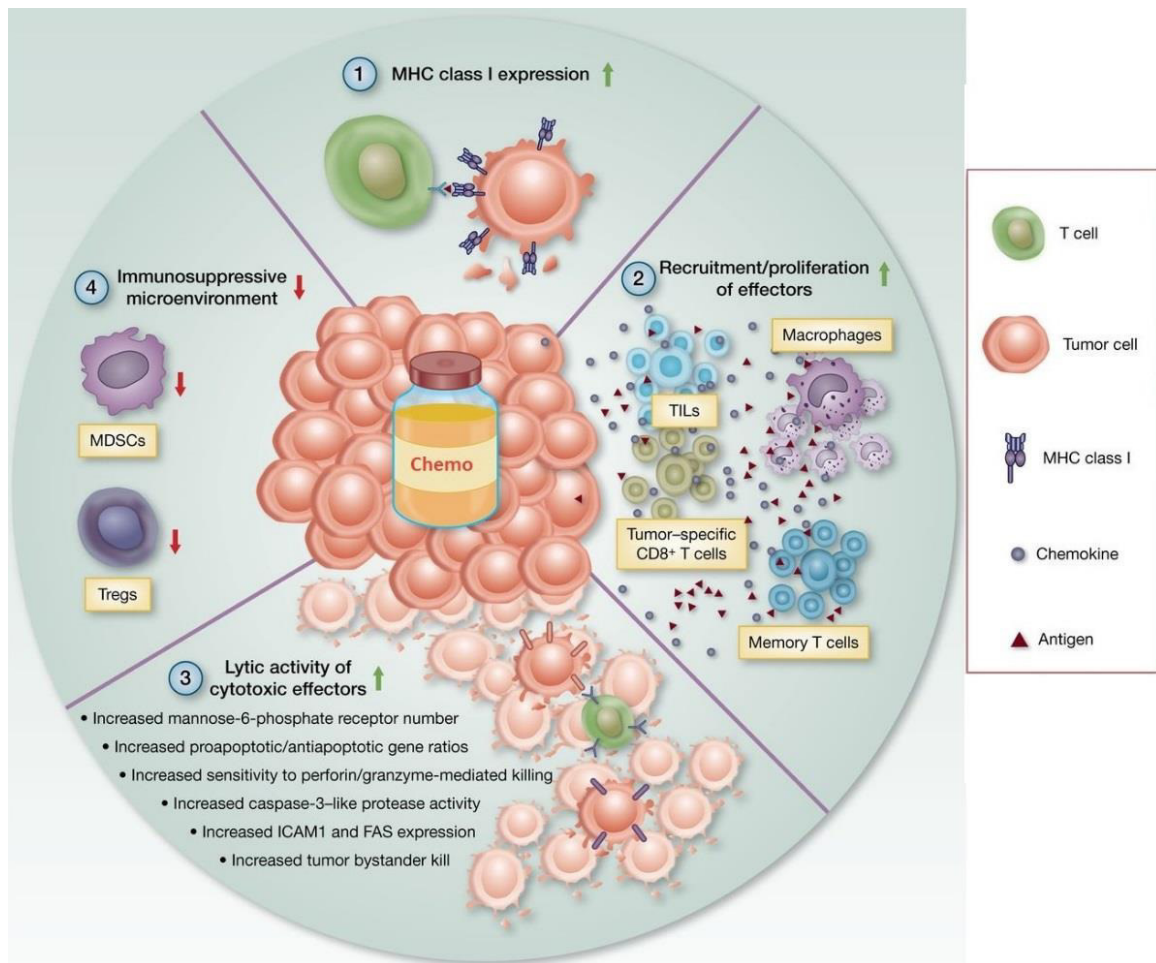
Figure I: Antitumor immunomodulation by conventional chemotherapy. Conventional antineoplastic drugs can activate anticancer immune responses through different mechanisms: (1) the enhancement of tumor immunovisibility by cytotoxic cell subsets or phagocytes, (2) the direct stimulation of T and B cell responses, (3) the increase of cytotoxic activity by effector cells, and (4) the inhibition of tumor-induced-suppressive mechanisms. Adapted from Biasi *et al*, 2014[22].

increases PD-L1 expression[23,20]. This is likely due to the cytotoxic properties of paclitaxel as there is evidence that low-dose paclitaxel preserves the immune system and treatment-mediated promotion of tumor-specific immunity[24]. Other results found that paclitaxel and carboplatin are able to polarize macrophages to an M1-like phenotype, deplete regulatory T cells and MDSCs, and augment CD4+ and CD8+ T cell trafficking[25], however those studies have not been conducted in ovarian cancer.

These findings suggest that complementary therapy of chemotherapy and immunotherapy may yield a synergistic antitumor response and improve the magnitude and frequency of responses in different cancers (Fig. II). A recent trial in non-small-cell lung cancer found that pembrolizumab plus carboplatin and pemetrexed increased objective response rates from 29 to 55% over chemotherapy alone[26]. In triple negative breast cancer patients, a study confirmed

that the addition of the anti-PD-L1 antibody atezolizumab to paclitaxel prolonged medium survival among patients compared to placebo[27].

Consequently, a number of phase II clinical trials are now investigating combination of chemotherapy and PD-(L)1 checkpoint blockade in ovarian cancers (NCT02440425, NCT02608684, NCT02726997)[28], but results are not available yet. An early phase III trial with avelumab +/- doxorubicin did not find any statistically significant improvement in overall survival of platinum-resistant or -refractory ovarian cancer[29]. Most of these clinical trials focus on immunomodulatory drugs that have been effective in other cancer types. However, ovarian carcinomas have a unique tumor microenvironment and treatments that benefit melanoma or bladder cancer patients may not be optimally suited for ovarian cancer patients[30]. A deeper understanding of the changes in the tumor microenvironment of ovarian tumors after chemotherapy treatment is needed to improve response rates in ovarian cancer patients and potentially achieve curative events.
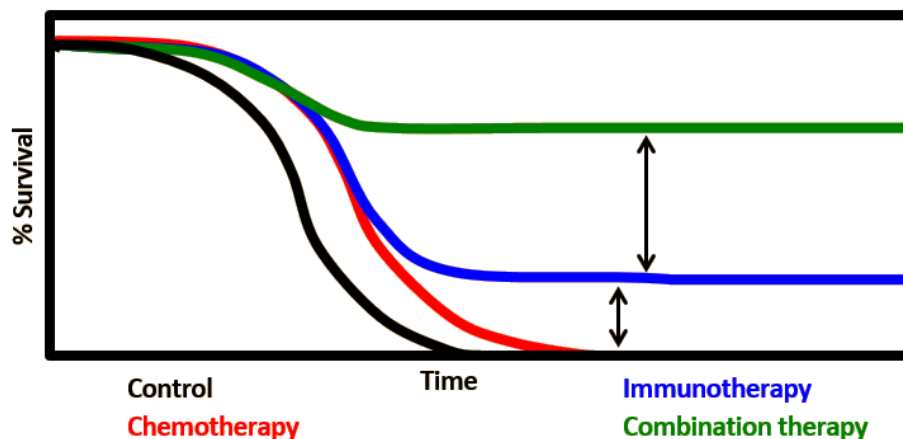
Figure II: Treatment outcomes in ovarian cancer. Depiction of Kaplan-Meier survival curve with chemotherapy agents (red line) as compared to no therapy (black line) indicating an improvement in median overall survival but lack of durable responses; improved median overall survival and durable responses in a fraction of patients treated with immunotherapy (blue line); possibility for improved median overall survival with durable responses for the majority of patients in the setting of combination treatment with chemotherapy and immunotherapy (green line). Adapted from Sharma *et al*, 2015[31].

1.3. Tumor microenvironment of ovarian carcinomas

Ovarian cancers have a number of immunosuppressive mechanisms which they employ to thwart immune attacks (Fig. III). While the number of tumor infiltrating lymphocytes (TILs) has been established as a positive prognostic factor[12], ovarian cancers are known to have large numbers of regulatory CD4$^+$ T cells (Tregs)[32]. Tregs play a central role in evading immune

destruction[33] and limiting antitumor immunity[34]. Their inhibitory activities are mediated through cytokines like TGF-β and IL-10 as well as through cell-cell interaction[35]. IL-10 is an immunosuppressive cytokine that inhibits the ability of antigen presenting cells (APCs) to present antigens to T cells in a variety of ways[36]. It has also been shown that IL-10 is directly upregulated as an adaptive resistance mechanism to PD-1 blockade[37]. Other cells populations that express IL-10 are tumor associated macrophages (TAMs) and myeloid derived suppressor cells (MDSCs)[38,39], which accumulate in high numbers in the local tumor environment of ovarian cancers[40]. They often express the immune inhibitory ligand PD-L1[41], but also secrete additional immunosuppressive factors like indoleamine-2,3-dioxygenase (IDO) in order to abolish activation of T cells via tryptophan catabolism[42] or arginase1 (Arg1), which metabolizes L-arginine and leads to T cell dysfunction[43].

Ovarian cancer cells themselves also upregulate PD-L1 to disrupt T cell mediated antitumor immunity[44]. Interestingly, PD-L1 expression of cancer cells is an indicator of a favorable prognosis in ovarian cancer[45], potentially because it is an indicator of high TIL infiltration. Furthermore, ovarian cancers are known to secrete high levels of vascular endothelial growth factor (VEGF), which is involved in angiogenesis[46]. Indeed, VEGF levels in the ascites of ovarian cancer patients are up to tenfold higher than levels in ascites associated with other solid tumors[47]. These high levels of VEGF are inversely correlated with survival[48] and correlate
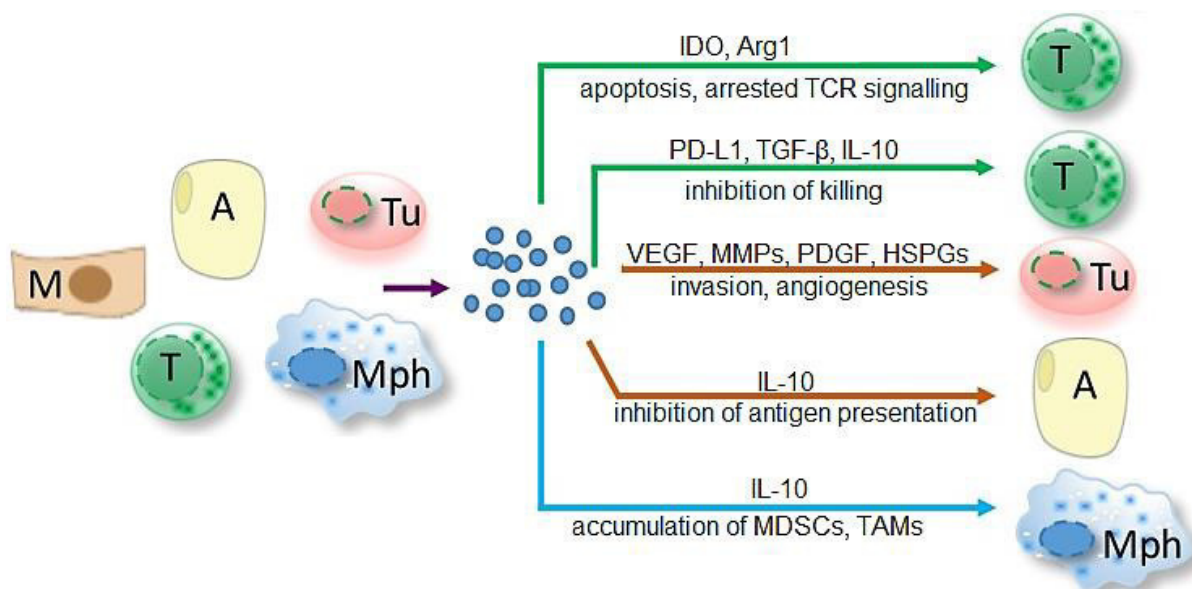
Figure III: Tumor microenvironment in ovarian cancer. Immunosuppressive factors are released by cells of the tumor microenvironment and shape cellular functions of both tumor cells and host cells via different pathways. Depicted examples affect major hallmarks of ovarian cancer to promote tumor growth and metastasis. A: APC; M: MDSC; Mph: macrophage; T: T cell; Tu: tumor cell. Adapted from Worzfeld *et al*, 2017[49].

directly with invasion and metastasis of ovarian cancer cells[50]. Other factors commonly found in the tumor microenvironment of ovarian cancer that facilitate tumor progression and metastasis are platelet derived growth factor (PDGF)[51], matrix metalloproteinases (MMPs)[52], and heparin sulfate proteoglycans (HSPGs)[53].

1.4. ID8-Vegf-Defb29 murine ovarian cancer tumor model

We selected the murine ovarian cell line ID8 for our project, which is a syngeneic mouse model frequently used for human ovarian cancer. ID8 is one of ten clonal lines established from late passaged C57BL/6 murine ovarian surface epithelial cells (MOSEC) and exhibited the highest tumor load[54]. In order to recapitulate the aggressive and immunosuppressive nature of ovarian carcinomas in the clinic, ID8 cells have previously been transduced with VEGFa and β-defensin-29 (Defb29)[55]. As described before, VEGFa is a critical factor in tumor invasion[56] by promoting tumor angiogenesis[46] and inhibiting dendritic cell (DC) differentiation and maturation[57]. Overexpression of VEGFa dramatically accelerates tumor growth and decreases medium survival times from 104 days (ID8) to 76 days (ID8-Vegfa)[55]. β-defensins are antimicrobial inflammatory peptides that use CCR6 to recruit immature DCs[58]. β-defensins works synergistically with VEGFa, whereby Defb29 recruits DCs into the tumor where they are then transformed by VEGFa into endothelial-like cells that engage in vasculogenesis and function as promoters of tumor progression. Thus, Defb29 significantly accelerates tumor growth and ascites formation of VEGFa over-expressing tumors and reduces survival time from 76 days (ID8-VEGFa) to 33 days (ID8-Vegfa-Defb29)[61]. In addition, ID8-Vegfa-Defb29
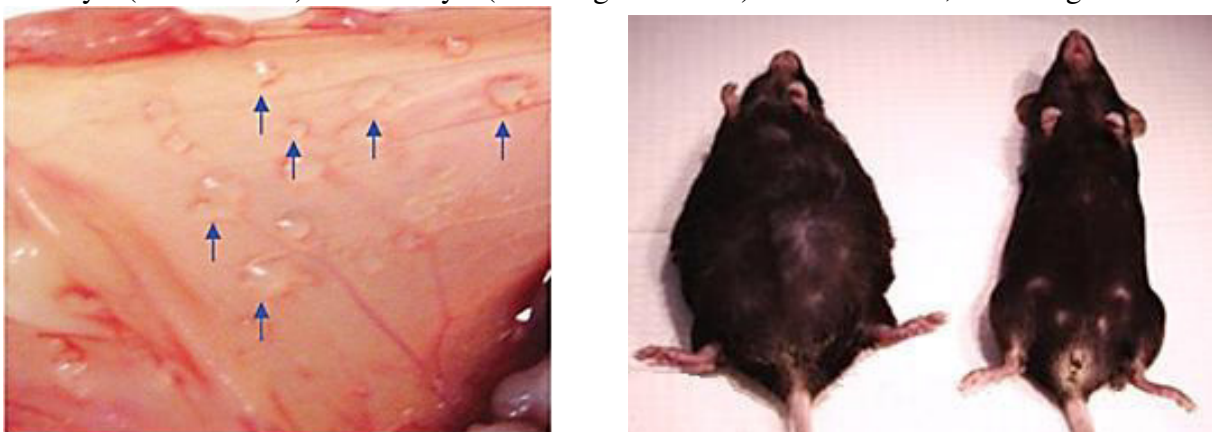
Figure IV: Tumor growth and ascites formation in C57B/6 mice with orthotopic ID8 tumors. (Left) Representative ID8-bearing mouse showing the tumor nodules on the peritoneal membranes. **(Right)** Representative image of an ID8 tumor-bearing mouse with ascites formation (animal on the left) and non-tumor bearing, PBS-injected mouse (animal on the right). Reprinted from Su *et al*, 2010 and Cho *et al*, 2013[59,60].

tumors display many of the characteristics of stage III human serous ovarian carcinomas[55,62]. After intraperitoneal (i.p.) injection tumor nodules are spread throughout the diaphragmatic peritoneum, the porta hepatis, and the pelvis and cellular ascites forms in late stages of cancer progression[55] (Fig. IV). Notably, ID8-Vegfa-Defb29 cells have to be injected i.p. since they fail to grow properly when inoculated subcutaneously (s.c.)[63].

1.5. Aims and objectives of the thesis

There is an urgent need to develop novel strategies for improving the outcomes of ovarian cancer patients. The main focus of this thesis was the identification of a mechanistically informed immunotherapy combination that synergizes with standard-of-care chemotherapy. Therefore, our first goal was examining the impact of the chemotherapy on the immune compartment of the tumor microenvironment in an aggressive murine model of ovarian cancer. Using the orthotopic, syngeneic ID8-Vegf-Defb29 model of murine ovarian cancer, we treated tumor-bearing mice with vehicle or chemotherapy and isolated peritoneal immune cells to test for differential gene and protein expression.

Based on these results, we selected various immunotherapies to evaluate their effectiveness when used in combination with chemotherapy. Survival experiments with tumor-bearing mice were conducted to test for synergy between standard-of-care chemotherapy and immunotherapy and to determine the most effective combination. The immunotherapy with the greatest survival benefit was selected and its impact on the tumor microenvironment was examined by flow cytometry analysis, using mice treated with vehicle, chemotherapy, immunotherapy, or the combination after tumor inoculation. We wanted to confirm that the combination therapy indeed works in a synergistic fashion and used the same treatment groups to conduct efficacy experiments with tumor-bearing mice. Subsequent survival studies with altered dosing schedules were conducted to verify that the efficacy of the combination is highly dependent on the temporal interplay between chemotherapy and immunotherapy, treatment duration, as well as timepoint of initiation.

Mechanistic studies are crucial to reveal the immune cell population(s) driving antitumor immunity. Therefore, we performed depletion experiments to investigate the importance of CD4$^+$ and CD8$^+$ T cells as well as CD11b$^+$ myeloid cells. We were expecting to identify at least one cell type essential for efficacy of combination therapy and intended to perform in-depth flow cytometry analysis for further evaluation of this population. To test the relevance of our model for clinical use, we analyzed human ovarian cancer samples before and after treatment

with chemotherapy for gene expression changes. As a final step, we translated our combination therapy into an aggressive model of murine lung cancer, in order to demonstrate efficacy in a solid tumor model with an entirely different tumor microenvironment.

Our hope for this work is to improve treatment options for ovarian cancer patients with a view towards curative outcomes. More broadly, this approach underscores the utility of leveraging mechanistic insights into how standard-of-care therapy impacts the immune compartment in order to identify complementary combination immunotherapy.

2. Materials

2.1. Laboratory equipment

Instrument	Manufacturer
Allegra X-15R Centrifuge	Beckman Coulter
Centrifuge 5417R	Eppendorf
CO_2 Water Jacketed Incubator	Forma Scientific
CQT202 Core Balance scale	Adam Equipment
Traceable Digital Callipers	Thermo Fisher Scientific
FACSAria IIIu	BD
FastPette	Labnet
MINIARCO animal trimmer	Wahl
NanoDrop 2000c Spectrophotometer	Thermo Fisher Scientific
nCounterMax	NanoString Technologies
Nikon Eclipse TS100 Microscope	Nikon
SP6800 Spectral Cell Analyzer	Sony Biotechnology
Ultrasonic cleaner	Branson
VortexGenie 2	Scientific Industries

2.2. Chemicals, reagents, and consumables

Product	Supplier
ACK Lysing buffer	Thermo Fisher Scientific
AlignCheck Alignment Beads	Sony Biotechnology
Aquaguard-1 solution	Promocell
Cell Activation Cocktail (with Brefeldin A)	BioLegend
Conical centrifuge tubes (15, 50 ml)	Thermo Fisher Scientific
Cryogenic vials	Corning
DEPC-treated water	Ambion
Disposable needles (20G, 21G, 27G)	BD
Disposable reagent reservoirs (25 ml)	VistaLab Technologies
Disposable syringes (1, 5 ml)	BD
Disposable Transfer Pipets (5 ml)	VWR
EASYstrainer (70 μm)	Greiner bio-one

Materials

EMD Millipore Stericup vacuum filter (1000 ml)	Thermo Fisher Scientific
Ethanol, 190 Proof	Thermo Fisher Scientific
Falcon Tissue Culture Dishes (60x15 mm)	Corning
Flat bottom plates (6, 12, 24, 96 well)	Corning
Filtered pipet tips (10, 20, 200, 1000 μl)	Denville
Isoflurane	Piramal Healthcare
Isopropanol	Fluka
Kimwipes	Kimtech
Micro Titer tubes (1.2 ml)	Thermo Fisher Scientific
Millex GP Filter Unit (0.22 μm)	Millipore
Nalgene Cryo Freezing Container	Thermo Fisher Scientific
Neubauer improved/bright-line counting chamber	Sigma-Aldrich
Nitril Exam Gloves	MediChoice
Parafilm M	Bemis NA
Polyethylene glycol 400	Sigma-Aldrich
Polystyrene Round-bottom tubes (5 ml)	Corning
Propylene glycol	Sigma-Aldrich
Protein Transport Inhibitor (with Monensin)	BD
RNase Zap	Thermo Fisher Scientific
Round bottom plate (96 well)	Corning
Safe-lock tubes (0.5, 1.5, 2.0 ml)	Sigma-Aldrich
Serological pipets (5, 10, 25, 50 ml)	Corning
Tissue culture flask/filter cap (75, 150 cm^2)	Corning
Trypan blue solution (0.4%)	Thermo Fisher Scientific
Trypsin-EDTA (0.25%)	Thermo Fisher Scientific
Tween80	Sigma-Aldrich
UltraComp Compensation Beads	Thermo Fisher Scientific
Unfiltered pipet tips (10, 20, 200, 1000 μl)	USA Scientific

2.3. Assay kits

Kits	Supplier
FoxP3 Staining Buffer Set	Thermo Fisher Scientific
PanCancer Immune Profiling Panel	NanoString Technologies
PureLink RNA Mini Kit	Ambion
Zombie Aqua™ Fixable Viability Kit	BioLegend

2.4. Media, supplements, and buffers

Product	Supplier
Beta-mercaptoethanol	Thermo Fisher Scientific
Fetal bovine serum (FBS)	Thermo Fisher Scientific
Dimethyl sulfoxide (DMSO)	Sigma-Aldrich
DMEM	Thermo Fisher Scientific
DPBS without Ca^{2+}, Mg^{2+} (1X)	Thermo Fisher Scientific
L-Glutamine (100X)	Thermo Fisher Scientific
Penicillin Streptomycin (100X)	Thermo Fisher Scientific
RPMI 1640 with L-glutamine	Thermo Fisher Scientific
Sodium pyruvate	Sigma-Aldrich

FBS serum were heat-inactivated and filtered through 0.22 μm pore-sized filters before being used as media supplements. Penicillin/Streptomycin (P/S) mix was also filtered through 0.22 μm filters before use.

Buffer/Medium	Components	Volume
FACS buffer	DPBS	485 ml
	FBS	15 ml
Freezing medium	FBS	9 ml
	DMSO	1 ml
ID8 medium	RPMI	437.5 ml
	FBS	50 ml
	Penicillin Streptomycin	5 ml
	L-Glutamine	5 ml
	Sodium Pyruvate	2.5 ml
	Beta-mercaptoethanol	2.15 μl
LLC medium	DMEM	440 ml
	FBS	50 ml
	Penicillin Streptomycin	5 ml
	Sodium Pyruvate	5 ml
T cell medium	RPMI	437.5 ml
	FBS	50 ml
	Penicillin Streptomycin	5 ml
	L-Glutamine	5 ml
	Sodium Pyruvate	2.5 ml
	Beta-mercaptoethanol	50 μl

2.5. Cell lines

Cell line	Type (derived from)	Mouse strain	Culture medium
ID8-Vegf-Defb29	Ovarian cancer	C57BL/6	ID8 medium
Lewis Lung Carcinoma	Lung cancer	C57BL/6	LLC medium

2.6. Drugs

Drug	Formulation	Supplier
2'3'-cGAMP	H_2O	Invivogen
Carboplatin	H_2O	Selleckchem
Gemcitabine HCl	0.9% saline	Selleckchem
GR-MD-02	0.9% saline	Galectin Therapeutics
LPS-B5	H_2O	Invivogen
Paclitaxel	1% DMSO 30% PEG 400 1% Tween80 dd H_2O	Selleckchem

2.7. Flow cytometry antibodies

Target	Isotype	Conjugate	Clone	Dilution	Vendor
Arg1	IgG	APC	Met1-Lys322	1:10	R&D Systems
B220	IgG2a, κ	PE	RA3-6B2	1:80	BioLegend
CD107a	IgG2a, κ	APC/Cy7	1D4B	1:20	BioLegend
CD11b	IgG2b, κ	PE/Cy5	M1/70	1:20	BioLegend
CD11c	IgG	BV421	N418	1:80	BioLegend
CD16/32	IgG2a, λ	-	93	1:200	BioLegend
CD3	IgG2b, κ	FITC	17A2	1:40	BioLegend
CD3	IgG2b, κ	APC	17A2	1:40	BioLegend
CD4	IgG2b, κ	PE/Cy5	GK1.5	1:200	BioLegend
CD44	IgG2b, κ	PE/Cy7	IM7	1:80	BioLegend
CD45	IgG2b, κ	AF 700	30-F11	1:200	BioLegend
CD69	IgG	BV421	H1.2F3	1:20	BioLegend
CD8a	IgG2b, λ	FITC	5H10-1	1:50	BioLegend
CD8a	IgG2a, κ	PE/Cy7	53-6.7	1:80	BioLegend
CD80	IgG	PE/Cy5	16-10A1	1:20	BioLegend

CD86	IgG2a, κ	BV605	GL-1	1:20	BioLegend
EOMES	IgG	AF488	Met1-Ser126	1:20	R&D Systems
F4/80	IgG2a, κ	PerCP/Cy5.5	BM8	1:20	BioLegend
FoxP3	IgG2b, κ	Pacific Blue	MF-14	1:50	BioLegend
Gal3	IgG1, κ	PE	Gal397	1:80	BioLegend
GZMB	IgG1, κ	PE/Cy7	QA16A02	1:20	BioLegend
ICOS	IgG2b, κ	PE	7E.17G9	1:20	BioLegend
IFNγ	IgG1, κ	PE-Dazzle 594	XMG1.2	1:300	BioLegend
IL-10	IgG2b, κ	PE/Cy7	JES5-16E3	1:80	BioLegend
IL-2	IgG2b, κ	Pacific Blue	JES6-5H4	1:200	BioLegend
IRF3	IgG	AF 647	D601M	1:100	CST
Ly6C	IgG2c, κ	AF700	HK1.4	1:200	BioLegend
Ly6G	IgG2a, κ	PerCP	1A8	1:80	BioLegend
MHCII	IgG2b, κ	PacificBlue	M5/114.15.2	1:200	BioLegend
NK1.1	IgG2a, κ	BV785	PK136	1:160	BioLegend
NKp46	IgG2a, κ	PE	29A1.4	1:20	BioLegend
PD-1	IgG2a, κ	BV605	29F.1A12	1:160	BioLegend
RORγt	IgG2b	PE	Met1-Arg10	1:10	R&D Systems
Tbet	IgG1, κ	BV605	4B10	1:20	BioLegend

2.8. *In vivo* antibodies

Target	Isotype	Conjugate	Clone	Vendor	Application
CD11b	Rat IgG2b, κ	-	M1/70	BioLegend	Dep
CD4	Rat IgG2b, κ	-	GK1.5	BioXCell	Dep
CD8α	Rat IgG2b, κ	-	2.43	BioXCell	Dep
Isotype Ctr	Rat IgG2b, κ	-	LTF-2	BioXCell	Dep/Neut
Isotype Ctr	Rat IgG1, κ	-	HRPN	BioXCell	Neut
4-1BB	Rat IgG2a	-	3H3	BioXCell	Neut
IL-10	Rat IgG1, κ	-	JES5-2A5	BioXCell	Neut
PD-1	Rat IgG2a	-	29F.1A12	BioXCell	Neut
PD-L1	Rat IgG2b, κ	-	10F.9G2	BioXCell	Neut

2.9. Mice

Female C57BL/6J mice (6 weeks old) from Jackson Laboratories (Stock #000664) were used in this study. Animal experiments were carried out in accordance with protocols approved by

the Dana-Farber Cancer Institute (DFCI) Institutional Animal Care and Use Committee (IACUC). Mice were housed in the animal facility of DFCI. Mice were house in sterile, individually ventilated cages (IVC). Ethical guidelines were followed according to the local regulations.

2.10. Additional software

Software	Developer
FACSDiva	BD
Flow Jo (V10)	Tree Star
GraphPad Prism (version 7.01)	GraphPad Software
Microsoft Office	Microsoft, USA
NanoDrop 2000/2000c	Thermo Fisher Scientific
nSolver 4.0	NanoString Technologies
SP6800	Sony Biotechnology
ToppGene Suite software	Cincinnati Children's Hospital Medical Center

3. Methods

3.1. Cell culture

ID8 murine ovarian cancer cells that overexpress VEGF-A and DEFB29 were kindly provided by Dr. Jose Conejo-Garcia, Moffitt Cancer Center and referred to as "ID8-Vegf-Defb29" within this manuscript. The murine Lewis Lung Carcinoma (LLC) lung cancer cell line was kindly provided by Dr. Harvey Cantor, Dana-Farber Cancer Institute, DFCI. All cell lines were cultured in the described culture medium (see Material section 2.4.) and maintained at 37°C and 5% CO_2. Cells were tested for mycoplasma contamination and found to be negative.

3.2. *In vivo* tumor models

For gene expression and flow analysis as well as survival experiments with the ID8-Vegf-Defb29 cell line, three million cancer cells were inoculated i.p. into the mice on day 0. Cells were inoculated in 200 μl/injection and injected using 27G needles. Tumor growth was measured using body weight and mice were sacrificed when body weight reached 150% or mice became moribund. Survival curves were generated using GraphPad Prism software. For efficacy studies with the LLC model, mice were shaved on the sides, anesthetized with isoflurane and subcutaneously (s.c.) injected with one million cells to generate a local tumor mass. Cells were inoculated in 100 μl/injection and injected using 27G needles. Tumor volume was measured using electronic calipers, and the volume was calculated using the formula (L x W^2)/2. Mice were sacrificed when tumor reached a volume of 2000 mm^3 or became necrotic. Tumor growth curves were generated using the GraphPad Prism software and plotted as fold change of tumor volume compared to day 16. All studies were performed in duplicate and included at least ten mice per group.

3.3. *In vivo* treatment

For the initial Nanostring and flow cytometry experiments, the mice were randomly assigned to treatment groups; 8 days after inoculation, mice were injected i.p. with vehicle control (0.5% DMSO + 15% PEG 400 + 0.5% Tween80 + ddH$_2$O) or a combination of paclitaxel (15 mg/kg; cat# S1150) and carboplatin (20 mg/kg; cat# S1215) (referred to as "chemotherapy" within this

manuscript). For the subsequent survival studies that included single immunotherapy, mice were injected with chemotherapy 8 days after inoculation followed by i.p. administration of either vehicle control or LPS-B5 (10mg/kg; cat# tlrl-pb5lps), GR-MD-02 (1.2 mg/dose), or anti-PD-1 antibody (0.2 mg/dose; clone 29F.1A12). For the survival studies including immunotherapy combinations, mice were injected with chemotherapy 8 days after inoculation followed by i.p. administration of various combinations of anti-IL-10 (0.25 mg/dose; clone JES5-2A5), 2'3'-cGAMP (0.01 mg/dose; cat# tlrl-nacga23-02), anti-PD-L1 (0.2 mg/dose; clone 10F.9G2), gemcitabine (1.2 mg/dose), anti-4-1BB (0.1 mg/dose; clone 3H3), and GR-MD-02 (1.2 mg/dose). A detailed description of the treatment schedule for each experiment is provided in the figure legends (Fig. 2,3,5,6,8). For subsequent flow experiments, mice received (i) vehicle control, (ii) paclitaxel and carboplatin, (iii) anti-IL-10, 2'3'-cGAMP, and anti-PD-L1, or (iv) paclitaxel, carboplatin, anti-IL-10, 2'3'-cGAMP, and anti-PD-L1 8 days after inoculation. For experiments with the LLC cancer cell line, mice were randomly assigned to treatment groups when tumors reached ~100 mm^3 (about 16 days after tumor inoculation), and received (i) vehicle control, (ii) paclitaxel and carboplatin, (iii) anti-IL-10, 2'3'-cGAMP, and anti-PD-L1, or (iv) paclitaxel, carboplatin, anti-IL-10, 2'3'-cGAMP, and anti-PD-L1.

3.4. Cell isolation

Cells were harvested from the peritoneal cavities of treated mice by peritoneal wash. Briefly, mice were mounted on Styrofoam and the outer skin was cut to expose the inner peritoneal skin. 5 ml ice-cold DPBS + 3% FBS was injected into the peritoneal cavity, the peritoneum was gently massaged, and the fluid containing peritoneal cells was collected through a 21G needle and placed on ice. The peritoneal skin was cut, and remaining fluid was collected using a transfer pipet. Cells were washed once, and red blood cells were removed by incubation with appropriate amount of ACK lysing buffer (cat# A1049201) for 3 min at RT. Reaction was stopped by adding 10 ml of medium and cells were washed once with FACS buffer and counted.

3.5. Cell sorting

Cells isolated from mice were stained with 4 μl/1x10^6 cells Zombie Aqua Fixable Viability Kit (cat# 423101) in 1 ml FACS buffer for 20 min on ice in the dark. 5 μl/1x10^6 cells anti-mouse CD16/32 antibody (cat# 101302, clone 93) was added to block unspecific antibody binding. Subsequently, cells were washed once and stained for anti-mouse CD45 (cat# 103131, clone

30-F11), anti-mouse CD3 (cat# 100236, clone 17A2), anti-mouse CD11b (cat# 101205, clone M1/70), anti-mouse B220 (cat# 103207, clone RA3-6B2), and anti-mouse NKp46 (cat# 137603, clone 29A1.4). Cells were then sorted on a BD FACSAria IIIu as ZombieAqua$^-$/CD45$^+$/CD3$^+$/CD11b$^{-/-}$/B220$^-$/NKp46$^-$ or ZombieAqua$^-$/CD45$^+$/CD3$^-$/CD11b$^+$/B220$^-$/NKp46$^-$ cells into RPMI 1640 medium containing 2% FBS at 4°C.

3.6. Nanostring

For Nanostring on murine myeloid and T cells sorted cells were pelleted, and RNA was isolated using the PureLink RNA Mini Kit (cat# 12183018A) according to manufacturer's instructions. Briefly, lysis buffer containing 2-mercaptoethanol was added to the cells and homogenized using a rotor-stator homogenizer at maximum speed for 30 sec. RNA was then bound, washed and eluted in 10 μl of RNase-free water. RNA quality and concentration were verified with the NanoDrop 2000c Spectrophotometer and 100 ng of RNA per sample was loaded on the nCounterMax instrument and run using the NS_MM_CancerImm_C3400 NanoString PanCancer Immune Profiling panel (NanoString Technologies). For human ovarian cancer samples, RNA was isolated from matched FFPE blocks taken from patients before treatment (biopsy) and after chemotherapy (surgical resection) and run using the NS_CancerImmune_C2929 NanoString PanCancer Immune Profiling panel (NanoString Technologies). Sample were analyzed using the Advanced Analysis Module of the nSolver^{TM} software[64]. In short, samples were automatically normalized using the best performing probes selected by the geNorm algorithm[65]. Selected housekeeping genes were confirmed to be stable with low variability and moderate expression levels. Differential expression was performed, and data displayed as volcano plots. p-values were adjusted using the Benjamini-Hochberg procedure. Top up- or downregulated genes as determined by the Advanced Analysis Module were plotted as a heatmap using the nSolver^{TM} software analysis function. For functional enrichment analysis genes were queried using the ToppFun tool of the ToppGene Suit software.

3.7. Flow cytometry

Cells were harvested from the peritoneal cavity by peritoneal wash as described above (see 3.4.) Cells were resuspended in T cell medium (see Material section 2.4.) at a concentration of 1.5x10^6/ml. Cell Activation Cocktail with Brefeldin A (cat# 423304) at a concentration of 2 μl/ml medium and GolgiStop™ protein transport inhibitor (cat# 554724) at a concentration

of 4 μl/6 ml medium were added for T cell stimulation and inspection of intracellular cytokines and cytolytic molecules. Cells were incubated for 4 hrs at 37°C and 5% CO_2. After that, cells were harvested, filtered through a 70 μm cell strainer, and washed once with FACS buffer. Cell were divided into samples and single stained controls and stained with Zombie Aqua Fixable Viability Kit (cat# 423101) and anti-mouse CD16/32 antibody (cat# 101302, clone 93) (see 3.5.). Subsequently, cells were washed once with FACS buffer and incubated with appropriate amount of surface antibodies in 100 μl FACS buffer (see Materials section 2.7.) for 30 min on ice in the dark. Cells were washed once with FACS buffer, pulse vortexed, and fixed using the Foxp3 Staining Buffer Set (cat# 00-5523-00) according to manufacturer's instructions. Briefly, cells were incubated in 100 μl Fixation/Permeabilization Buffer for 20 min on ice in the dark and then washed twice with 1 x Permeabilization Buffer. After fixation, cells were stained for intracellular proteins with appropriate amount of antibodies in 50 μl 1 x Permeabilization Buffer for 60 min on ice in the dark. Cell were then washed twice with 1 x Permeabilization Buffer before being resuspended in 70 - 100 μl of FACS buffer for flow analysis. Flow cytometry was performed on a Sony SP6800 Spectral Analyzer, compensation was calculated using the SP6800 software, and cell population were gated and analyzed using the FlowJo software (see Supplementary Fig. 3). Bar plots were generated using the GraphPad Prism software. All antibodies were purchased from BioLegend, R&D Systems, or Cell Signaling Technology (see Materials section 2.7.).

3.8. Depletion of CD4+ T cells, CD8+ T cells, or CD11b+ cells

In order to evaluate which immune cells are required to confer the observed antitumor effect, specific cell subsets (CD4+ T cells, CD8+ T cells, or CD11b+ cells) were depleted by administering depleting antibodies i.p., beginning one day prior to chemotherapy. The antibodies used for depletion were anti-mouse CD4 (cat# BE0003-1, clone GK1.5), anti-mouse CD8a (cat# BE0061, clone 2.43), and anti-mouse CD11b (cat# 101231, clone M1/70). Two-hundred μg of anti-CD4 or anti-CD8a was administered every three days, or 100 μg of anti-CD11b was administered every two days. A detailed description of the treatment schedule is provided in the figure legend (Fig. 6). Depletion of CD4+ T cells, CD8+ T cells, and CD11b+ cells was confirmed by flow cytometry of leukocytes isolated from the blood of mice to which antibodies or isotype antibody (cat# BE0090, clone LTF-2) had been administered. Briefly, three and six days after initiation of treatment blood was collected from mice via submandibular bleeds. Cells were washed once, and red blood cells were removed by incubation with

appropriate amount of ACK lysing buffer (cat# A1049201) for 5 min at RT. Reaction was stopped by adding 10 ml of medium and cells were washed once with FACS buffer and counted. Cell were stained with Zombie Aqua Fixable Viability Kit (cat# 423101) and anti-mouse CD16/32 antibody (cat# 101302, clone 93) (see 3.5.). Cell were stained and analyzed by flow cytometry as described in 3.7.

3.9. Statistical methods

Statistical methods were not used to predetermine necessary sample size. The sample sizes were selected based on the results of pilot experiments so that relevant statistical tests could reveal significant differences between experimental groups. Statistical analysis was performed using GraphPad Prism software. Data are presented as mean ± SEM, as indicated in the Figure legends. The Student's t-test or one-way ANOVA with Tukey's post-hoc test was used to determine statistical significance between two groups and several groups, respectively. For survival analysis, the Log-rank (Mantel-Cox) test was employed. * $p \leq 0.05$, ** $p \leq 0.01$, *** $p \leq 0.001$, **** $p \leq 0.0001$.

4. Results

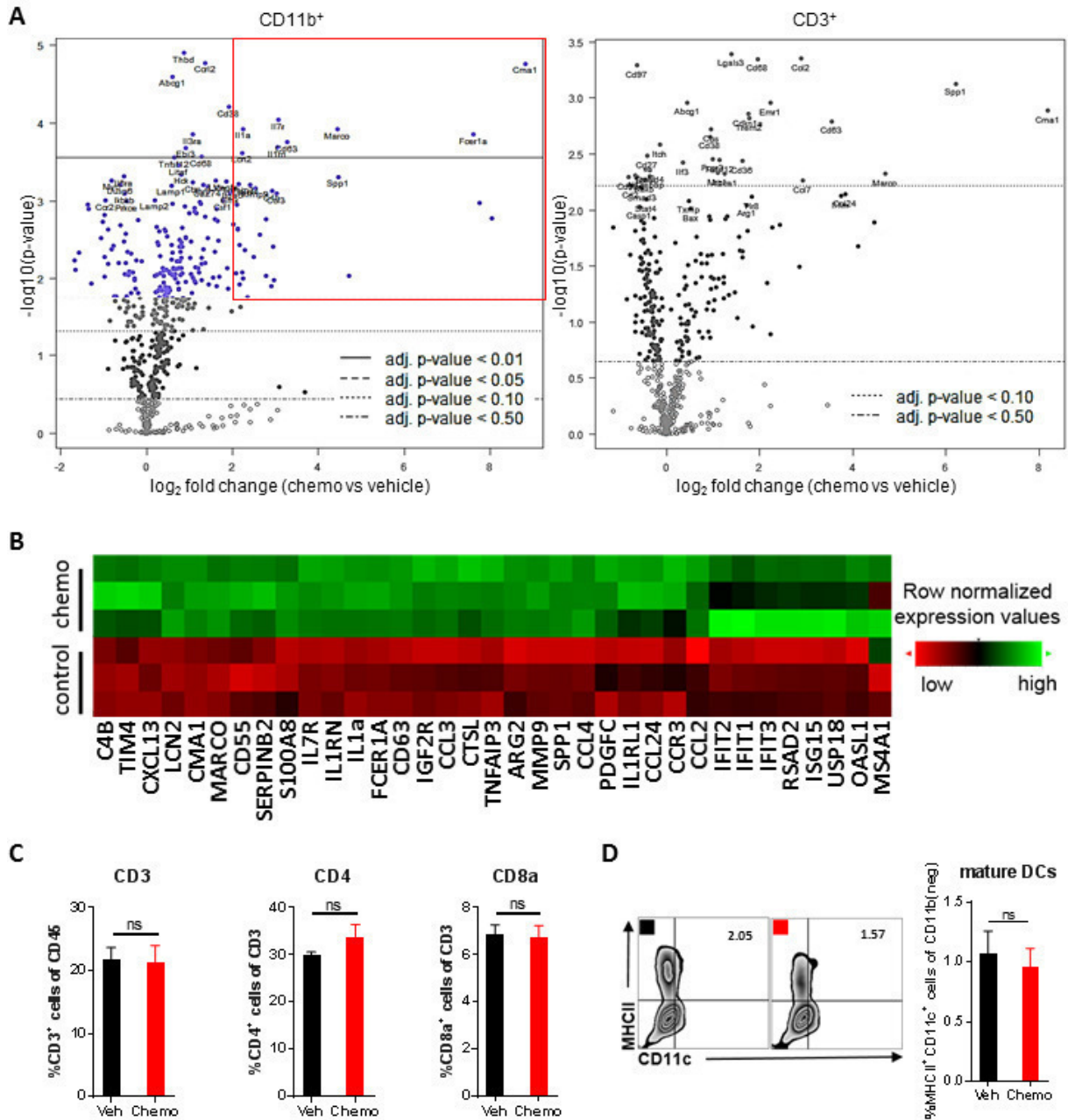## 4.1. Chemotherapy induces acute immunosuppression among innate immune cells specifically

Author	Author position	Scientific ideas %	Data generation %	Analysis & interpretation %	Paper writing %
Christina Hartl	1st	80 %	93 %	90 %	95 %
Adrian Bertschi	2nd	0 %	5 %	0 %	0 %
Carolin Andresen	4th	0 %	2 %	0 %	0 %
Michael Goldberg	8th	20 %	0 %	10 %	5 %
Title of paper:	Combination therapy targeting both innate and adaptive immunity improves survival in a pre-clinical model of ovarian cancer				
Status in publication process:	under review				

In this study, we examined the effects of standard-of-care chemotherapy on the peritoneal immune compartment of mice harboring ovarian cancer. These insights were sought to enable identification of a mechanistically informed immunotherapy that could combine synergistically with chemotherapy and thereby increase overall survival. As described in section 1.4., we selected the orthoptic, syngeneic ID8-Vegf-Defb29 ovarian cancer model because it is an aggressive variant of the parental ID8 cell line that robustly recapitulates many features of advanced human ovarian cancer[66]. Consistent with clinical presentation, treatment with chemotherapy alone is not curative in this model, which exhibits low sensitivity to checkpoint blockade monotherapy (Supplementary Fig. 1A,B).

Peritoneal leukocytes were harvested from tumor-bearing mice two days after treatment with a single dose of paclitaxel and carboplatin – the standard of care for ovarian cancer patients. This time point was chosen to inspect the short-term consequences of standard-of-care chemotherapy on the immune system, as we sought to initiate immunotherapy concomitantly in order to leverage the benefits of chemotherapy and mitigate against its drawbacks. Nanostring-mediated analysis of FACS-sorted $CD11b^+$ or $CD3^+$ leukocytes revealed a selective induction of differential gene expression in myeloid cells (Fig. 1A; Supplementary Fig. 2). Among $CD11b^+$ cells, mRNA expression was increased for 200 genes, 35 of which were upregulated more than 2-fold (Fig. 1B). In contrast, no significantly differential gene expression was detected among $CD3^+$ T cells using an adjusted p-value of 0.05 or lower. Flow cytometric analysis of peritoneal leukocytes confirmed that chemotherapy predominantly affected the myeloid compartment, as

evidenced by a lack of change in the proportion of CD3^{+}, CD4^{+}, and CD8^{+} T cells (Fig. 1C; Supplementary Fig. 3) and mature dendritic cells (MHCII^{+}) (Fig. 1D). Consistently, the number of macrophages (F4/80^{+}) was increased, and the proportion of MDSCs (Ly6G^{+}/Ly6C^{+}) and CD11b^{+} cells that expressed the immunosuppressive factors ARG1 and IL-10 was similarly elevated (Fig. 1E)[43,67,38]. Together, these data indicate that chemotherapy induces acute immunosuppression in this model.
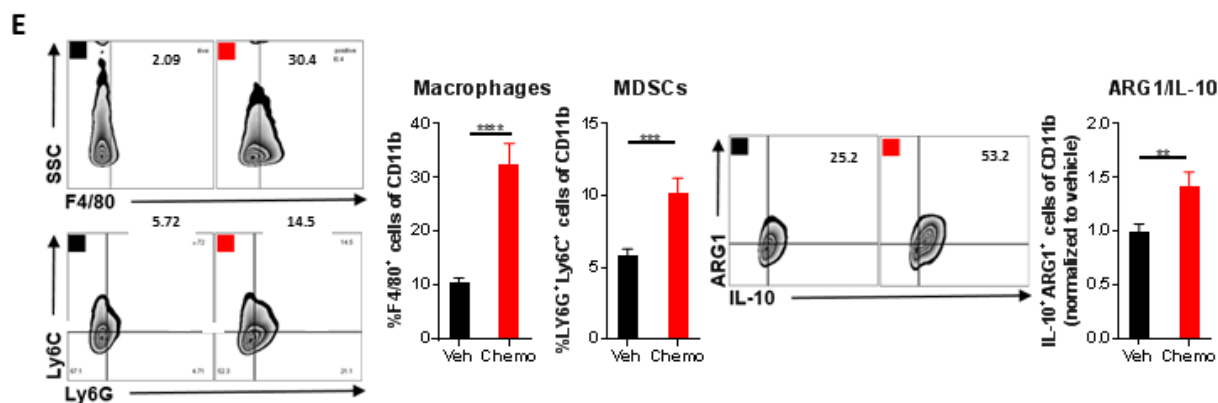
Figure 1. Treatment with paclitaxel and carboplatin induces acute immunosuppression that is mediated by innate immune cells. Mice were inoculated orthotopically with ID8-Vegf-Defb29 ovarian cancer cells. Eight days later, the mice were injected with vehicle (Veh) or chemotherapy (Chemo). Two days later, peritoneal cells were harvested for analysis. (**A**) Volcano plots of gene expression data sets derived from FACS-sorted leukocytes (CD11b^{+} and CD3^{+}). All probe sets are shown. The top 40 differentially expressed genes are named, and highlight coloring was applied to significantly differentially expressed (adj. p-value < 0.05) probe sets. The experiment was performed once with n=3 biological replicates. (**B**) A heatmap of the top 35 upregulated genes after chemotherapy treatment in FACS-sorted CD11b^{+} cells. (**C**) Peritoneal cell suspensions were assessed by flow cytometry. Bar graphs show quantification of flow cytometry gating of CD3^{+} T cells, CD4^{+} T cells, and CD8^{+} T cells. (**D**) Flow cytometry gating of subsets of MHCII^{+} mature dendritic cells are shown as scatter plots and quantified at right. (**E**) Flow cytometry gating of subsets of F4/80[+] macrophages are shown as scatter plots and quantified at right. Increased numbers of Ly6G^{+}Ly6C^{+} myeloid derived suppressor cells, immunosuppressive ARG1^{+} myeloid cells, and IL-10^{+} macrophages are observed following chemotherapy. The experiment was performed twice with n=4 biological replicates. Statistics were calculated using a two-sided unpaired t-test. Data are presented as mean ± SEM * p≤0.05, ** p≤0.01, **** p≤0.0001

4.2. Combination with single immunotherapy does not increase survival

Author	Author position	Scientific ideas %	Data generation %	Analysis & interpretation %	Paper writing %
Christina Hartl	1st	90 %	90 %	95 %	100 %
Adrian Bertschi	2nd	0 %	10 %	0 %	0 %
Michael Goldberg	8th	10 %	0 %	5 %	0 %
Title of paper:	Combination therapy targeting both innate and adaptive immunity improves survival in a pre-clinical model of ovarian cancer				
Status in publication process:	under review				

To identify an immunotherapy that best synergizes with paclitaxel and carboplatin, we compared the relative efficacy of several immunotherapies targeting different arms of the immune system. In order to enhance the antitumor reaction and attenuate the immunosuppressive environment, we chose to complement chemotherapy with LPS-B5, a principal component of gram-negative bacteria and an activator of toll-like receptors (TLRs) 2 and 4 with the subsequent induction of NF-κB and the production of pro-inflammatory cytokines. It has previously been shown to be a potent adjuvant in *in vivo* models of melanoma tumors[68]. We also included an inhibitor for Galectin-3 (GR-MD-02), a protein that is widely expressed on all types of immune cells (macrophages, monocytes, dendritic cells, eosinophils, mast cells, natural killer cells, and activated T and B cells) and cancer cells and induces cancer growth, angiogenesis, and immune cell apoptosis[69,70]. Its expression was upregulated on various immune cells four days after treatment with chemotherapy (Supplementary Fig. 4). Finally, to target the adaptive immune system and boost T cell response against cancer cells we included antibodies for PD-1[71]. Immunotherapies were administered promptly after chemotherapy into tumor-bearing mice and dosed as described (see Methods; Fig. 2). Paclitaxel and carboplatin in the absence of immunotherapy (Chemo) were administered as a control. Tumor burden was monitored using ascites as a surrogate for disease progression and it as found that no combination therapy extended survival over chemotherapy alone (Fig. 2A-C). These results suggested that solely targeting one part of the immune system was not sufficient in this model, and to significantly extend survival a more aggressive approach would likely be necessary.
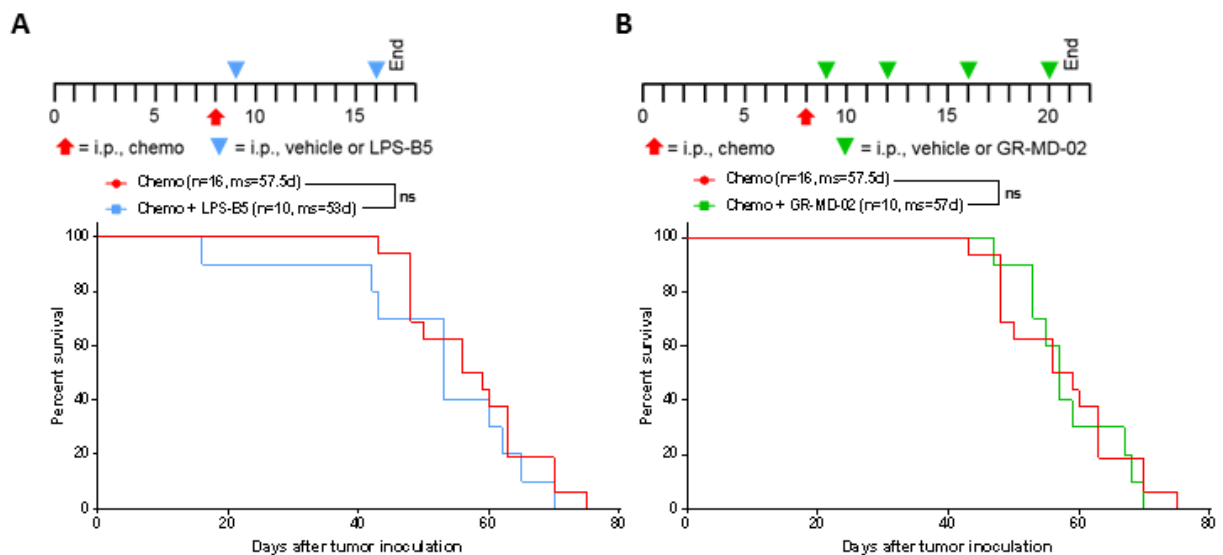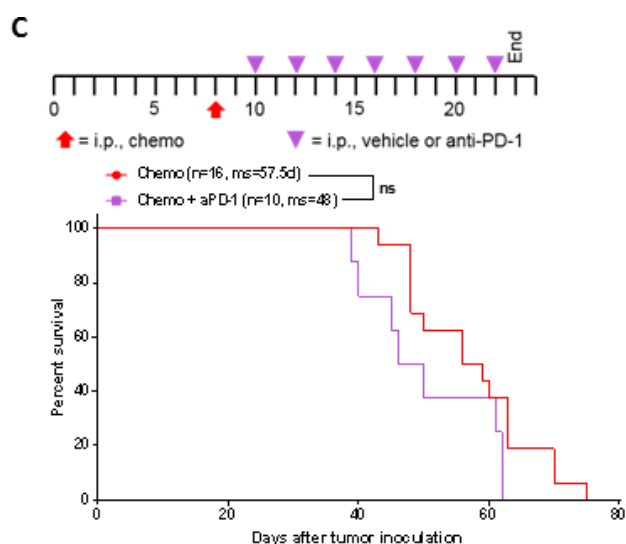
Figure 2. Combination with single immunotherapy does not increase survival. Different combinations of chemotherapy and immunotherapy were tested *in vivo* for synergy. Kaplan-Meier curves are shown for mice treated with chemotherapy and (**A**) LPS-B5, (**B**) GR-MD-02, or (**C**) PD-1 antibody. (**A-C**) All combination treatments were compared to chemotherapy and isotype control for immunotherapy (Chemo) eight days after inoculation of ID8-Vegf-Defb29 cells. The number of mice per group (n) and median survival (ms) are listed. The experiment was performed with biological replicates twice. Statistics were calculated relative to the group treated with chemotherapy only using the Log-rank (Mantel-Cox) test.

4.3. STING agonism combined with neutralization of IL-10 and PD-L1 after chemotherapy increases survival

Author	Author position	Scientific ideas %	Data generation %	Analysis & interpretation %	Paper writing %
Christina Hartl	1st	80 %	95 %	95 %	90 %
Regina Bou Puerto	3rd	0 %	5 %	0 %	0 %
Michael Goldberg	8th	20 %	0 %	5 %	10 %
Title of paper:	Combination therapy targeting both innate and adaptive immunity improves survival in a pre-clinical model of ovarian cancer				
Status in publication process:	under review				

Since single immunotherapy was inadequate to slow tumor growth, we decided to simultaneously target multiple aspects of the immune system in combination with chemotherapy. We also selected a wider number of immunotherapies for subsequent testing.

In order to stimulate the adaptive arm of the immune system, we selected an agonist of 4-1BB, a co-stimulatory receptor expressed on activated T and NK cells and important regulator of immune responses that can increase the intratumor persistence of tumor-specific cytotoxic T cells resulting in enhanced tumor cell killing[72,73]. We opted to exchange anti-PD-1 for an antibody targeting its ligand as it also enhances cytotoxic function[74] but has previously shown to have a higher affinity in mice (data not shown). Neutralization of the PD-1 pathway is likely to be the backbone of immunotherapy for treatment of ovarian cancer[31]; however, since anti-PD-(L)1 monotherapy of ovarian cancer is inadequate in the clinic[15] and has not yielded synergistic results in our previous experiment (Fig. 2C), we decided to simultaneously target the innate immune system.

We tested the Galectin-3 inhibitor GR-MD-02 as complement to the adaptive immunotherapy as well as an antibody against interleukin-10 (anti-IL-10) a negative regulator of immune function[38,75], which is found in high levels in ascites of ovarian cancer patients and consistently correlates with advanced disease and poor prognosis[76]. Its expression was upregulated on myeloid cells shortly after chemotherapy, as determined by flow cytometry (Fig. 1E). Gemcitabine is a chemotherapy known to preferentially deplete immunosuppressive MDSCs[77], and 2'3'-cGAMP is an agonist of Stimulator of interferon genes (STING) that potently induces production of type I interferons[78]. GR-MD-02 and agonist anti-4-1BB were combined with either anti-IL-10 or 2'3'-cGAMP. Anti-PD-L1 and 2'3'-cGAMP were combined with gemcitabine or anti-IL-10. 2'3'-cGAMP and anti-IL-10 were combined with an activator of the adaptive immune system: anti-PD-L1 or agonist anti-4-1BB. Immunotherapies were administered promptly after chemotherapy into tumor-bearing mice and dosed as described (see Methods; Fig. 3). Paclitaxel and carboplatin in the absence of immunotherapy (Chemo) were administered as a control.

It was confirmed that combination of immunotherapy and chemotherapy can significantly extend survival in some groups relative to chemotherapy only control (Fig. 3A-E). Notably, not all combinations increased survival equally.

GR-MD-02, which inhibits M2 macrophage polarization and angiogenesis, had little impact relative to anti-IL-10 and 2'3'-cGAMP (Fig. 3A,B,D). Gemcitabine provided some benefit but was inferior to anti-IL-10 (Fig. 3C,E). As a complement to anti-IL-10 and 2'3'-cGAMP, anti-PD-L1 conferred greater survival benefit than agonist anti-4-1BB (Fig. 3D,E). These data suggest that both the neutralization of immunosuppressive cytokines (anti-IL-10) and the induction of an inflammatory innate immune response (2'3'-cGAMP) are essential for establishing meaningful antitumor immunity following chemotherapy. Furthermore, the

increased survival conferred by anti-PD-L1 therapy (Fig. 3E) suggests an essential role of T cells in mediating anti-tumor effects, though this effect is likely enabled by the continued dosing of the antibody beyond the neuralization of acute immunosuppression. These results suggest that immunotherapy targeting both innate (anti-IL-10; 2'3'-cGAMP) and adaptive (anti-PD-L1) immune function generated the greatest survival benefit.
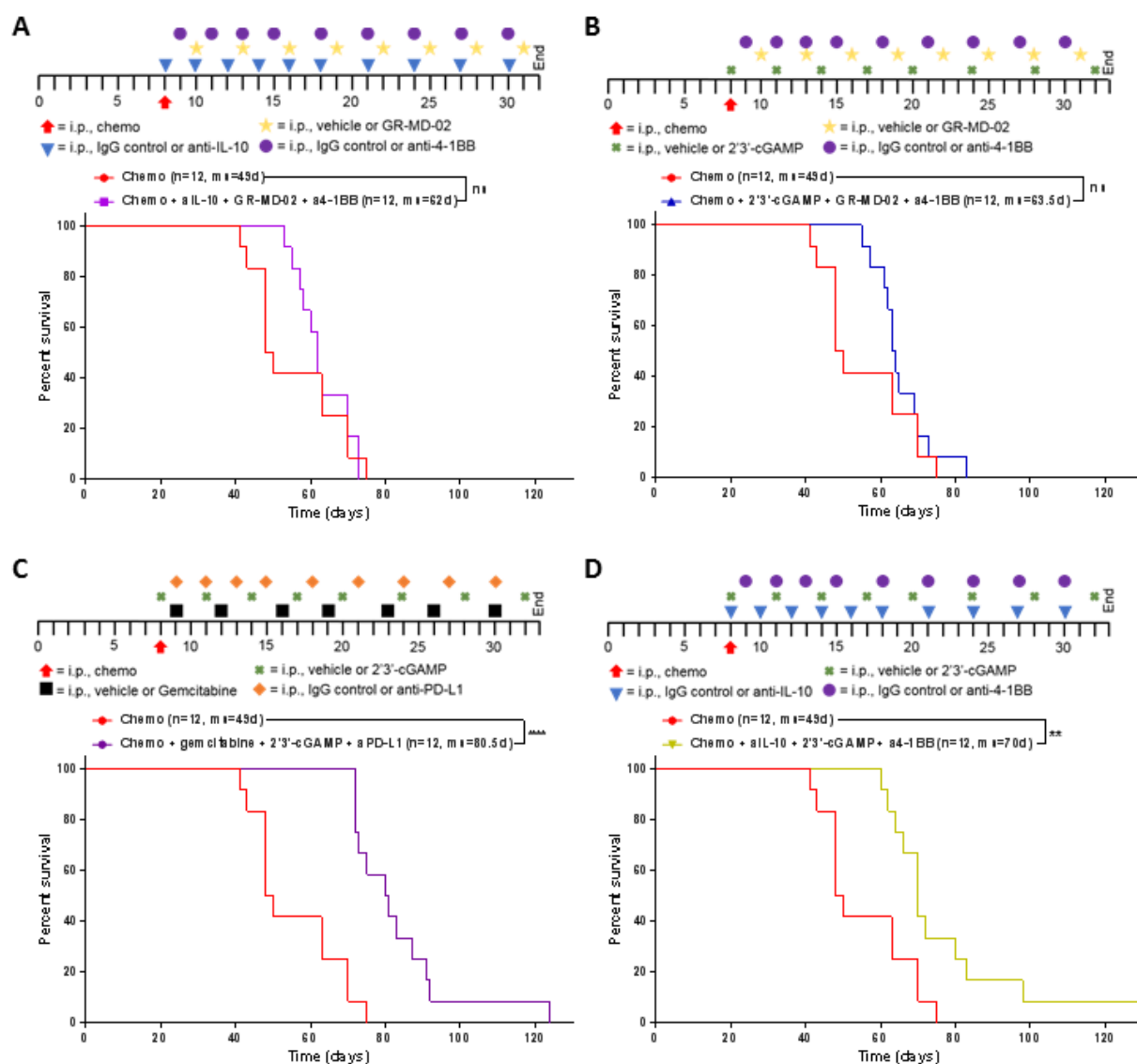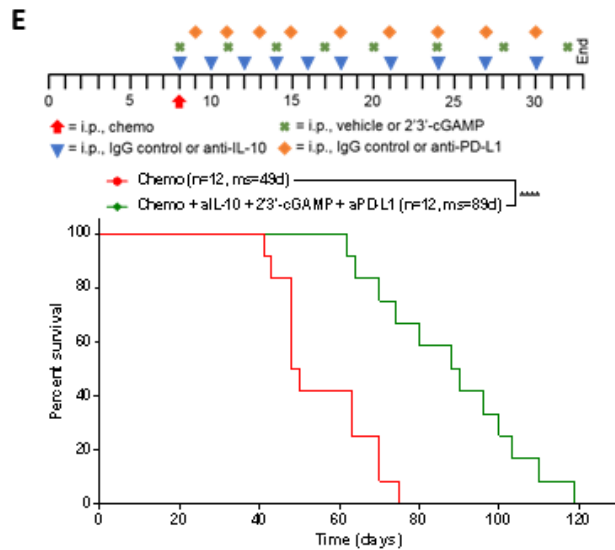
Figure 3. STING agonism combined with neutralization of IL-10 and PD-L1 after chemotherapy increases survival. Different combinations of chemotherapy and immunotherapy were tested *in vivo* for synergy. Kaplan-Meier curves are shown for mice treated with chemotherapy and (**A**) anti-IL-10, GR-MD-02, and anti-4-1BB, (**B**) 2'3'-cGAMP, GR-MD-02, and anti-4-1BB (**C**) gemcitabine, 2'3'-cGAMP, and anti-PD-L1, (**D**) anti-IL-10, 2'3'-cGAMP, and anti-4-1BB, or (**E**) anti-IL-10, 2'3'-cGAMP, and anti-PD-L1 or with chemotherapy and (**A-E**) isotype control (Chemo) 8 days after inoculation of ID8-Vegf-Defb29 cells. The number of mice per group (n) and median survival (ms) are listed. The experiment was performed with biological replicates twice. Statistics were calculated relative to the group treated with chemotherapy only using the Log-rank (Mantel-Cox) test. ** $p \leq 0.01$, **** $p \leq 0.0001$.

4.4. Combination therapy reverses the myeloid cell-mediated immunosuppression and promotes infiltration of activated DCs and T cells

Author	Author position	Scientific ideas %	Data generation %	Analysis & interpretation %	Paper writing %
Christina Hartl	1st	95 %	100 %	95 %	95 %
Michael Goldberg	8th	5 %	0 %	5 %	5 %
Title of paper:	Combination therapy targeting both innate and adaptive immunity improves survival in a pre-clinical model of ovarian cancer				
Status in publication process:	under review				

To dissect the changes among immune cell subsets following administration of combination therapy on a cellular and molecular level, we assessed the immune cells recovered from the peritoneal cavity for expression of lineage and activation markers. Leukocytes were recovered from mice four days after initiation of treatment for flow cytometric analysis. We observed a

significant decrease in macrophage numbers (CD11b$^+$F4/80$^+$) after treatment with immunotherapy (Fig. 4A). Similarly, the numbers of ARG1$^+$ and IL-10$^+$ myeloid cells, which are highly immunosuppressive, were decreased (Fig. 4B). After exposure to combination therapy, more dendritic cells were present in the tumor microenvironment, which were highly activated by chemotherapy as indicated by the elevated expression of costimulatory molecules CD86 and CD80 (Fig. 4C). Furthermore, increased expression of IRF3, a transcription factor in the STING pathway[79], suggested activation by chemotherapy as well as 2'3'-cGAMP[80] (Fig. 4D). The activation of dendritic cells translated into robust T cell priming as evidenced by a strong adaptive antitumor response. The number of CD3$^+$ T cells was increased after treatment with combination chemotherapy and immunotherapy but not after either therapy alone or vehicle (Fig. 4E). While the numbers of CD4$^+$ and CD8$^+$ T cells did not change (Supplementary Fig. 5), increased expression of the early activation marker CD69, the degranulation marker CD107a, the cytokine IL-2, and the cytolytic molecule granzyme B (GZMB) were detected (Fig. 4E, Supplementary Fig. 6). The relatively short time between treatment and analysis might explain why significant changes in expression of IFNγ or PD-1 were not observed (Supplementary Fig. 7). Together, these results indicate that combination of immunotherapy targeting both the innate and adaptive arms of the immune system can reverse the immunosuppressive phenotype of myeloid cells induced by chemotherapy and can commensurately lead to activation of T cells.
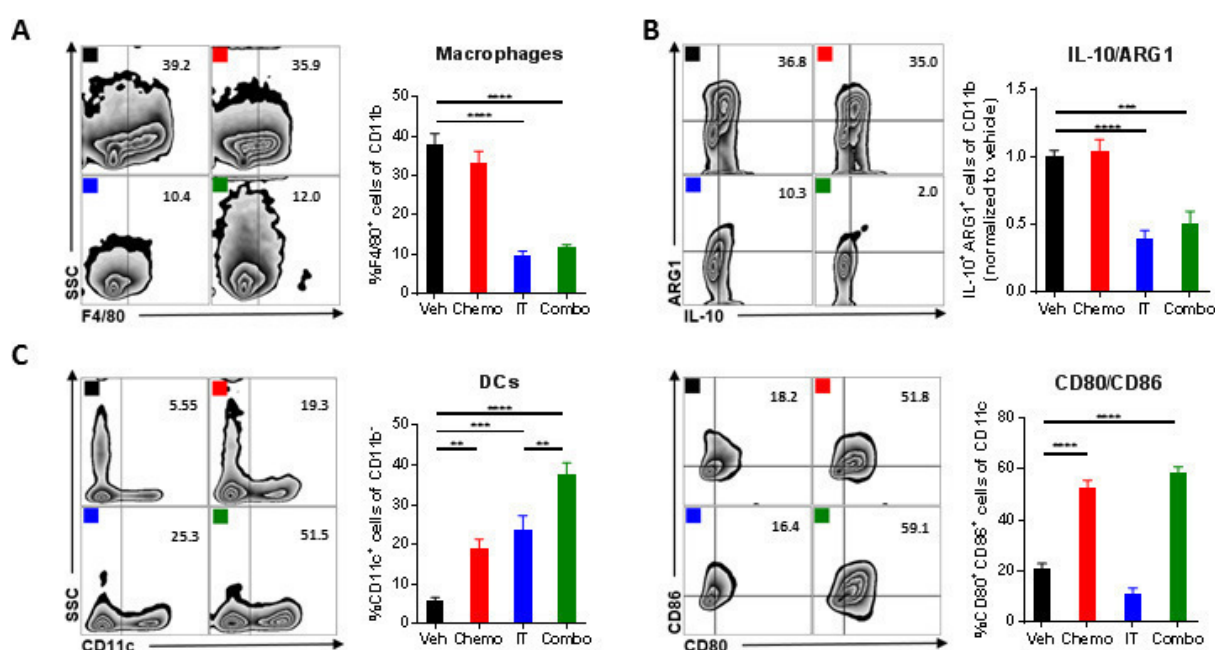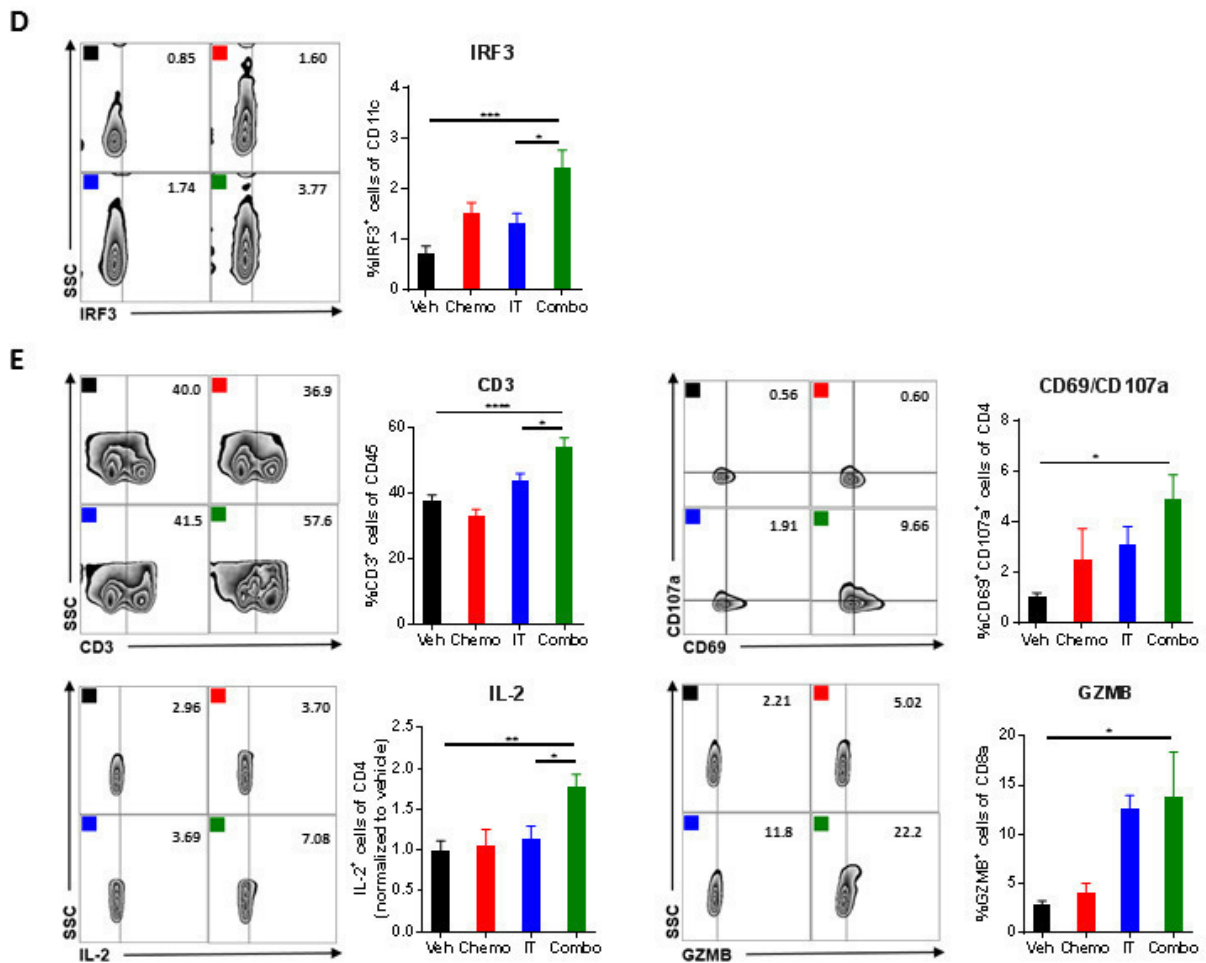
Figure 4. Combination therapy reverses the myeloid cell-mediated immunosuppression and promotes infiltration of activated DCs and T cells. (A) Peritoneal cell suspensions from tumor-bearing mice treated with vehicle (Veh); chemotherapy (Chemo); anti-IL-10, 2'3'-cGAMP, and anti-PD-L1 immunotherapy (IT); or both Chem and IT (Combo) were assessed by flow cytometry 4 days after initiation of treatment. **(A,B)** Decreased numbers of myeloid cells with immunosuppressive phenotypes are observed upon Combo treatment. **(A)** Decreased numbers of F4/80[+] macrophages are observed upon treatment with immunotherapy (IT and Combo) **(B)** Flow cytometry gating of subsets of ARG1^{+}IL^{+} myeloid cells are shown as scatter plots and quantified at right. **(C,D)** Increased numbers of mature dendritic cells are observed upon Combo treatment. **(C)** Flow cytometry gating of subsets of CD11c^{+} dendritic cells are shown as scatter plots and quantified at right. Numbers of CD11c^{+} cells expressing co-stimulatory molecules are quantified. **(D)** STING activation is pharmacodynamically confirmed by expression of IRF3. **(E)** The adaptive immune system is also impacted by Combo therapy. Quantitation of flow cytometry gating of CD3^{+} T cells, CD4^{+} T cells, and CD8^{+} T cells is shown. Increased numbers of CD3^{+} T cells expressing the activation marker CD69, the pro-inflammatory cytokine IL-2, and the cytolytic molecules CD107a and GZMB are observed. The experiment was performed twice with n=4 biological replicates. Statistics were calculated using one-way ANOVA with Tukey's multiple comparisons test. Data are presented as mean $\pm$ SEM * $p \leq 0.05$, ** $p \leq 0.01$, *** $p \leq 0.001$, **** $p \leq 0.0001$.

4.5. Survival benefit of combination therapy is strongly influenced by dosing schedule

Author	Author position	Scientific ideas %	Data generation %	Analysis & interpretation %	Paper writing %
Christina Hartl	1st	95 %	95 %	95 %	95 %
Emily Cheney	5th	0 %	5 %	0 %	0 %
Michael Goldberg	8th	5 %	0 %	5 %	5 %
Title of paper:	Combination therapy targeting both innate and adaptive immunity improves survival in a pre-clinical model of ovarian cancer				
Status in publication process:	under review				

Next, we confirmed that chemotherapy and immunotherapy indeed work synergistically by comparing the combination of chemotherapy plus immunotherapy (Combo) to separate therapy with paclitaxel and carboplatin (Chemo) or anti-IL-10, 2'3'-cGAMP, and anti-PD-L1 immunotherapy (IT). Studies confirmed that while each therapy (chemotherapy/immunotherapy) alone significantly improves survival, the combination imparted a much larger benefit (Fig. 5A). Initial repolarization of the immune compartment can sometimes be sufficient to increase survival and enhance the antitumor effects of chemotherapy. To determine if prolonged immunotherapy is necessary for efficacy, we dosed mice with the combination for either the full three weeks (Combo) or just one week (Combo short). Dosing for only one week completely abrogates the survival benefit of the combination (Fig. 5B), revealing that merely repolarizing the immune environment shortly after chemotherapy is not adequate and highlighting the importance of directly augmenting the adaptive immune system thereafter. It is thus possible that continued immunotherapy – beyond three weeks – could potentially further increase survival or even be curative.

Next, we investigated the importance of the early repolarization phase and the temporal interplay between chemotherapy and immunotherapy dosing. We dosed mice with chemotherapy on day 8 post-tumor inoculation in combination with immunotherapy beginning on day 8 (Combo) or day 12 (Delayed IT). We chose a delay of four days to minimize the possibility that any effects on survival would be caused by a dearth of therapy early in the course of disease progression, as might be expected if the therapy was delayed by one week or more. Still, a delay of just four days was sufficient to abolish the benefit of the combination therapy (Fig. 5C), supporting the notion that the immunosuppressive effects of chemotherapy are acute and that immediate intervention with immunotherapy is essential. This highlights the enormous importance of a well-designed treatment schedule in the clinic to maximize patient outcome. In the clinic, ovarian cancer is often diagnosed at a late stage when patients have

already developed extensive primary tumors and metastases[81]. Therefore, we investigated whether our combination would have the same survival benefit when given to mice at a relatively late stage of cancer progression. Mice were treated with combination therapy beginning either on day 8 (Combo) or day 22 (Combo late). Results show that mice treated later do not benefit from the combination therapy (Fig. 5D). The results show that our immunotherapy works synergistically with standard-of-care chemotherapy in this model, but the dosing schedule is crucial to conferring benefit. Furthermore, the largest survival benefit is achieved when immunotherapy is given concomitant with chemotherapy at an early stage of disease for an extended period of time.
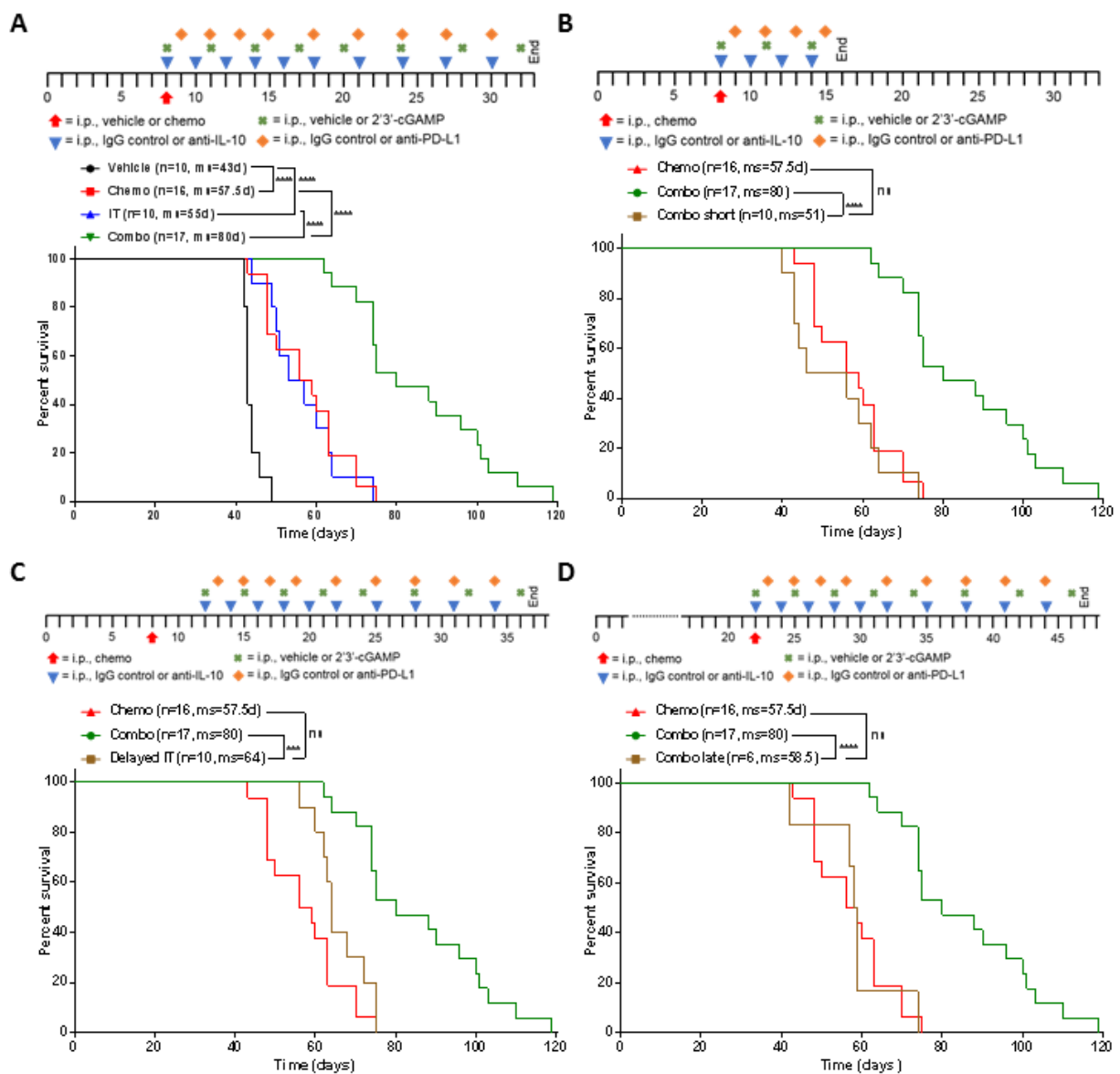

Figure 5. Survival benefit conferred by the combination therapy is superior to chemotherapy or immunotherapy alone and strongly influenced by dosing schedule. Different dosing schedules were tested to understand the temporal interaction between chemotherapy and immunotherapy in ID8-Vegf-

Defb29-tumor bearing mice. Each is depicted above the Kaplan-Meier curves. (**A**) A Kaplan-Meier curve is shown comparing combination therapy (Combo) to chemotherapy (Chemo) or immunotherapy (IT) alone as well as vehicle only (Vehicle). (**B**) A Kaplan-Meier curve is shown comparing three weeks of treatment (Combo) to one week of immunotherapy treatment (Combo short) following chemotherapy. (**C**) A Kaplan-Meier curve is shown comparing immunotherapy initiated on the same day as chemotherapy (Combo) to immunotherapy initiated 4 days later (Delayed IT). (**D**) A Kaplan-Meier curve is shown comparing combination therapy initiated on day 8 (Combo) to combination therapy initiated on day 22 (Combo late). (**B-D**) Treatment groups are compared to chemotherapy and isotype control (Chemo). The number of mice per group (n) and median survival (ms) are listed. All experiments were performed with biological replicates at least twice. Statistics were calculated using the Log-rank (Mantel-Cox) test. *** $p \leq 0.001$, **** $p \leq 0.0001$.

4.6. CD4$^+$ T cells are critical for the efficacy of this combination therapy

Author	Author position	Scientific ideas %	Data generation %	Analysis & interpretation %	Paper writing %
Christina Hartl	1st	85 %	100 %	90 %	85 %
Elizabeth Mittendorf	6th	0 %	0 %	5 %	0 %
Jennifer Guerriero	7th	10 %	0 %	5 %	0 %
Michael Goldberg	8th	5 %	0 %	0 %	15 %
Title of paper:	Combination therapy targeting both innate and adaptive immunity improves survival in a pre-clinical model of ovarian cancer				
Status in publication process:	under review				

Having shown that immunotherapy activates both innate and adaptive immune cells, we subsequently sought to investigate the mechanistic pathway and effector cells underlying the enhanced antitumor immune response upon combination therapy. To this end, we treated mice with combination therapy and additionally depleted CD11b$^+$ cells, CD8$^+$ T cells, or CD4$^+$ T cells (Supplementary Fig. 8). Survival studies indicated that only CD4$^+$ T cells are required for antitumor response (Fig. 6A). Mice whose CD4$^+$ T cells had been depleted failed to benefit from combination therapy.

To dissect the cellular and molecular changes among CD4$^+$ T cells after immunotherapy, we harvested leukocytes in the peritoneal cavity after 13 days of combination treatment and assessed their phenotype and function status with a focus on CD4$^+$ T cells. In line with the survival studies, we saw a 3-fold increase in the proportion of CD4$^+$ T cells with combination therapy, while the percentage of CD8$^+$ T cells was unchanged (Fig. 6B). Looking into the

phenotype of these CD4$^+$ T cells, we found that immunotherapy alone or in combination caused a highly significant increase in Th17 cells, as indicated by expression of the transcription factor RORγt (Fig. 6C). Interestingly, the percentage of regulatory FoxP3$^+$ CD4+ T cells among total CD4$^+$ T cells was also significantly increased with combination therapy (Fig. 6C). In contrast, the involvement of T-bet-expressing Th1 cells in mediating antitumor immunity in this model is likely minor, as numbers were found to be low overall and not impacted by combination therapy (Supplementary Fig. 9). The proportion of CD4$^+$ T cells expressing ICOS, CD44, and PD-1 were markedly elevated by immunotherapy, indicating that these cells are antigen-experienced and highly active (Fig. 6D). When looking for cells that could potentially mediate this CD4$^+$ T cell antitumor immunity, we observed a 2.5-fold increase in dendritic cells (Fig. 6E) and in mature dendritic cells (CD11c$^+$MHCII$^+$) (Supplementary Fig. 10).

CD4$^+$ T cells have several means by which to kill cancer cells. It has been previously shown that they can kill cancer cells directly through granzyme-dependent cytotoxic activity[82]. Indeed, combination therapy induces significant expression of GZMB and EOMES by CD4$^+$ T cells, and immunotherapy alone or in combination with chemotherapy increased the proportion of epithelial cancer cells that expressed MHCII (Fig. 6F). These results indicate that CD4$^+$ T cells are essential for extending survival in this model and that antitumor immunity is likely mediated by both Th17 helper cells as well as GZMB$^+$EOMES$^+$ cytotoxic CD4$^+$ T cells.
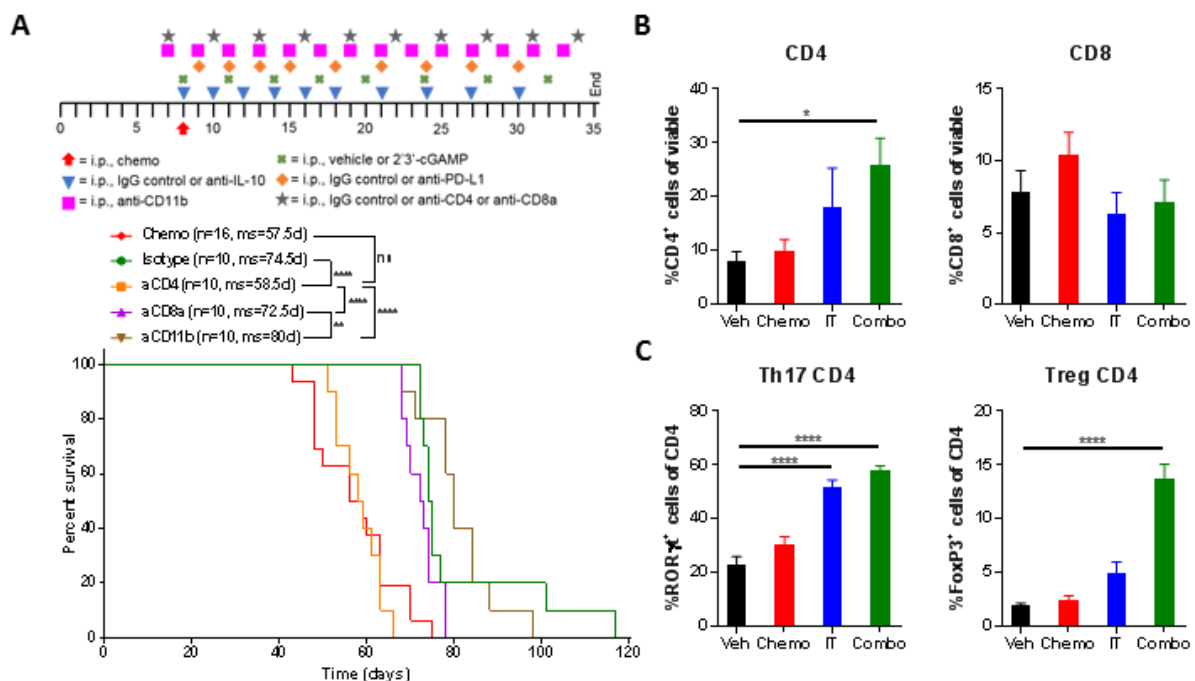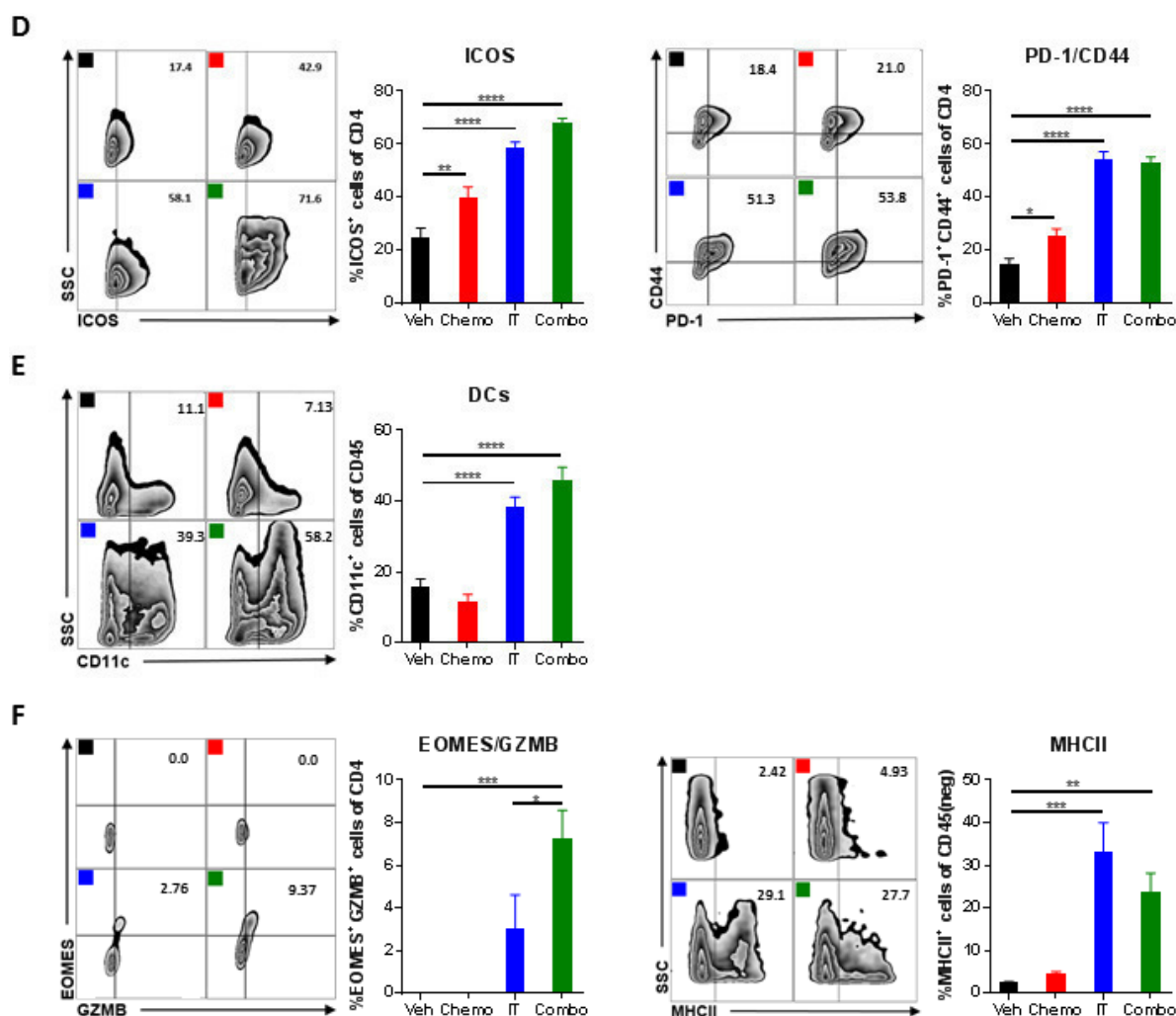
Figure 6. **CD4+ T cells are critical for the efficacy of the combination therapy.** (**A**) Specific immune cell subsets (CD4+ T cells, CD8+ T cells, or CD11b+ cells) were depleted to explore their relative contribution to the observed efficacy. Kaplan-Meier curves are shown for all groups described compared to isotype control. The number of mice per group (n) and median survival (ms) are listed. All experiments were performed twice with n=5 biological replicates. Dosing schedule is shown at the top of the figure. Statistics were calculated using the Log-rank (Mantel-Cox) test. ** $p \leq 0.01$, **** $p \leq 0.0001$. (**B-G**) Peritoneal cell suspensions from tumor-bearing mice treated with vehicle (Veh); chemotherapy (Chemo); anti-IL-10, 2'3'-cGAMP, and anti-PD-L1 immunotherapy (IT); or both Chemo and IT (Combo) were assessed by flow cytometry 13 days after initiation of treatment. (**B**) Bar graphs show quantification of flow cytometry gating of CD4+ and CD8+ T cells. (**C**) Increased numbers of RORγt- and FoxP3-expressing CD4+ T cells are observed with Combo therapy. (**D**) CD4+ T cells expressing activation markers are observed. (**E**) Increased numbers of dendritic cells are observed upon Combo treatment even at this late timepoint. (**F**) Flow cytometry gating of subsets of GZMB expressing CD4+ T cells are shown as scatter plots and quantified at right. MHCII-expression on cancer cells is confirmed. The experiment was performed twice with n=4 biological replicates. Statistics were

calculated using one-way ANOVA with Tukey's multiple comparisons test. Data are presented as mean ± SEM * $p \leq 0.05$, ** $p \leq 0.01$, *** $p \leq 0.001$, **** $p \leq 0.0001$.

4.7. Human ovarian cancer samples exhibit similar immunosuppressive shift after chemotherapy

Author	Author position	Scientific ideas %	Data generation %	Analysis & interpretation %	Paper writing %
Christina Hartl	1st	90 %	100 %	100 %	100 %
Michael Goldberg	8th	10 %	0 %	0 %	0 %
Title of paper:	Combination therapy targeting both innate and adaptive immunity improves survival in a pre-clinical model of ovarian cancer				
Status in publication process:	under review				

In an effort to translate this work into the clinical setting, we obtained matched samples from patients before they received paclitaxel and carboplatin chemotherapy (pre-treatment samples from biopsy) and after chemotherapy (post-treatment samples from surgical resection) (Supplementary Table S1) and analyzed these samples for gene expression changes using Nanostring. While we did not see a shift in genes related to the myeloid compartment, the majority of immune related genes were downregulated after chemotherapy (Fig. 7A). Due to the small number of patient samples available and the high degree of heterogeneity among them, significantly differential gene expression was observed for only nine genes, which were down-regulated by more than 1.5-fold (Fig. 7B). When queried for their biological function using the ToppGene Suit gene list enrichment analysis tool, these mRNAs highly correlated with pattern recognition receptor signaling and the production of type I interferons (Fig. 7C). These results indicate that chemotherapy in ovarian cancer patients severely impedes the antitumor immune reaction.
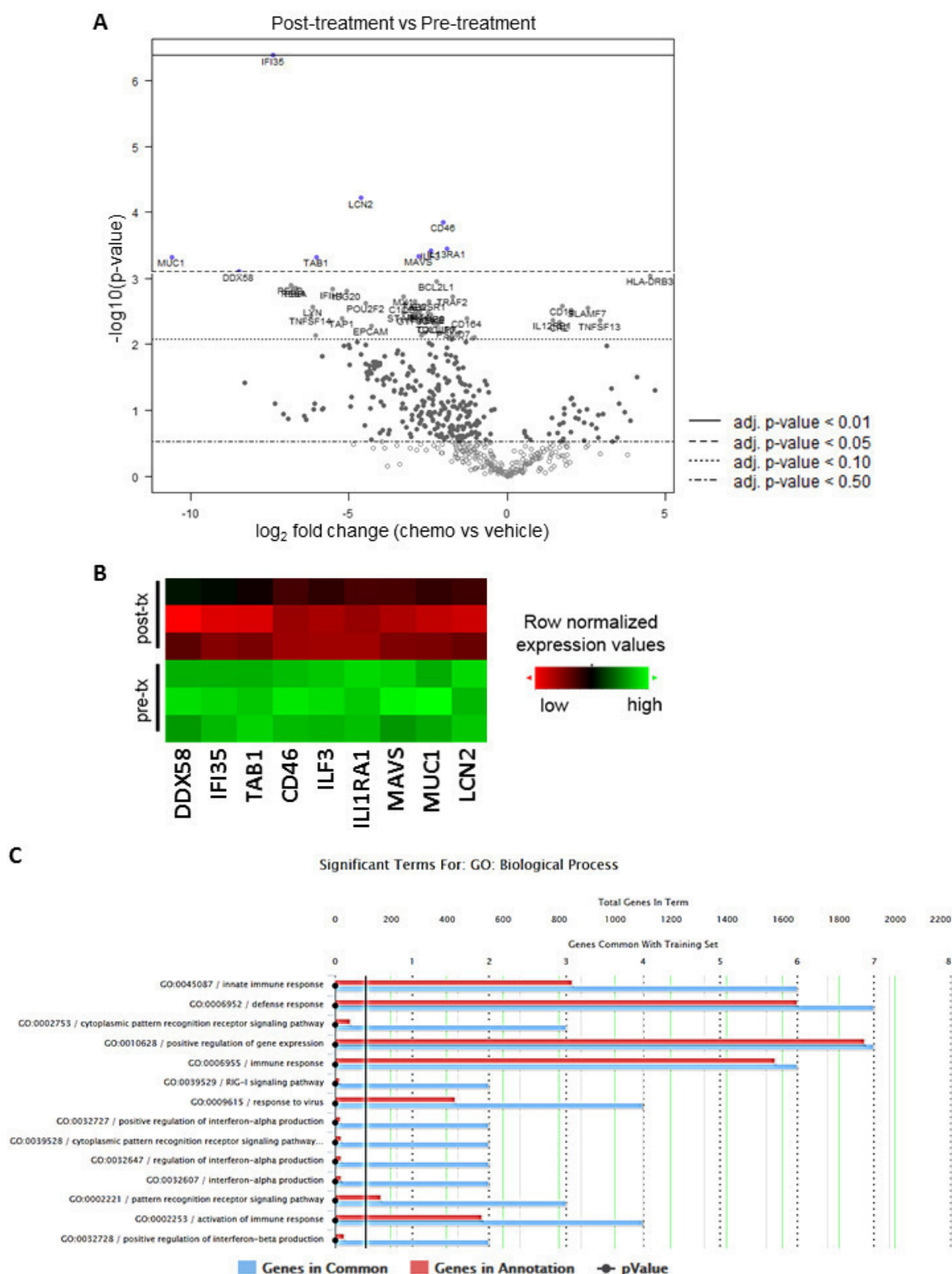
Figure 7. **Human ovarian cancer samples exhibit similar immunosuppressive shift after chemotherapy.** RNA was isolated from matched patient-derived FFPE blocks before treatment with paclitaxel and carboplatin and after chemotherapy and analyzed for gene expression using Nanostring. (**A**) Volcano plot of gene expression data sets derived from matched patient samples. All probe sets are shown. The top 40 differentially expressed genes are named, and highlight coloring was applied to

significantly differentially expressed (adj. p-value < 0.05) probe sets. The experiment was performed once with n=3 biological replicates. (**B**) A heatmap of the top 9 downregulated genes after chemotherapy treatment. (**C**) The 9 significantly downregulated genes after chemotherapy treatment with a fold change ≥ 1.5 were queried for their biological function using the ToppGene Suite gene list enrichment analysis tool.

4.8. Efficacy of this combination therapy is similarly exhibited in a subcutaneous lung cancer model

Author	Author position	Scientific ideas %	Data generation %	Analysis & interpretation %	Paper writing %
Christina Hartl	1st	95 %	100 %	90 %	85 %
Jennifer Guerriero	7th	0 %	0 %	10 %	0 %
Michael Goldberg	8th	5 %	0 %	0 %	15 %
Title of paper:	Combination therapy targeting both innate and adaptive immunity improves survival in a pre-clinical model of ovarian cancer				
Status in publication process:	under review				

To test the efficacy of this new combination therapy in a second solid tumor model, the treatment was administered to mice harboring established Lewis Lung Carcinoma (LLC) tumors. Like ovarian cancer, lung carcinomas are treated with paclitaxel and carboplatin as a standard-of-care in the clinic[83]; however, lung cancer exhibits a different tumor microenvironment, so it was not obvious that the combination would be similarly effective in this context. Tumors were allowed to grow to roughly 100 mm^3 prior to commencement of therapy: paclitaxel and carboplatin (Chemo); anti-IL-10, 2'3'-cGAMP, and anti-PD-L1 immunotherapy (IT); chemotherapy plus immunotherapy (Combo); or control (Vehicle). Tumor volume measurements confirmed that while chemotherapy alone had no influence on tumor growth, immunotherapy alone was able to delay tumor growth, and combination therapy had by far the largest benefit (Fig. 8). These results suggest that the combination treatment of chemotherapy and anti-IL-10, 2'3'-cGAMP, and anti-PD-L1 has the potential to slow tumor growth in aggressive forms of cancer.
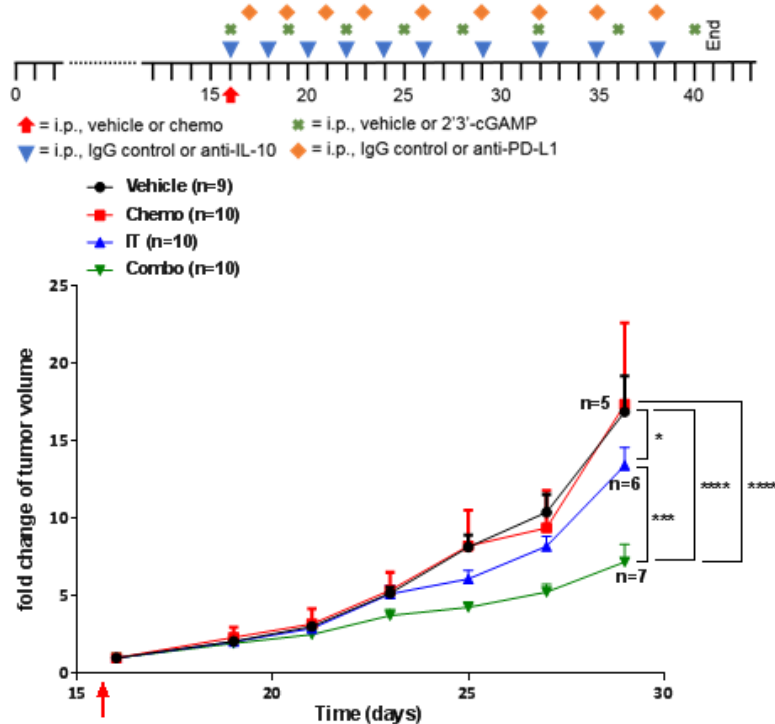
Figure 8. Efficacy of combination therapy is similarly observed in a subcutaneous lung cancer model. Combination therapy was tested in the murine LLC lung cancer model. Tumors were allowed to grow to an average of 100mm^3 per group before initiation of treatment (red arrow). Average fold change of tumor volume of mice treated with combination therapy (Combo), chemotherapy (Chemo) alone, or immunotherapy (IT) alone as well as vehicle only (Vehicle). The number of mice per group (n) are listed. All experiments were performed with biological replicates twice. Statistics were calculated using two-way ANOVA and the Log-rank (Mantel-Cox) test. * $p \leq 0.05$, *** $p \leq 0.001$, **** $p \leq 0.0001$.

5. Discussion

5.1. Combination therapy targeting both innate and adaptive immunity improves survival

In this study, we identified a complementary combination immunotherapy that, when administered together with standard chemotherapy, is able to significantly extend the survival of mice harboring aggressive models of ovarian cancer and lung cancer. The components of the combination were selected based on analysis of gene expression and flow cytometry data. It was further determined that the temporal interplay between chemotherapy and immunotherapy was as important as the components.

To achieve substantial survival benefit in the orthotopic ID8-Vegf-Defb29 ovarian cancer model, we found that chemotherapy had to be complemented by immunomodulators targeting both the innate and adaptive arms of the immune system. As shown in literature and discussed earlier, it has been shown that paclitaxel and carboplatin can be immunostimulatory[84,85]. However, dosing is critical to focus the effects of paclitaxel from purely tumor suppressive to immunostimulatory. While low doses of paclitaxel have shown to enhance early DC maturation through TLR4 signaling and activate CD8$^+$ T cells[86,87], clinical doses of paclitaxel are cytotoxic. Following injection of both cytotoxic compounds in our model, we observed an immunosuppressive shift in the tumor microenvironment, as denoted by an increased myeloid cell population shortly after chemotherapy (Fig. 1).

Immune checkpoint blockade is a powerful means by which to enhance the antitumor activity of T cells, and previous work in murine models of ovarian cancer has demonstrated the efficacy of PD-1 pathway blockade when combined with blockade of another immune checkpoint or with a vaccine[88,89]. Unfortunately, these treatment regimens have not been observed to be similarly effective when translated to patients[90,14,91]. Factors that may account for the differential responses include the inability to recreate the orthotopic tumor microenvironment upon inoculating cancer cells subcutaneously as well as the use of a much less aggressive model that does not recapitulate the clinical setting quite as well. Our approach improves on past research by selecting a more realistic cancer model that is inoculated orthotopically and in line with clinical finding, PD-1 blockade as well as other single immunotherapies show no significant improvement in survival when combined with chemotherapy (Fig. 2).

Ovarian cancer often involves a highly immunosuppressive milieu that includes anti-inflammatory cytokines and often a dearth of effector T cells[92]. Therefore, successful treatment

of ovarian cancer in the clinic may require immunotherapy combinations that are able to stimulate antigen presenting cells, attenuate the immunosuppressive microenvironment, and enhance T cell stimulation and functionality. Consistent with what has been reported from early clinical studies[15], our work shows that PD1 pathway blocking is largely ineffective as monotherapy for treatment of ovarian cancer- (Supplementary Fig. 1B). However, anti-PD-L1 therapy can be highly effective if combined with chemotherapy and other immunotherapies that address the innate arm of the immune system (Fig. 3C,E).

5.2. The importance of the STING pathway

We hypothesize that neutralization of IL-10 in conjunction with production of type I interferons (IFNs) – induced by 2'3'-cGAMP-mediated activation of the STING pathway – reverses the tumor microenvironment from immunosuppressive to immunostimulatory. Typically STING gets activated as a response to detection of cytosolic DNA in the context of antimicrobial immune response (Fig. V). First, cyclic GMP-AMP synthase (cGAS) binds DNA and produces cyclic dinucleotide species – including 2'3'-cGAMP – which activates STING protein. STING then in turn re-localizes from the endoplasmic reticulum (ER) to the Golgi and recruits the kinase TBK1[93]. This leads to phosphorylation of IRF3 and production of type I IFNs and other pro-inflammatory cytokines that boost the immune response[94]. Besides bacterial DNA, DNA-damaging chemotherapy can yield DNA fragments that translocate to the cytosol, where they activate cGAS, leading to production of 2'3'-cGAMP intracellularly[95]. Indeed, in an ovarian cancer model cisplatin led to activation of the cGAS/STING pathway, which in turn boosted tumor immunogenicity by increasing MHC I expression[96]. Furthermore, combination therapy of 2'3'-cGAMP with the DNA damaging chemotherapeutic drug 5-fluorouracil (5-FU) (Li) or radiation therapy[97] showed synergistic anti-tumor effects in models of colon cancer. In our study, chemotherapy and immunotherapy contribute equally to STING activation, as evidenced by increased expression of IRF3 (Fig. 4D). Still, chemotherapy is insufficient to generate meaningful survival benefit, for which combination with immunotherapy is required. Previous work has shown that a majority of ovarian cancer cell lines exhibit a diminished cGAS expression and also impaired cytosolic DNA signaling[98]. Although that study did not test the ID8 cell line, it is possible that it also exhibits a dysfunctional cGAS pathway. Therefore, DNA leakage caused by chemotherapy is likely insufficient in our model and direct STING activation by 2'3'-cGAMP is needed in addition for meaningful induction of immune response.

The STING pathway is an attractive target in immuno-oncology as it can also lead to potent adaptive antitumor response, which is likely mediated by activation of DCs[99]. DCs are shown to depend on STING function *in vivo* to efficiently prime IFN-dependent CD8^{+} T cell responses to tumor antigens[100]. In line with this, our results show that chemotherapy leads to initial activation and maturation of dendritic cells, while immunotherapy drives a significant increase in the number of DCs and maintains their activation (Fig. 4C). In this immunostimulatory environment created by anti-IL-10 and 2'3'-cGAMP, antitumor efficacy of T cells is further improved by the addition of PD-L1 blockade. In fact, recent work in a murine model of *Brca*-deficient ovarian cancer has demonstrated that the STING pathway is required for the T cell-mediated cytotoxicity of PARP inhibitors, which is mediated by DCs[101]. Interestingly, in that study STING activation also synergized with PD-1 checkpoint blockade therapy.
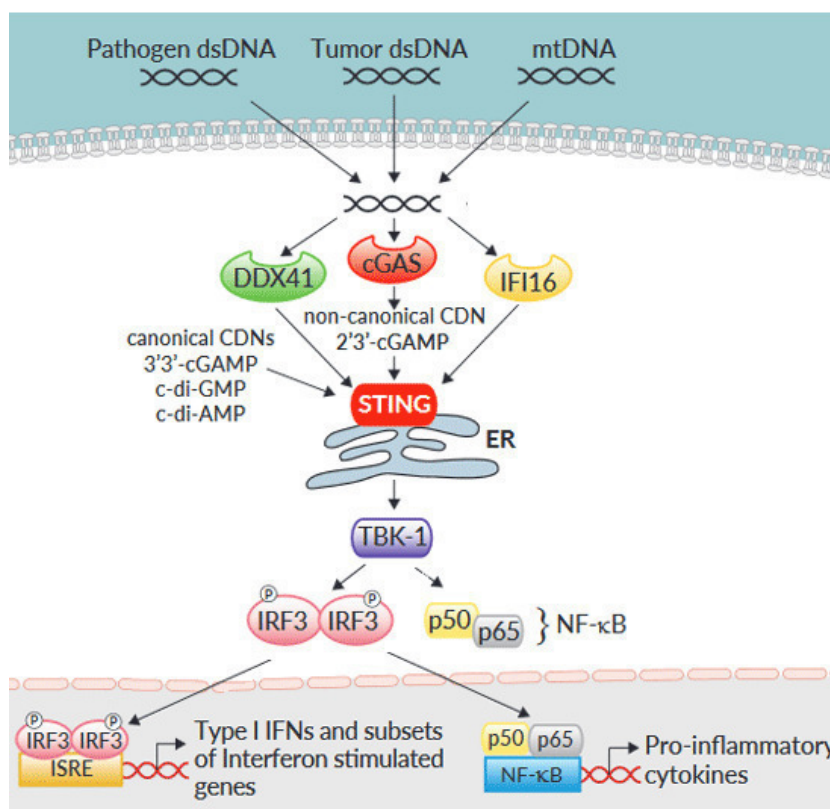
Figure V: The STING signaling pathway. DNA is a pathogen-associated molecular pattern when it is delivered to the host cytoplasm by microbial infection and is a danger-associated molecular pattern when enters the cytoplasm from the nucleus (e.g., through DNA damage), mitochondria or dead cells. Cytosolic DNA binds to and activates cGAS, which catalyzes the synthesis of 2′3′-cGAMP. 2′3′-cGAMP binds to the ER adaptor STING, which traffics to the Golgi apparatus. STING then activates TBK1. TBK1 phosphorylates STING, which in turn recruits IRF3 for phosphorylation by TBK1. Phosphorylated IRF3 dimerizes and then enters the nucleus, where it functions with NF-kB to turn on the expression of type I interferons and other immunomodulatory molecules. Adapted from Invivogen[102].

5.3. CD4+ T cells as mediators of antitumor immunity

Historically, cytotoxic CD8+ T cells have been the main focus of adaptive antitumor therapies to date[103,104,105]. They carry the T cell receptor (TCR) co-receptor CD8, which can recognize cell intrinsic antigens presented via MHC class I molecules on any cell and induce direct killing of infected and malignant cells[106]. However, depletion studies show that CD4+ T cells become the main driver of tumor growth delay in our model (Fig. 6A). We hypothesize that activation and stimulation of CD4+ T cells is mediated by DCs, which in turn get activated by both chemotherapy and immunotherapy. CD4+ T cells – also known as T helper (Th) cells – are crucial to the development of immune responses and for protection against malignancies by recruiting cells of the innate immune system and activating adaptive effector cells[107]. Th cells carry the T cell receptor (TCR) co-receptor CD4, which can recognize antigens bound by the MHC class II complex[108]. Typically, this complex is only expressed on professional APCs and unlike CD8+ T cells, Th cells are known to kill indirectly via secondary effector cells[109,110,111,112]. CD4+ T cells are very diverse and can express a variety of transcription factors that determine their function, phenotype, and capacity for persistence. Using flow cytometry, we determined that combination therapy causes a 3-fold increase in Th17 cells, which are characterized by expression of the transcription factor retinoic acid receptor-related orphan nuclear receptor γ (RORγt) (Fig. 6C) and secretion of IL-17[113].

The role of Th17 cells in antitumor immunity is controversial. Some studies have found early immunosuppressive and tumor promoting effects of Th17 cells[114,115]. However, our results suggest that they are essential for protection against tumor progression. Indeed, it has been found that Th17 cells play an inhibitory role in tumorigenesis[116] and are involved in inflammation and recruitment of innate immunity[117]. Furthermore, they can stimulate CXCL9 and CXCL10 production to recruit effector T cells to the tumor microenvironment and display a great degree of plasticity, rendering them capable of acquiring functional characteristics of Th1 cells in human ovarian cancers[118] (Fig. VI). Th1 cells are characterized by expression of the transcription factor Tbet (T-box transcription factor TBX21) and secret IFNγ and TNFα. In our study, we found no increase in Th1 cells after immunotherapy (Supplementary Fig. 9) and along with that no change in IFNγ expression. Classically, Th1 effector cells were thought to be the most potent CD4+ subpopulation mediating anticancer function[119], but more recent studies revealed that Th17-polarized cells were even more effective than Th1 cells in antitumor immunity against different models of melanoma[120,121]. One key advantage of Th17 cells might be their resistance to senescence mediated by the transcription factor RORγt[122]. Studies using

adoptive therapy have found that even after 3 weeks, Th17 cells do not exhibit hallmarks of senescence or apoptosis and retain robust antitumor efficacy *in vivo* compared to Th1 cells[123]. CD4^{+} T cells acquire a highly antitumor phenotype upon combination therapy, as evidenced by an increased proportion of cells expressing activation markers (ICOS, PD-1, CD44) (Fig. 6D). It has been shown that ICOS expression is critical for development of human Th17 cells and antitumor activity in mesothelioma[124]. CD4^{+} T cells can eliminate cancer cells directly in a perforin/granzyme B-dependent manner or indirectly via secondary effector cells. Notably, 13 days after initiation of combination therapy, far more CD4^{+} T cells express granzyme B and

Figure VI: A proposed model for Th cell subset evolution in antitumor immunity. Th cells can play a central role in tumor rejection by recognizing and killing malignant cells directly. Indirect recognition of tumor-associated antigens can result in the activation of APCs, which in turn are capable of activating cytotoxic CD8^{+} T cells and NK cells. Tumor-specific Th17-polarized cells are plastic and can evolve into t-bet-expressing Th1-like population secreting IFN-γ that can eliminate tumor cells. Th17-polarized cells are closely related to induced-FOXP3^{+} regulatory cells (iTreg), which might negatively influence antitumor immunity. There is a considerable plasticity between iTreg and Th17 cells. Reprinted from Muranski *et al*, 2009[120].

EOMES (Fig. 6F). Together with the upregulation of MHCII^{+} expression on cancer cells, this phenomenon hints at a direct cytotoxic activity for the CD4^{+} T cells. Such functionality has been previously proposed in a model of melanoma, wherein antitumor activity was solely dependent on transferred CD4^{+} T cells[82,108].

As previously described, indirect mechanisms of cancer cell killing induced by CD4^{+} T cells are largely dependent on IFNγ and effector cells like macrophages and/or NK cells[110,112,109]. However, we did not observe increased secretion of IFNγ after combination therapy and our depletion study revealed that delayed tumor growth is independent of CD11b^{+} myeloid cells, which include macrophages. It is likely that NK cells are affected by CD4^{+} T cells, as we see an increase in GZMB expression in CD45^{+}CD3[-]cells, as well as elevated PD-1 expression on NK cells after combination treatment[125,126]. However, the number of NK cells is not increased by immunotherapy and further studies are warranted to confirm the involvement of NK cells.

The data also demonstrate a significant increase in FoxP3^{+} Treg cells with combination therapy. While it has been shown that there is plasticity among naïve FoxP3^{+} Treg cells that are capable of converting into FoxP3^{-} Th17 progenitors in humans[127,128], the immunosuppressive effects of regulatory T cells may be the ultimate cause of the tumors escaping immune surveillance. Future studies will need to address this issue by investigating the role of regulatory T cells in this model. Potentially, the addition of an CTLA-4 antibody that targets these cells could further improve survival.

While past research has often focused predominantly on the immunosuppressive properties of CD4^{+} T cells[129], the data presented herein underline the complexity of CD4^{+} T cell plasticity and support the importance of conducting further research on exploiting the antitumor function of CD4^{+} T cells in immuno-oncology.

5.4. The importance of an optimized dosing schedule

Given the growing numbers of clinicals trials involving combination therapy, our work on the temporal interplay of chemotherapy and immunotherapy is highly relevant. It has been previously reported that paclitaxel and carboplatin chemotherapy augments anti-tumor immunity through a powerful cytotoxic T lymphocyte response and proposed a period of 12-14 days after chemotherapy as the optimal opportunity for T cell-focused immunotherapy[130]. However, that work is mainly based on analysis of *in vitro* cultured T cells isolated from human ovarian cancer patients and this context fails to recapitulate the complex interactions in the

tumor microenvironment and the immunosuppressive influence of myeloid cells. Furthermore, the selection of their measurement timepoints misses the early effects of chemotherapy.

Our work shows that the impact of chemotherapy on the innate immune system is acute and that the benefits of combination therapy are lost when administration of immunotherapy is delayed (Fig. 5C). This finding is consistent with a clinical study in forty patients with advanced ovarian cancer found that administration of immunotherapy on the same day as chemotherapy produced a significantly faster humoral immunity compared to dosing one week after chemotherapy[131]. Overall, the immune responses were stronger and more common and measured parameters favored the schedule with simultaneous immunotherapy and chemotherapy. It therefore stands to reason that immunotherapies targeting the innate immune system should be administered concomitant with chemotherapy.

Still, consistent with the work of Wu *et al.*, our results and unpublished data also show that T cells were not stimulated by chemotherapy during the first 7 days after chemotherapy, hinting that – unlike anti-IL-10 and 2'3'-cGAMP – anti-PD-L1 dosing could be delayed until the T cell compartment is fully primed without compromising survival benefits. The optimal timing of immunotherapy is therefore also dependent on the area of immune activation that is modified. Therapies attenuating the immunosuppressive effects of chemotherapy and boosting DC presentation need to be given earlier, followed by agents promoting T cell priming and differentiation. In contrast, therapies enhancing T cell function and tumor cell lysis should be given after T cell priming is complete and continued throughout treatment to maintain effector T cell activation and prevent exhaustion[132]. Tumor derived immunosuppression persists and grows throughout tumor progression and therapies addressing this should be continued throughout treatment[133].

5.5. Translation of combination therapy into the clinic

A more sequential, serial delivery of immunotherapy could also reduce the likelihood and severity of adverse events (AEs), which have been frequently reported with administration of combination immunotherapy in the clinic[134]. Although we did not detect any toxicity among mice following administration of five different drugs in our study, this will likely be a greater concern among patients. Numerous phase I clinical trials have been conducted using PD-(L)1 blockade. A review assessing the incidence of immune-related AEs found that about 27% of patients develop AEs of any grade during treatment and around 6% of patients develop severe grade AEs[135]. A Phase Ib trial with pembrolizumab specifically in patients with advanced

ovarian cancers reported that treatment-related AEs occurred in 73% of patients but no deaths occurred, and treatment was not discontinued due to AEs[17]. The effects of IL-10 inhibition have not yet been studied in a clinical trial; however, Merck recently published their early data on the use of STING agonist MK-1454 in combination with pembrolizumab in patients with advanced solid tumors. Treatment-related AEs occurred in 23 of 28 (82%) patients and lead to trial discontinuation in 2 (7%) patients. Interestingly, combination immunotherapy leads to partial responses in 25% of patients[136]. Another phase I trial which employed the STING agonist ADU-S100 saw no dose-limiting toxicities when administered alone or in combination with the anti-PD-1 antibody spartalizumab[137]. Overall, most immune-related AEs caused by immunotherapy are reversible and easily managed. Importantly, immune toxicity may be associated with the antitumor response and treatment of AEs has a potential detrimental impact on anticancer efficacy[138].

It is likely that aggressive ovarian cancers which do not respond to combination therapy with chemotherapy and single agent immunotherapy to date will be treated with a combination of several immunotherapies in the future. Currently, a Phase III clinical trial in newly diagnosed advanced ovarian cancer is administering five different drugs, including the standard-of-care chemotherapy carboplatin and paclitaxel, the PARP inhibitor olaparib as well as immunotherapy against VEGFa and PD-L1[139]. Another early combination trial combines cyclophosphamide and fludarabine with adoptive T cell transfer (ACT) and immunotherapies against PD-L1 and IL-2[140].

5.6. Extension of combination therapy to other cancer indications

The fact that the combination of chemotherapy with anti-IL-10, 2'3'-cGAMP, and anti-PD-L1 was effective not only against ovarian cancer, but also against lung cancer (Fig. 8), which presents a completely different tumor microenvironment suggests that this combination approach could potentially be employed in a variety of tumors. Besides lung and ovarian, also cervical and uterine cancers are treated with paclitaxel and carboplatin combination[141,142]. Similar to ovarian cancers, the prognosis of patients with metastatic or relapsed cervical and uterine cancers is poor and novel treatment options are needed as chemotherapy alone is rarely curative. Indeed, in uterine cancers there has been a focus on DC immunotherapies and evidence is emerging that the tumor microenvironment of these cancers is also highly infiltrated with arginase-expressing MDSCs[143]. Our combination therapy could be the optimal therapy to address both DCs and immunosuppression.

In addition to gynecological cancers, there are other tumors which are characterized by the spreading of cancer cells throughout the peritoneal cavity and development of ascites. Metastatic colorectal, stomach, pancreatic, liver, and renal cancers all frequently lead to ascites and combination therapy could prove beneficial in these patients as well[144,145,146,147,148]. Pancreatic cancer specifically is known to evade the host immune surveillance by manipulating immune cells to establish an immunosuppressive tumor microenvironment and similar to ovarian cancer it expresses significantly increased amounts of VEGF[149,150]. Furthermore, monotherapy with immune checkpoint blockade fails to have antitumor effects in pancreatic cancer[151], and current clinical trials also employ a five-drug regimen combining chemotherapy and immunotherapy to improve survival[152]. Combination of chemotherapy with anti-IL-10, 2'3'-cGAMP, and anti-PD-L1 could be a viable alternative in this cancer that has been impervious to past immunotherapies.

5.7. Outlook

This study has made great advancements in understanding the impact of chemotherapy on the tumor microenvironment in ovarian cancer and identified a combination therapy that addresses the immunosuppressive effects of paclitaxel and carboplatin. Cellularly, we found that CD4$^+$ T cell are the main driver of antitumor immunity, but it remains unclear whether this is mediated solely by direct cytotoxicity via GZMB. Using blocking antibodies for GMZB or MHC class II in *ex vivo* studies with CD4$^+$ T cells and MHC class II expressing tumor cells harvested from the peritoneal cavity of combination therapy-treated mice could reveal the importance of direct cytotoxicity. In addition, future work should examine the role of NK cells as potential secondary effector cells in the tumor microenvironment using depletion studies. Flow cytometry could further confirm if NK cells express GZMB and activity against tumor cells should be validated in *ex vivo* cytotoxicity assays. Since indirect killing activity of CD4$^+$ T cells is usually conferred by IFNγ or TNFα[82,108,109], depletion antibodies should be used to uncover their role in antitumor immunity.

We hypothesize that the increased number of Tregs present in the tumor microenvironment after combination therapy prevents long-term efficacy. Since Tregs are characterized by high CTLA4 expression[153], the addition of an anti-CTLA-4 antibody to mediate increased survival should be examined. Furthermore, the significant increase in ICOS expression by CD4$^+$ T cells needs to be further investigated. A previous study that found high expression of ICOS on CD4$^+$

T cell cells after targeted therapy used an ICOS agonist to further increase antitumor activity[154]. It should be examined if this could also be exploited in our model.

Since the STING pathway is gaining more traction in immunotherapy, a closer investigation of the impact of 2'3'-cGAMP on the tumor microenvironment would be helpful. Specifically, analysis of type I IFN upregulation and MHC class I expression via flow cytometry and activation of the NK-κB pathway using western blot. To get an overall picture of the changes in gene expression, we would like to perform a second Nanostring after administration of immunotherapy or combination therapy. Furthermore, the importance of DCs for combination therapy should be confirmed with depletion experiments using CD11c-DTR-GFP transgenic mice, in which DCs can be selectively depletion by diphtheria toxin administration[155]. While our results suggest that DCs are vital for antitumor immunity, another study using the ID8-Vegf-Defb29 ovarian cancer model paradoxically found that DC depletion decreases tumor growth and enhances effect of chemotherapy[156].

A major drawback of the ID8-Vegf-Defb29 ovarian cancer model is the inability to assess intraperitoneal tumor growth other than by total animal weight and ascites development. In order to provide a more reliable measure for the success of immunotherapies, the ID8-Vegf-Defb29 cells could be labelled with a luciferase reporter to measure intraperitoneal growth of cancer cells via *in vivo* imaging system (IVIS). However, luciferase itself can induce a cellular immune response, which could limit tumor growth and reproducibility[157].

For a model that captures spontaneous tumor development in the ovarian epithelium, genetically engineered mouse models (GEMMs) could be used to test the efficacy of this combination. However, while many GEMMs are implemented to study other tumor entities, not many models exist for ovarian cancer yet[158].

In order to analyze the contribution of each immunotherapy to survival increase, survival experiments should be performed combining chemotherapy with anti-IL-10 and 2'3'-cGAMP, anti-IL-10 and anti-PD-L1, or 2'3'-cGAMP and anti-PD-L1. As previously shown, duration of immunotherapy treatment strongly influences outcome. Therefore, survival experiments should be performed in which immunotherapy treatment is extended beyond three weeks. Also, in this context a more sequential delivery of immunotherapy should be tested. Our results suggest that T cells are not getting activated or differentiated in the first 4 days after combination therapy. Thus, it is possible that anti-PD-L1 antibodies are not conferring any benefits in this early phase when T cell exhaustion has not happened yet. In an effort to design a more optimized dosing schedule, anti-IL-10 and 2'3'-cGAMP could be administered concomitant with chemotherapy,

while anti-PD-L1 administration is delayed, extended beyond three weeks, and potentially supplemented at a later time by anti-CTLA-4 and/or an ICOS agonist.

Our human data mostly confirms immunosuppression after chemotherapy in ovarian cancer, but the low number of samples limits the strength of our findings. Ideally, we could perform gene expression analysis and flow cytometry on a much larger cohort of matched pre- and post-treatment patient samples.

Finally, we are proposing to repeat combination therapy with subclinical doses of paclitaxel and carboplatin. Conventionally, chemotherapy is designed to kill rapidly dividing cells and it is often administered at the highest dose possible without causing life-threatening side effects[159]. New studies are suggesting that this is counterproductive to the anti-angiogenic and immune modulatory effects of many chemotherapies[160]. With the broader application of cancer immunotherapy, low-dose metronomic chemotherapy should become a crucial alternative to conventional chemotherapy[161].

5.8. Conclusion

In conclusion, we found a combination treatment of chemotherapy and immunotherapy that markedly prolongs survival in murine models of ovarian and lung cancer. The use of anti-IL-10, 2'3'-cGAMP, and anti-PD-L1 engages both the innate and adaptive arms of the immune system. Thereby, immunotherapy counteracts the immunosuppressive shift mediated by the myeloid cell population while chemotherapy effectively activated dendritic cells. Together, they increase the expression of pro-inflammatory molecules as well as the numbers of activated T cells and mature dendritic cells. The data indicate that survival benefit is strongly dependent on a mechanistically informed dosing schedule. On a cellular level, Th17 CD4+ T cells appear to be particularly important, and their effects are thought to be mostly mediated directly via GZMB. We verified that chemotherapy also downregulates the immune system of the tumor microenvironment in the clinical setting using human samples of advanced ovarian cancers. We believe that these data support the utility of clinical trials for ovarian cancer patients that combine immunotherapies that target both innate and adaptive immunity. As importantly, they underscore the importance of tumor-reactive CD4+ T cells in mediating anti-tumor immunity. Finally, the complete loss of efficacy upon delayed or abbreviated administration of the immunotherapies highlights the need to be thoughtful about dosing regimens in the clinic.

6. References

1. Bray F, Ferlay J, Soerjomataram I, Siegel RL, Torre LA, et al. Global cancer statistics 2018: GLOBOCAN estimates of incidence and mortality worldwide for 36 cancers in 185 countries. CA Cancer J Clin. 2018;68(6):394-424.

2. ACS. Cancer facts & figures. American Cancer Society, 2018.

3. ORCFA. Statistics. Ovarian Cancer Research Fund Alliance, 2018.

4. MayoClinic: ovarian cancer. https://www.mayoclinic.org/diseases-conditions/ovarian-cancer/ symptoms-causes/syc-20375941. Accessed 01 February 2019.

5. Kroeger PT & Drapkin R. Pathogenesis and heterogeneity of ovarian cancer. Curr Opin Obstet Gynecol. 2016;29(1):26-34.

6. du Bois A, Luck HJ, Bauknecht T, Mobus V, Bochtler H, Diergarten K, et al. Phase I/II study of the combination of carboplatin and paclitaxel as first-line chemotherapy in patients with advanced epithelial ovarian cancer. Ann Oncol. 1997;8:355–361.

7. Hennessy BT, Coleman RL, Markman M. Ovarian cancer. Lancet. 2009;374:1371.

8. Heintz AP, Odicino F, Maisonneuve P, et al. Carcinoma of the ovary. FIGO 26th annual report on the results of treatment in gynecological cancer. Int J Gynaecol Obstet. 2006;95:S161–S192.

9. Ozga M, Aghajanian C, Myers-Virtue S, McDonnell G, Jhanwar S, Hichenberg S, Sulimanoff I. A systematic review of ovarian cancer and fear of recurrence. Palliat Support Care. 2015;13:1771-1780.

10. Luvero D, Milani A, Ledermann JA. Treatment options in recurrent ovarian cancer: latest evidence and clinical potential. Ther Adv Med Oncol. 2014;6(5):229-39.

11. Sato E, Olson SH, Ahn J, Bundy B, Nishikawa H, Qian F, Jungbluth AA, Frosina D, Gnjatic S, Ambrosone C, et al. Intraepithelial CD8+ tumor-infiltrating lymphocytes and a high CD8+/regulatory T cell ratio are associated with favorable prognosis in ovarian cancer. Proc Natl Acad Sci U S A. 2005;102:18538–18543.

12. Zhang L, et al. Intratumoral T cells, recurrence, and survival in epithelial ovarian cancer. N Engl J Med. 2003;348(3):203–213.

13. Kandalaft L E, Powell DJ, Singh N, Coukos G. Immunotherapy for ovarian cancer: what's next? J Clin Oncol. 2011;29:925-933.

14. Brahmer JR, Tykodi SS, Chow LQ, Hwu WJ, Topalian SL, Hwu P, Drake CG, Camacho LH, Kauh J, Odunsi K, Pitot HC, Hamid O, Bhatia S, Martins R, Eaton K, Chen S, Salay TM, Alaparthy S, Grosso JF, Korman AJ, Parker SM, Agrawal S, Goldberg SM, Pardoll DM, Gupta A, Wigginton JM. Safety and activity of anti-PD-L1 antibody in patients with advanced cancer. N Engl J Med. 2012;366:2455–2465.

15. Hamanishi J, Mandai M, Ikeda T, et al. Safety and antitumor activity of anti-PD-1 antibody, nivolumab, in patients with platinum-resistant ovarian cancer. J Clin Oncol. 2015;33:4015–4022

16. Disis ML, Taylor MH, Kelly K, et al. Efficacy and safety of avelumab for patients with recurrent or refractory ovarian cancer: phase 1b results from the JAVELIN solid tumor trial. JAMA Oncol. 2019 [Epub ahead of print].

17. Varga A, Piha-Paul SA, Ott PA, et al. Pembrolizumab in patients with programmed death ligand 1-positive advanced ovarian cancer: analysis of KEYNOTE-028. Gynecol Oncol. 2018;S0090-8258(18):31418-5.

18. Odunsi K. Immunotherapy in ovarian cancer. Ann Oncol. 2017;28(suppl_8):viii1-viii7.

19. Bracci L, Schiavoni G, Sistigu A & Belardelli F. Immune-based mechanisms of cytotoxic chemotherapy: implications for the design of novel and rationale-based combined treatments against cancer. Cell Death Differ. 2014;21:15-25.

20. Peng J, Hamanishi J, Matsumura N, et al. Chemotherapy induces programmed cell death-ligand 1 overexpression via the nuclear factor-kappab to foster an immunosuppressive tumor microenvironment in ovarian cancer. Cancer Res 2015;75:5034–5045.

21. Kampan NC, Madondo MT, McNally OM, et al. Paclitaxel and its evolving role in the management of ovarian cancer. Biomed Res Int 2015;413076:18–21.

22. de Biasi AR, Villena-Vargas J, Adusumilli PS. Cisplatin-induced antitumor immunomodulation: a review of preclinical and clinical evidence. Clin Cancer Res. 2014;20(21):5384-5391.

23. Chan OT & Yang LX. The immunological effects of taxanes. Cancer Immunol Immunother. 2000;49(4–5):181–185.

24. Chang CL, Hsu YT, Wu CC, et al. Dose-dense chemotherapy improves mechanisms of antitumor immune response. Cancer Res 2013;73:119–127.

25. Khairallah AS, Genestie C, Auguste A, Leary A. Impact of neoadjuvant chemotherapy on the immune microenvironment in advanced epithelial ovarian cancer: prognostic and therapeutic implications. Int J Cancer. 2018;143:8-15.

26. Langer CJ, Gadgeel SM, Borghaei H, et al. Carboplatin and pemetrexed with or without pembrolizumab for advanced, non-squamous non-small-cell lung cancer: a randomised, phase 2 cohort of the open-label KEYNOTE-021 study. Lancet Oncol. 2016;17:1497-1508.

27. Schmid P, Adams S, Rugo HS, Schneeweiss A, Barrios CH, Iwata H, et al. Atezolizumab and nab-paclitaxel in advanced triple-negative breast cancer. N Engl J Med. 2018;379:2108-2121.

28. Pakish JB & Jazaeri AA. Immunotherapy in gynecologic cancers: are we there yet?. Curr Treat Options Oncol. 2017;18(10):59.

29. Pfizer press release details https://investors.pfizer.com/investor-news/press-release-details/2018/Merck-KGaA-Darmstadt-Germany-and-Pfizer-Provide-Update-on-Avelumab-in-Platinum-Resistant-Refractory-Ovarian-Cancer/default.aspx. Accessed 05 February 2019.

30. Kreuzinger C, Geroldinger A, Smeets D, Braicu EI, Sehouli J, et al. A complex network of tumor microenvironment in human high-grade serous ovarian cancer. Clin Cancer Res. 2017;23:7621–7632.

31. Sharma P & Allison JP. Immune checkpoint targeting in cancer therapy: toward combination strategies with curative potential. *Cell*. 2015;161(2):205-214.

32. Landskron J, Helland Ø, Torgersen KM, Aandahl EM, Gjertsen BT, Bjørge L, Taskén K. Activated regulatory and memory T-cells accumulate in malignant ascites from ovarian carcinoma patients. Cancer Immunol Immunother. 2015;64:337–347.

33. Sehouli J, Loddenkemper C, Cornu T, et al. Epigenetic quantification of tumor-infiltrating T-lymphocytes. Epigenetics. 2011;6(2):236-246.

34. Redjimi N, Raffin C, Raimbaud I, Pignon P, Matsuzaki J, Odunsi K, et al. CXCR3+ T regulatory cells selectively accumulate in human ovarian carcinomas to limit type I immunity. Cancer Res. 2012;72(17):4351–4360.

35. Kryczek I, Liu R, Wang G, Wu K, Shu X, Szeliga W, et al. FOXP3 defines regulatory T cells in human tumor and autoimmune disease. Cancer Res. (2009) 69:3995–4000.

36. Mittal SK & Roche PA. Suppression of antigen presentation by IL-10. Curr Opin Immunol. 2015;34:22-27.

37. Lamichhane P, Karyampudi L, Shreeder B, et al. IL10 release upon PD-1 blockade sustains immunosuppression in ovarian cancer. Cancer Res. 2017;77(23):6667-6678.

References

38. Ruffell B, Chang-Strachan D, Chan V, Rosenbusch A, Ho CMT, Pryer N, Daniel D, Hwang ES, Rugo HS and Coussens LM. Macrophage IL-10 blocks CD8+ T cell-dependent responses to chemotherapy by suppressing IL-12 expression in intratumoral dendritic cells. Cancer Cell 2014;26:623-637.

39. Hart KM, Byrne KT, Molloy MJ, Usherwood EM, Berwin B. IL-10 immunomodulation of myeloid cells regulates a murine model of ovarian cancer. Front Immunol. 2011;2:29.

40. Khan AN, Kolomeyevskaya N, Singel KL, et al. Targeting myeloid cells in the tumor microenvironment enhances vaccine efficacy in murine epithelial ovarian cancer. Oncotarget. 2015;6(13):11310-11326.

41. Webb JR, Milne K, Kroeger DR, et al. PD-L1 expression is associated with tumor-infiltrating T cells and favorable prognosis in high-grade serous ovarian cancer. Gynecol Oncol 2016;141:293–302.

42. Qian F, Villella J, Wallace PK, Mhawech-Fauceglia P, Tario JD, Andrews C, Matsuzaki J, Valmori D, Ayyoub M, Frederick PJ. Efficacy of levo-1-methyl tryptophan and dextro-1-methyl tryptophan in reversing indoleamine-2, 3-dioxygenase–mediated arrest of T-cell proliferation in human epithelial ovarian cancer. Cancer Res. 2009;69:5498–5504.

43. Rodriguez PC, Ochoa AC. Arginine regulation by myeloid derived suppressor cells and tolerance in cancer: mechanisms and therapeutic perspectives. Immunol Rev. 2008;222:180–191.

44. Aust S, Felix S, Auer K, et al. Absence of PD-L1 on tumor cells is associated with reduced MHC I expression and PD-L1 expression increases in recurrent serous ovarian cancer. Sci Rep. 2017;7:42929.

45. Darb-Esfahani S, Kunze CA, Kulbe H, et al. Prognostic impact of programmed cell death-1 (PD-1) and PD-ligand 1 (PD-L1) expression in cancer cells and tumor-infiltrating lymphocytes in ovarian high grade serous carcinoma. Oncotarget. 2015;7(2):1486-1499.

46. Gerhardt H, Golding M, Fruttiger M, et al. VEGF guides angiogenic sprouting utilizing endothelial tip cell filopodia. J Cell Biol. 2003;161(6):1163-1177.

47. Zebrowski BK, Liu W, Ramirez K, Akagi Y, Mills GB, Ellis LM. Markedly elevated levels of vascular endothelial growth factor in malignant ascites. Ann Surg Oncol. 1999;6:373–378.

48. Rudlowski C, Pickart A-K, Fuhljahn C, Friepoertner T, Schlehe B, Biesterfeld S, and Schroeder W. Prognostic significance of vascular endothelial growth factor expression in ovarian cancer patients: a long-term follow-up. Int J Gynecol Cancer. 2006;16:183-189.

49. Worzfeld T, Pogge von Strandmann E, Huber M, et al. The unique molecular and cellular microenvironment of ovarian cancer. Front Oncol. 2017;7:24.

50. Ueda M, Terai Y, Kumagai K, Ueki K, Yamaguchi H, Akise D, et al. Vascular endothelial growth factor c gene expression is closely related to invasion phenotype in gynecological tumor cells. Gynecol Oncol. 2001;82:162–166.

51. Cimpean AM, Cobec IM, Ceaușu RA, Popescu R, Tudor A, Raica M. Platelet derived growth factor bb: a "must-have" therapeutic target "redivivus" in ovarian cancer. Cancer Genomics Proteomics. 2016;13(6):511-517.

52. Kamat AA, Fletcher M, Gruman LM, et al. The clinical relevance of stromal matrix metalloproteinase expression in ovarian cancer. Clin Cancer Res. 2006;12(6):1707-1714.

53. Davies EJ, Blackhall FH, Shanks JH, David G, McGown AT, Swindell R, et al. Distribution and clinical significance of heparan sulfate proteoglycans in ovarian cancer. Clin Cancer Res. 2004;10:5178–5186.

54. Roby KF, Taylor CC, Sweetwood JP, Cheng Y, Pace JL, Tawfik O, Persons DL, Smith PG, Terranova PF. Development of a syngeneic mouse model for events related to ovarian cancer. Carcinogenesis. 2000;21(4):585–591.

55. Zhang L, Yang N, Garcia JR, Mohamed A, Benencia F, Rubin SC, et al. Generation of a syngeneic mouse model to study the effects of vascular endothelial growth factor in ovarian carcinoma. Am J Pathol. 2002;161:2295–2309.

56. Ohm JE & Carbone DP. Vegf as a mediator of tumor-associated immunodeficiency. Immunol Res. 2001;23:263–272.

57. Gabrilovich DI, et al. Production of vascular endothelial growth factor by human tumors inhibits the functional maturation of dendritic cells. Nat Med. 1996;2:1096–1103.

58. Yang D, et al. β-defensins: linking innate and adaptive immunity through dendritic and T cell CCR6. Science. 1999:286:525–528.

59. Su F, Kozak KR, Imaizumi S, et al. Apolipoprotein A-I (apoA-I) and apoA-I mimetic peptides inhibit tumor development in a mouse model of ovarian cancer. Proc Natl Acad Sci U S A. 2010;107(46):19997-20002.

60. Cho S, Sun Y, Soisson AP, Dodson MK, Peterson CM, Jarboe EA, et al. Characterization and evaluation of pre-clinical suitability of a syngeneic orthotopic mouse ovarian cancer model. Anticancer Res. 2013;33:1317–1324.

References

61. Conejo-Garcia JR, Benencia F, Courreges MC, Kang E, Mohamed-Hadley A, Buckanovich RJ, et al. Tumor-infiltrating dendritic cell precursors recruited by a beta-defensin contribute to vasculogenesis under the influence of Vegf-A. Nat Med. 2004;10:950–958.

62. Fong MY & Kakar SS. Ovarian cancer mouse models: a summary of current models and their limitations. J Ovarian Res. 2009;2(1):12.

63. Hernandez L, Kim MK, Lyle LT, et al. Characterization of ovarian cancer cell lines as in vivo models for preclinical studies. Gynecol Oncol. 2016;142(2):332-430.

64. Geiss GK, Bumgarner RE, Birditt B, Dahl T, Dowidar N, Dunaway DL, et al. Direct multiplexed measurement of gene expression with color-coded probe pairs. Nat Biotechnol. 2008;26:317–325.

65. Vandesompele J, De Preter K, Pattyn F, et al. Accurate normalization of real-time quantitative RT-PCR data by geometric averaging of multiple internal control genes. Genome Biol. 2002;3(7):Research0034.

66. Cubillos-Ruiz JR, Benencia F, Courreges M-C, Kang E, Mohamed-Hadley A, Buckanovich R J, Holtz D O, Jenkins A, Na H, Zhang L, Wagner D S, Katsaros D, Caroll R & Coukos G. Tumor-infiltrating dendritic cell precursors recruited by a β-defensin contribute to vasculogenesis under the influence of Vegf-A. Nature Medicine 2004;10:950–958.

67. Bronte V & Zanovello P. Regulation of immune responses by L-arginine metabolism. Nat Rev Immunol. 2005;5:641–654.

68. Oberli MA, Reichmuth AM, Dorkin JR, et al. Lipid nanoparticle assisted mRNA delivery for potent cancer immunotherapy. Nano Lett. 2016;17(3):1326-1335.

69. Newlaczyl AU & Yu LG. Galectin-3–a jack-of-all-trades in cancer. Cancer Lett. 2011;313:123-128.

70. de Oliveira FL, Gatto M, Bassi N, et al. Galectin-3 in autoimmunity and autoimmune diseases. Exp Biol Med. 2015;240(8):1019-1028.

71. Wong RM, Scotland RR, Lau RL, Wang C, Korman AJ, Kast WM, et al. Programmed death-1 blockade enhances expansion and functional capacity of human melanoma antigen-specific CTLs. Int Immunol. 2007;19(10):1223–1234.

72. Long AH, Haso WM, Shern JF, Wanhainen KM, Murgai M, Ingaramo M, et al. 4-1BB costimulation ameliorates T cell exhaustion induced by tonic signaling of chimeric antigen receptors. Nat Med. 2015;21:581–590.

73. Weigelin B, Bolaños E, Teijeira A, et al. Focusing and sustaining the antitumor CTL effector killer response by agonist anti-CD137 mAb. *Proc Natl Acad Sci U S A*. 2015;112(24):7551-6.

74. Mony JT, et al. Anti-PD-L1 prolongs survival and triggers T cell but not humoral anti-tumor immune responses in a human MUC1-expressing preclinical ovarian cancer model. Cancer immunology, immunotherapy CII. 2015;64:1095–1108.

75. Funasaka T, Raz A, Nangia-Makker P. Galectin-3 in angiogenesis and metastasis. Glycobiology 2014;24:886–891.

76. Lane D, Matte I, Garde-Granger P, Bessette P, Piché A. Ascites IL-10 promotes ovarian cancer cell migration. Cancer Microenviron. 2018;11(2-3):115-124.

77. Eriksson E, Wenthe J, Irenaeus S, Loskog A, Ullenhag G. Gemcitabine reduces MDSCs, tregs and TGFβ-1 while restoring the teff/treg ratio in patients with pancreatic cancer. J Transl Med. 2016;14:282.

78. Zhang X, et al. Cyclic GMP-AMP containing mixed phosphodiester linkages is an endogenous high-affinity ligand for STING. Mol Cell 2013;51:226-235.

79. Liu S, Cai X, Wu J, Cong Q, Chen X, et al. Phosphorylation of innate immune adaptor proteins MAVS, STING, and TRIF induces IRF3 activation. Science 2015;347:2630.

80. Li T, Cheng H, Yuan H, Xu Q, Shu C, Zhang Y, Xu P, Tan J, Rui Y, Li P, Tan X. Antitumor activity of cGAMP via stimulation of cGAS-cGAMP-STING-IRF3 mediated innate immune response. Scientific Reports. 2016;6:19049.

81. Siegel RL, Miller KD, Jemal A, Cancer statistics 2017. CA Cancer J Clin. 2017;67:7-30.

82. Quezada SA, Simpson TR, Peggs KS, Merghoub T, Vider J, Fan X, Blasberg R, Yagita H, Muranski P, Antony PA, et al. Tumor-reactive CD4(+) T cells develop cytotoxic activity and eradicate large established melanoma after transfer into lymphopenic hosts. J Exp Med. 2010;207:637-650.

83. Rozzi A, Nardoni C, Corona M, Restuccia MR, Falbo T, Lanzetta G. Weekly regimen of paclitaxel and carboplatin as first-line chemotherapy in elderly patients with stage IIIB-IV non small cell lung cancer (NSCLC): Results of a phase II study. J. Chemother. 2010;22:419–423.

84. Javeed A, Ashraf M, Riaz A, Ghafoor A., Afzal S, Mukhtar MM. Paclitaxel and immune system. Eur J Pharm Sci. 2009;38:283–290.

85. Machiels J-PH, Reilly RT, Emens LA, Ercolini AM, Lei RY, Weintraub D, Okoye FI, Jaffee EM. Cyclophosphamide, doxorubicin, and paclitaxel enhance the antitumor immune response of granulocyte/macrophage-colony stimulating factor-secreting whole-cell vaccines in HER-2/neu tolerized mice. Cancer Res. 2001;61(9):3689-3697.

86. Pfannenstiel LW, Lam SS, Emens LA, Jaffee EM, Armstrong TD. Paclitaxel enhances early dendritic cell maturation and function through TLR4 signaling in mice. Cell Immunol. 2010;263(1):79–87.

87. Hsu FT, Chen TC, Chuang HY, Chang YF, Hwang JJ. Enhancement of adoptive T cell transfer with single low dose pretreatment of doxorubicin or paclitaxel in mice. Oncotarget. 2015;6(42):44134-44150.

88. Duraiswamy J, Kaluza KM, Freeman GJ, Coukos G. Dual blockade of PD-1 and CTLA-4 combined with tumor vaccine effectively restores T-cell rejection function in tumors. Cancer Res. 2013;73(12):3591–3603.

89. Duraiswamy J, Freeman GJ, Coukos G. Therapeutic PD-1 pathway blockade augments with other modalities of immunotherapy T-cell function to prevent immune decline in ovarian cancer. Cancer Res. 2013;73:6900–6912.

90. Hodi FS, Butler M, Oble DA, et al. Immunologic and clinical effects of antibody blockade of cytotoxic T lymphocyte-associated antigen 4 in previously vaccinated cancer patients. Proc Natl Acad Sci U S A. 2008;105(8):3005-3010.

91. Diefenbach CSM, Gnjatic S, Sabbatini P, Aghajanian C, Hensley ML, Spriggs DR, Iasonos A, Lee H, Dupont B, Pezzulli S, et al. Safety and immunogenicity study of NY-ESO-1b peptide and montanide ISA-51 vaccination of patients with epithelial ovarian cancer in high-risk first remission. Clin Cancer Res. 2008;14:2740–2748.

92. Preston CC, Goode EL, Hartmann LC, Kalli KR, Knutson KL. Immunity and immune suppression in human ovarian cancer. Immunotherapy. 2011;3(4):539-556.

93. Tanaka Y & Chen ZJ. STING specifies IRF3 phosphorylation by TBK1 in the cytosolic DNA signaling pathway. Sci Signal. 2012;5(214):ra20.

94. Bose D. cGAS/STING pathway in cancer: Jekyll and Hyde story of cancer immune response. Int J Mol Sci. 2017;18(11):2456.

95. Harding SM, Benci JL, Irianto J, Discher DE, Minn AJ, Greenberg RA. Mitotic progression following DNA damage enables pattern recognition within micronuclei. Nature. 2017;548:466–470.

96. Grabosch S, Bulatovic M, Zeng F, Ma T, Zhang L, Ross M, Brozick J, Fang Y, et al. Cisplatin-induced immune modulation in ovarian cancer mouse models with distinct inflammation profiles. Oncogene. 2018 [Epub ahead of print].

97. Deng L, Liang H, Xu M, et al. STING-dependent cytosolic DNA sensing promotes radiation-induced type I interferon-dependent antitumor immunity in immunogenic tumors. Immunity. 2014;41(5):843-852.

98. De Queiroz NMGP, Xia T, Konno H, Barber GN. Ovarian cancer cells commonly exhibit defective STING signaling which affects sensitivity to viral oncolysis. Mol Cancer Res. 2018 [Epub ahead of print].

99. Barber GN. STING: infection, inflammation and cancer. Nat Rev Immunol. 2015;15(12):760-770.

100. Klarquist J, Hennies CM, Lehn MA, Reboulet RA, Feau S, Janssen EM. STING-mediated DNA sensing promotes antitumor and autoimmune responses to dying cells. J Immunol. 2014;193(12):6124-6134.

101. Ding L, Kim HJ, Wang Q, Kearns M, Jiang T, Ohlson CE, Li BB, Xie S, Liu FJ, Stover EH, Howitt BE, Bronson RT, Lazo S, Roberts TM, Freeman GJ, Konstantinopoulos P, Matulonis UA, Zhao JJ. PARP inhibition elicits STING-dependent antitumor immunity in Brca1-deficient ovarian cancer. Cell Rep. 2018;25(11):2972-2980.

102. InvivoGen infocus: follow the path to STING. https://www.invivogen.com/sites/default/files/ invivogen/resources/documents/invivogen-infocus-sting-2018.pdf. Accessed 07 February 2019.

103. Pardoll DM & Topalian SL. The role of CD4+ T cell responses in antitumor immunity. Curr Opinion Immunol. 1998;10:588–594.

104. Reiser J & Banerjee A. Effector, memory, and dysfunctional CD8(+) T cell fates in the antitumor immune response. J Immunol Res. 2016;2016:8941260.

105. Dovedi SJ, Lipowska-Bhalla G, Beers SA, et al. Antitumor efficacy of radiation plus immunotherapy depends upon dendritic cell activation of effector CD8+ T cells. Cancer Immunol Res. 2016;4(7):621-630.

106. Dockree T, Holland CJ, Clement M, et al. CD8+ T-cell specificity is compromised at a defined MHCI/CD8 affinity threshold. Immunol Cell Biol. 2016;95(1):68-76.

107. Knutson KL & Disis ML. Tumor antigen-specific T helper cells in cancer immunity and immunotherapy. Cancer Immunol Immun. 2005;54:721–728.

References

108. Haabeth OA, Tveita AA, Fauskanger M, Schjesvold F, Lorvik KB, Hofgaard PO, et al. How do CD4(+) T cells detect and eliminate tumor cells that either lack or express MHC class II molecules? Front Immunol. 2014;5:174.

109. Perez-Diez A, Joncker NT, Choi K, et al. CD4 cells can be more efficient at tumor rejection than CD8 cells. Blood. 2007;109(12):5346-5354.

110. Mumberg D, Monach PA, Wanderling S, et al. CD4(+) T cells eliminate MHC class II-negative cancer cells in vivo by indirect effects of IFN-gamma. Proc Natl Acad Sci U S A. 1999;96(15):8633-8638.

111. Hung K, Hayashi R, Lafond-Walker A, Lowenstein C, Pardoll D, Levitsky H. The central role of CD4(+) T cells in the antitumor immune response. J Exp Med. 1998;188(12):2357-2368.

112. Corthay A, Skovseth DK, Lundin KU, Røsjø E, Omholt H, Hofgaard PO, et al. Primary antitumor immune response mediated by CD4+ T cells. Immunity. 2005;22:371–383.

113. Muranski P & Restifo NP. Essentials of Th17 cell commitment and plasticity. Blood. 2013;121(13):2402–2414.

114. Guéry L & Hugues S. Th17 cell plasticity and functions in cancer immunity. Biomed Res Int. 2015;2015:314620.

115. Asadzadeh Z, Mohammadi H, Safarzadeh E, Hemmatzadeh M, Mahdian-Shakib A, Jadidi-Niaragh F, Azizi G, Baradaran B. The paradox of Th17 cell functions in tumor immunity. Cell Immunol. 2017;322:15–25.

116. Tong Z, Yang XO, Yan H, et al. A protective role by interleukin-17F in colon tumorigenesis. PLoS One. 2012;7(4):e34959.

117. Wilson NJ, Boniface K, Chan JR, McKenzie BS, Blumenschein WM, Mattson JD, Basham B, Smith K, Chen T, Morel F, et al. Development, cytokine profile and function of human interleukin 17-producing helper T cells. Nat Immunol. 2007;8:950–957.

118. Kryczek I, Banerjee M, Cheng P, Vatan L, Szeliga W, Wei S, et al. Phenotype, distribution, generation, and functional and clinical relevance of Th17 cells in the human tumor environments. Blood. 2009;114:1141–1149.

119. Nishimura T, et al. The critical role of Th1-dominant immunity in tumor immunology. Cancer Chemother Pharmacol. 2000;46(Suppl):S52–S61.

120. Muranski P & Restifo NP. Adoptive immunotherapy of cancer using CD4+ T cells. Curr Opin Immunol. 2009;21:200–208.

121. Martin-Orozco N, Muranski P, Chung Y, et al. T helper 17 cells promote cytotoxic T cell activation in tumor immunity. Immunity. 2009;31(5):787-798.

122. He YW, Deftos ML, Ojala EW, Bevan MJ. RORgamma t, a novel isoform of an orphan receptor, negatively regulates Fas ligand expression and IL-2 production in T cells. Immunity. 1998;9(6):797-806.

123. Bowers JS, Nelson MH, Majchrzak K, et al. Th17 cells are refractory to senescence and retain robust antitumor activity after long-term ex vivo expansion. JCI Insight. 2017;2(5):e90772. Published 2017 Mar 9. doi:10.1172/jci.insight.90772

124. Paulos CM, Carpenito C, Plesa G, et al. The inducible costimulator (ICOS) is critical for the development of human T(H)17 cells. Sci Transl Med. 2010;2(55):55ra78.

125. Benson DM, Bakan CE, Mishra A, et al. The PD-1/PD-L1 axis modulates the natural killer cell versus multiple myeloma effect: a therapeutic target for CT-011, a novel monoclonal anti-PD-1 antibody. Blood. 2010;116(13):2286-2294.

126. Beldi-Ferchiou A, Lambert M, Dogniaux S, et al. PD-1 mediates functional exhaustion of activated NK cells in patients with Kaposi sarcoma. Oncotarget. 2016;7(45):72961-72977.

127. Valmori D, Raffin C, Raimbaud I, Ayyoub M. Human RORγt$^+$ TH17 cells preferentially differentiate from naive FOXP3$^+$Treg in the presence of lineage-specific polarizing factors. Proc Natl Acad Sci U S A. 2010;107(45) 19402–19407.

128. Yang XO, Nurieva R, Martinez GJ, et al. Molecular antagonism and plasticity of regulatory and inflammatory T cell programs. Immunity. 2008;29(1):44-56.

129. DeNardo DG, Barreto JB, Andreu P, Vasquez L, Tawfik D, Kolhatkar N, Coussens LM CD4(+) T cells regulate pulmonary metastasis of mammary carcinomas by enhancing protumor properties of macrophages. Cancer Cell. 2009;16:91–102.

130. Wu X, Feng QM, Wang Y, Shi J, Ge HL, Di W. The immunologic aspects in advanced ovarian cancer patients treated with paclitaxel and carboplatin chemotherapy. Cancer Immunol Immunother. 2010;2:279–291.

131. Braly P, Nicodemus CF, Chu C, Collins Y, Edwards R, Gordon A, McGuire W, Schoonmaker C, Whiteside T, Smith LM. et al. The immune adjuvant properties of front-line carboplatin-paclitaxel: a randomized phase 2 study of alternative schedules of intravenous oregovomab chemoimmunotherapy in advanced ovarian cancer. J Immunother. 2009;32(1):54–65.

References

132. Vanneman M & Dranoff G. Combining immunotherapy and targeted therapies in cancer treatment. Nat Rev Cancer. 2012;12(4):237-251.

133. Wesolowski R, Duggan MC, Stiff A, et al. Circulating myeloid-derived suppressor cells increase in patients undergoing neo-adjuvant chemotherapy for breast cancer. Cancer Immunol Immunother. 2017;66(11):1437-1447.

134. Gangadhar TC & Vonderheide RH. Mitigating the toxic effects of anticancer immunotherapy. Nat Rev Clin Oncol. 2014;11:91-99.

135. Wang PF, Chen Y, Song SY, et al. Immune-related adverse events associated with anti-PD-1/PD-L1 treatment for malignancies: a meta-analysis. Front Pharmacol. 2017;8:730.

136. Merck press release details. https://investors.merck.com/news/press-release-details/2018/First-Presentation-of-Early-Data-for-Mercks-Investigational-STING-Agonist-MK-1454-in-Patients-with-Advanced-Solid-Tumors-or-Lymphomas-at-ESMO-2018-Congress/default.aspx. Accessed 12 February 2019.

137. Aduro Biotech press release. http://investors.aduro.com/phoenix.zhtml?c=242043&p=irol-newsArticle&ID=2376492. Accessed 12 February 2019.

138. Michot JM, Bigenwald C, Champiat S, Collins M, Carbonnel F, Postel-Vinay S, et al. Immune-related adverse events with immune checkpoint blockade: a comprehensive review. Eur J Cancer 2016;54:139–148.

139. NIH: U.S. national library of medicine. https://clinicaltrials.gov/ct2/show/NCT03737643. Accessed 12 February January 2019.

140. NIH: U.S. national library of medicine. https://clinicaltrials.gov/ct2/show/NCT03158935. Accessed 12 February January 2019.

141. Salihi R, Leunen K, Moerman P, Amant F, Neven P, Vergote I. Neoadjuvant weekly paclitaxel-carboplatin is effective in stage I-II cervical cancer. Int J Gynecol Cancer. 2017;27(6):1256–1260.

142. Otsuki A, Watanabe Y, Nomura H, Futagami M, Yokoyama Y, Shibata K, Kamoi S, Arakawa A, Nishiyama H, Katsuta T, et al. Paclitaxel and carboplatin in patients with completely or optimally resected carcinosarcoma of the uterus: a phase II trial by the Japanese uterine sarcoma group and the Tohoku gynecologic cancer unit. Int J Gynecol Cancer. 2015;25:92–97.

143. Coosemans A, Tuyaerts S, Vanderstraeten A, Vergote I, Amant F, Van Gool SW. Dendritic cell immunotherapy in uterine cancer. Hum Vaccin Immunother. 2014;10(7):1822-1827.

144. Lu CS, Lin JK, Chen WS, et al. Intraperitoneal ziv-aflibercept effectively manages refractory ascites in colorectal cancer patients. Oncotarget. 2016;8(22):36707-36715.

145. Maeda H, Kobayashi M, Sakamoto J. Evaluation and treatment of malignant ascites secondary to gastric cancer. World J Gastroenterol. 2015;21(39):10936-10947.

146. Takahara N, Isayama H, Nakai Y, et al. Pancreatic cancer with malignant ascites: clinical features and outcomes. Pancreas 2015;44:380–385.

147. Kew MC, Dos Santos HA, Sherlock S. Diagnosis of primary cancer of the liver. Br Med J. 1971;4(5784):408-411.

148. Sidana A, Kadakia M, Friend JC, et al. Determinants and prognostic implications of malignant ascites in metastatic papillary renal cancer. Urol Oncol. 2016;35(3):114.e9-114.e14.

149. Banerjee K, Kumar S, Ross KA, Gautam S, Poelaert B, Nasser MW, Aithal A, Bhatia R, Wannemuehler MJ, Narasimhan B, et al. Emerging trends in the immunotherapy of pancreatic cancer. Cancer Lett. 2018;417:35–46.

150. Okuyama R, Aruga A, Hatori T, Takeda K, Yamamoto M. Immunological responses to a multi-peptide vaccine targeting cancer-testis antigens and VEGFRs in advanced pancreatic cancer patients. Oncoimmunology. 2013;2(11):e27010.

151. Feng M, Xiong G, Cao Z, Yang G, Zheng S, Song X, You L, Zheng L, Zhang T, Zhao Y. PD-1/PD-L1 and immunotherapy for pancreatic cancer. Cancer Lett. 2017;407:57–65.

152. NIH: U.S. national library of medicine. https://clinicaltrials.gov/ct2/show/NCT03193190. Accessed 12 February January 2019.

153. Tanaka A & Sakaguchi S. Regulatory T cells in cancer immunotherapy. Cell Res. 2016;27(1):109-118.

154. Wang W, Marinis JM, Beal AM, Savadkar S, Wu Y, Khan M, Taunk PS, Wu N, Su W, Ahsan A, Kurz E, Chen T, Yaboh I, Li F, Gutierrez J, Diskin B, Hundeyin M, et al. RIP1 kinase drives macrophage-mediated adaptive immune tolerance in pancreatic cancer. Cancer Cell. 2018;34(5):757-774.e7.

155. Probst HC, Tschannen K, Odermatt B, Schwendener R, Zinkernagel RM, Van Den Broek M. Histological analysis of CD11c-DTR/GFP mice after in vivo depletion of dendritic cells. Clin Exp Immunol. 2005;141(3):398-404.

156. Huarte E, Cubillos-Ruiz JR, Nesbeth YC, et al. Depletion of dendritic cells delays ovarian cancer progression by boosting antitumor immunity. Cancer Res. 2008;68(18):7684-7691.

157. Baklaushev VP, Kilpeläinen A, Petkov S, et al. Luciferase expression allows bioluminescence imaging but imposes limitations on the orthotopic mouse (4T1) model of breast cancer. Sci Rep. 2017;7(1):7715.

158. Konstantinopoulos PA & Matulonis UA. Current status and evolution of preclinical drug development models of epithelial ovarian cancer. Front Oncol. 2013;3:296.

159. Kerbel RS & Kamen BA. The anti-angiogenic basis of metronomic chemotherapy. Nat Rev Cancer. 2004;4:423–436.

160. Hanahan D, Bergers G, Bergsland E. Less is more, regularly: metronomic dosing of cytotoxic drugs can target tumor angiogenesis in mice. J Clin Invest. 2000;105(8):1045-1047.

161. Dalgleish AG & Stern PL. The failure of radical treatments to cure cancer: can less deliver more?. Ther Adv Vaccines Immunother. 2018;6(5-6):69-76.

7. Supplements

Supplementary Table S1. Information on patient samples used for gene expression analysis

Patient	Time btw diagnosis and surgery	Time btw surgery and last chemo	Time btw last chemo and recurrence	Time btw recurrence and last follow-up
A	3.5 months	4 months	3.5 months	0.5 months
B	2.5 months	2.5 months	-	-
C	4 months	4 months	10.5 months from last chemo to last follow-up	
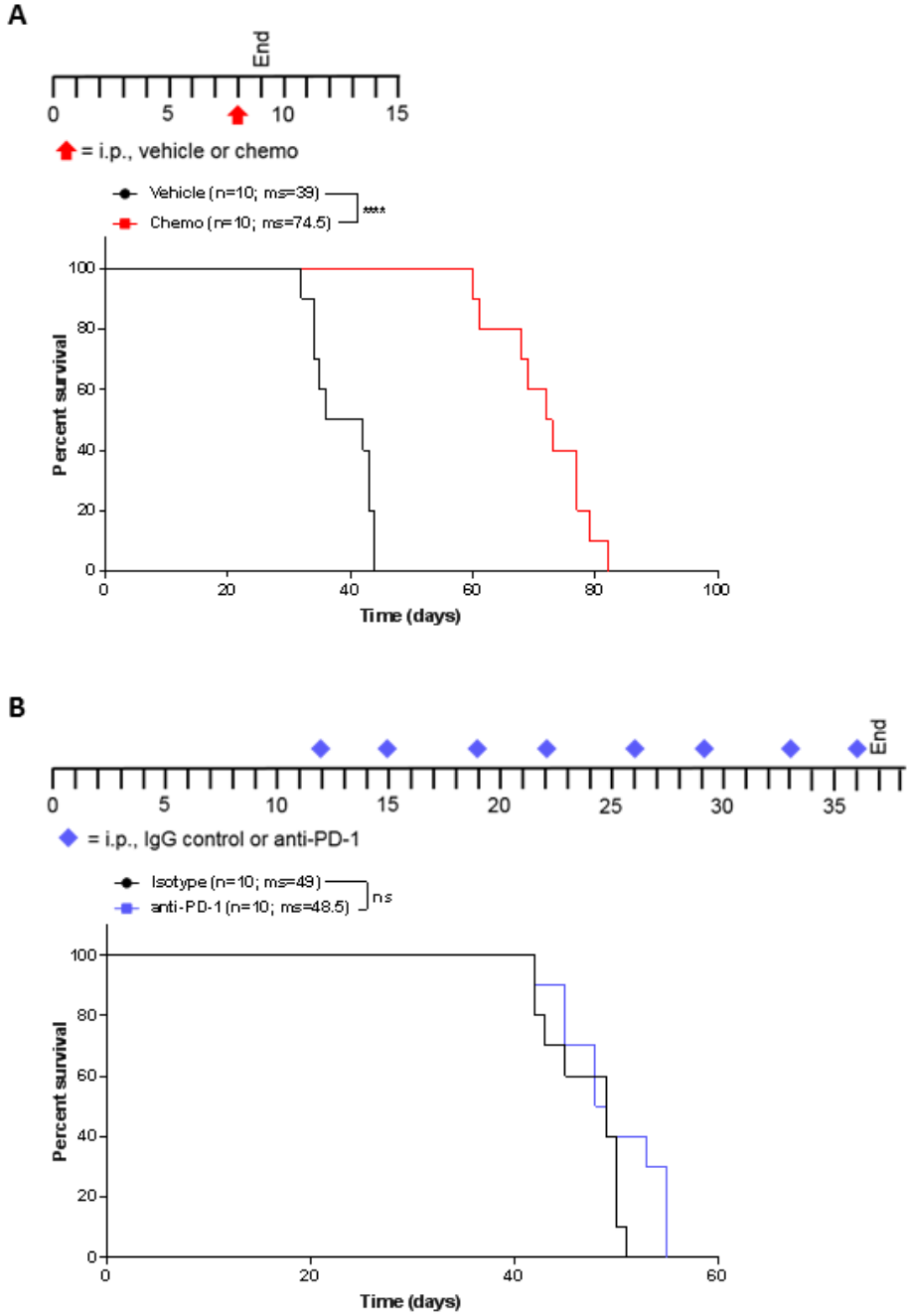
Supplementary Figure 1. Chemotherapy prolongs survival, but PD-1 checkpoint blockade monotherapy does not. (**A**) Mice were inoculated with ID8-Vegf-Defb29 cancer cells. Eight days later, mice were injected with either vehicle or paclitaxel and carboplatin (Chemo). A Kaplan-Meier curve is shown. (**B**) Mice were inoculated with ID8-Vegf-Defb29 cancer cells. Twelve days later, treatment with anti-PD-1 checkpoint blockade or isotype was initiated. The number of mice per group (n) and median survival (ms) are listed. All experiments were performed with biological replicates twice. Statistics were calculated using the Log-rank (Mantel-Cox) test. **** p≤0.0001.

A

Significant Terms For: Pathway
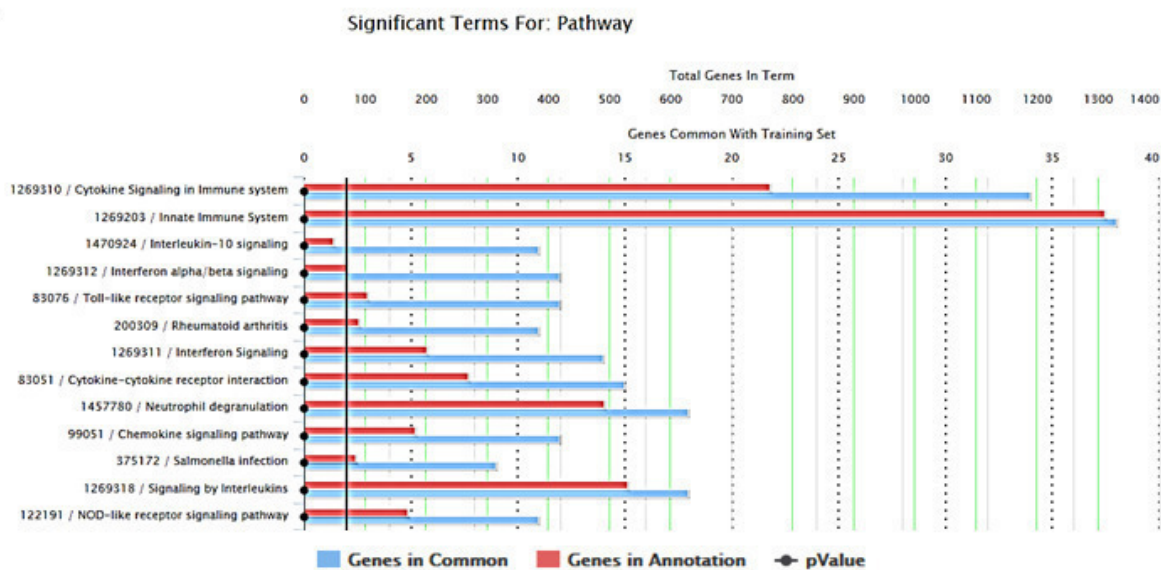
B

| #	ID	Name	pValue	FDR B&H	Genes from Input	Genes in Annotation
1	M2568	Genes up-regulated in lung tissue upon LPS aspiration with mechanical ventilation (MV) compared to control (PBS aspiration without MV).	8.832E-38	6.185E-34	25	128
2	19795415-Table1	Mouse Lung Beisiegel09 262genes	9.697E-29	3.395E-25	23	207
3	16479545-Table2	Mouse Lung not cancer Kahnert06 70genes	3.788E-28	8.842E-25	16	50
4	12446012-Table2	Mouse Immune Carmody02 151genes	1.415E-25	2.478E-22	18	112
5	20220088-SuppTable2a	Human Immune Allen10 106genes	2.142E-24	3.000E-21	17	103
6	M3302	Genes down-regulated in comparison of unstimulated peripheral blood mononuclear cells (PBMC) 3 days after stimulation with YF17D vaccine versus PBMC 7 days after the stimulation.	4.178E-24	4.877E-21	20	199
7	20460173-ImmPortAntimicrobials	Human Immune Kong10 544genes ImmPort Antimicrobials	3.231E-23	3.233E-20	25	469
8	M3010	Genes transcriptionally modulated in the blood of multiple sclerosis patients in response to subcutaneous treatment with recombinant IFNB1 [GeneID = 3456].	3.775E-23	3.304E-20	16	95
9	M14829	Genes down-regulated in hematopoietic precursor cells conditionally expressing HOXA9 and MEIS1 [GeneID=3205;4211].	8.957E-23	6.970E-20	15	77
10	M3296	Genes down-regulated in comparison of unstimulated peripheral blood mononuclear cells (PBMC) 1 day after stimulation with YF17D vaccine versus PBMC 7 days after the stimulation.	1.744E-22	1.036E-19	19	199
11	M5932	Genes defining inflammatory response.	1.922E-22	1.036E-19	19	200
12	M5913	Genes up-regulated in response to IFNG [GeneID=3458].	1.922E-22	1.036E-19	19	200
13	M7237	Genes down-regulated in thymus cortical regions: subcapsular versus central cortical.	1.922E-22	1.036E-19	19	200
14	16081686-SuppTable2	Human Lymphoma Tome05 357genes	3.171E-21	1.586E-18	17	155
15	M3288	Genes down-regulated in comparison of unstimulated peripheral blood mononuclear cells (PBMC) versus PBMC 7 days after stimulation with YF17D vaccine.	7.418E-21	3.056E-18	18	200
16	M9572	Genes up-regulated in cells from peripheral lymph nodes: T reg versus T conv.	7.418E-21	3.056E-18	18	200
17	M7320	Genes up-regulated in HMC-1 (mast leukemia) cells: incubated with the peptide ALL1 and then treated with Cl-IB-MECA [PubChem=3035850] versus stimulation by T cell membranes.	7.418E-21	3.056E-18	18	200
18	M1430	Genes defining differentiation potential of the bipotential myeloid cell line FDB.	9.472E-21	3.685E-18	17	165
19	17174972-TableS1	Human Zola07 426genes CellDifferentiationMarkers	1.089E-20	4.014E-18	21	345
20	M1920	Genes forming the macrophage-enriched metabolic network (MEMN) claimed to have a causal relationship with the metabolic syndrom traits.	1.273E-20	4.458E-18	32	1210

Supplementary Figure 2. Functional enrichment analysis of unsorted cells highlights the importance of the innate immune system. Mice were inoculated with ID8-Vegf-Defb29 cancer cells. Eight days later, mice were injected with either vehicle or paclitaxel and carboplatin (Chemo). Two days thereafter, peritoneal cells were recovered and assessed by gene expression analysis. (**A**) The top 84 significantly upregulated genes after chemotherapy treatment with a fold change ≥ 1 were queried for their pathway interactions using the ToppGene Suite gene list enrichment analysis tool. (**B**) The genes induced by chemotherapy had a significant correlation with myeloid cell populations.
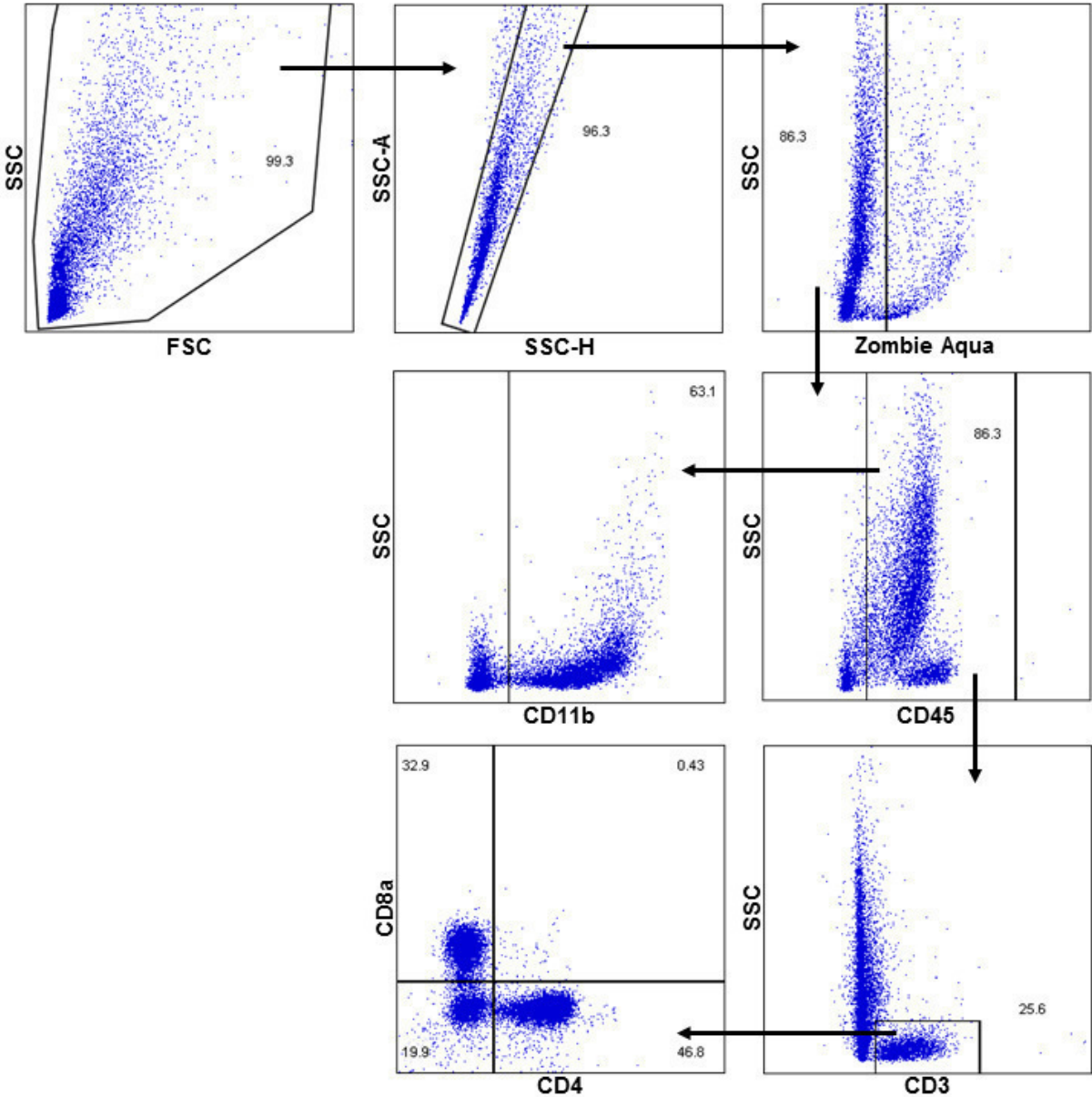
Supplementary Figure 3. Gating strategy used in flow cytometric analysis of immune cells harvested from the peritoneal cavity after treatment. Flow cytometric data were analyzed using FlowJo software.
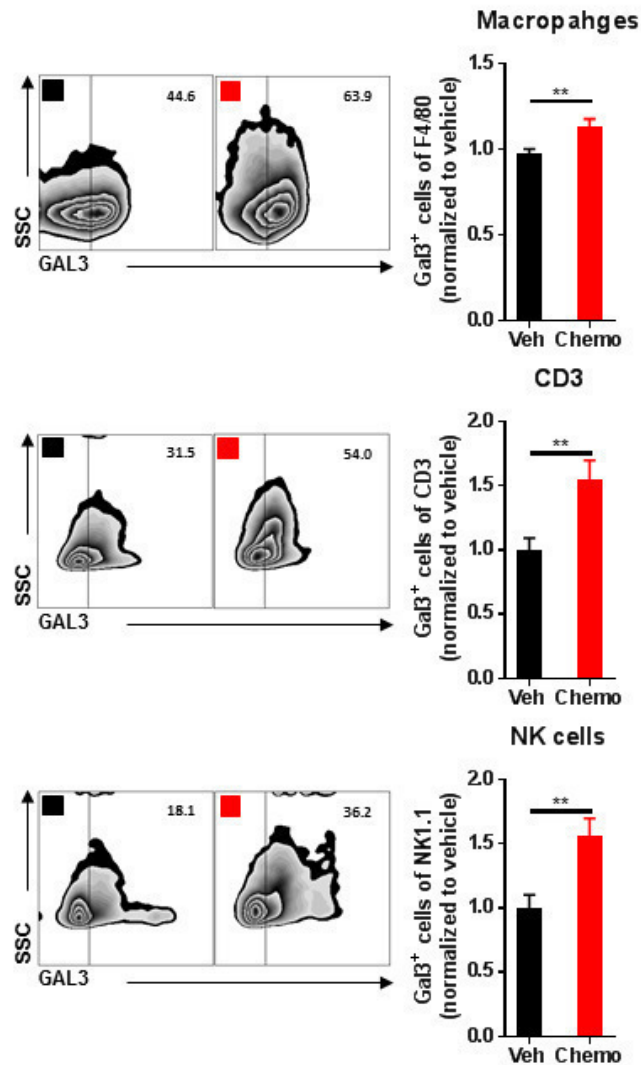
Supplementary Figure 4. Galectin3 is upregulated after chemotherapy treatment. Mice were treated with vehicle (Veh) or chemotherapy (Chemo) 8 days after ID8-VEGF-Defb29 tumor inoculation and peritoneal cells were assessed by flow cytometry 4 days after initiation of treatment. Flow cytometry gating of subsets of GAL3+ expressing CD11b+ myeloid cells, CD3+ T cells, and NK cells are shown as scatter plots and quantified at right. Experiment was performed twice with n=5 biological replicates. Statistics were calculated using a two-sided unpaired t-test. Data are presented as mean ± SEM ** p≤0.01
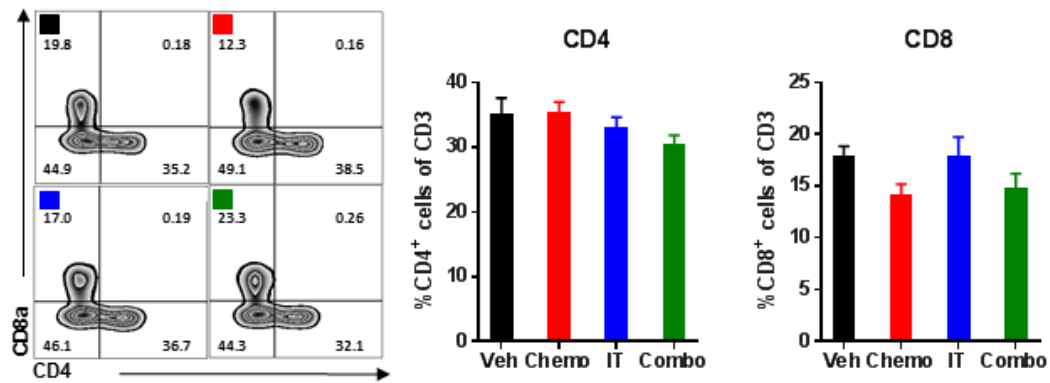
Supplementary Figure 5. Proportion of CD4+ and CD8+ T cells is not affected shortly after treatment. Peritoneal cells harvested from mice treated with vehicle (Veh); chemotherapy (Chemo); anti-IL-10, 2'3'-cGAMP, and anti-PD-L1 immunotherapy (IT); or both Chem and IT (Combo) were assessed by flow cytometry four days after initiation of treatment. Flow cytometry gating of subsets of CD4+ and CD8+ expressing CD3+ T cells are shown as scatter plots and quantified at right. Experiment was performed twice with n=4 biological replicates. Statistics were calculated using one-way ANOVA with Tukey's multiple comparisons test. Data are presented as mean ± SEM.
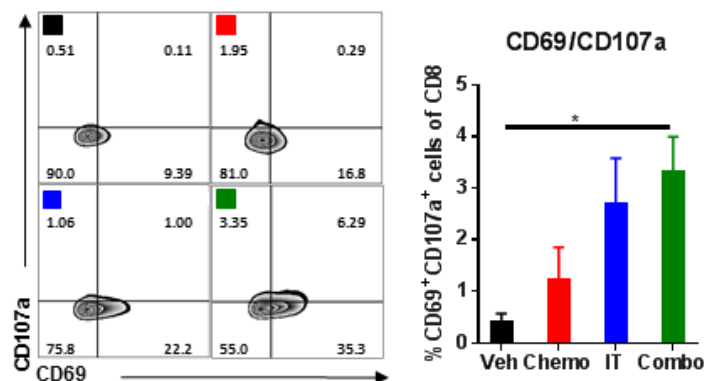
Supplementary Figure 6. Combination therapy increases the proportion of differentiated CD8+ T cells. Peritoneal cells harvested from mice treated with vehicle (Veh); chemotherapy (Chemo); anti-IL-10, 2'3'-cGAMP, and anti-PD-L1 immunotherapy (IT); or both Chemo and IT (Combo) were assessed by flow cytometry four days after initiation of treatment. Flow cytometry gating of subsets of CD69 and CD107a expressing CD8+ T cells are shown as scatter plots and quantified at right. Experiment was performed twice with n=4 biological replicates. Statistics were calculated using one-way ANOVA with Tukey's multiple comparisons test. Data are presented as mean ± SEM * p≤0.05.
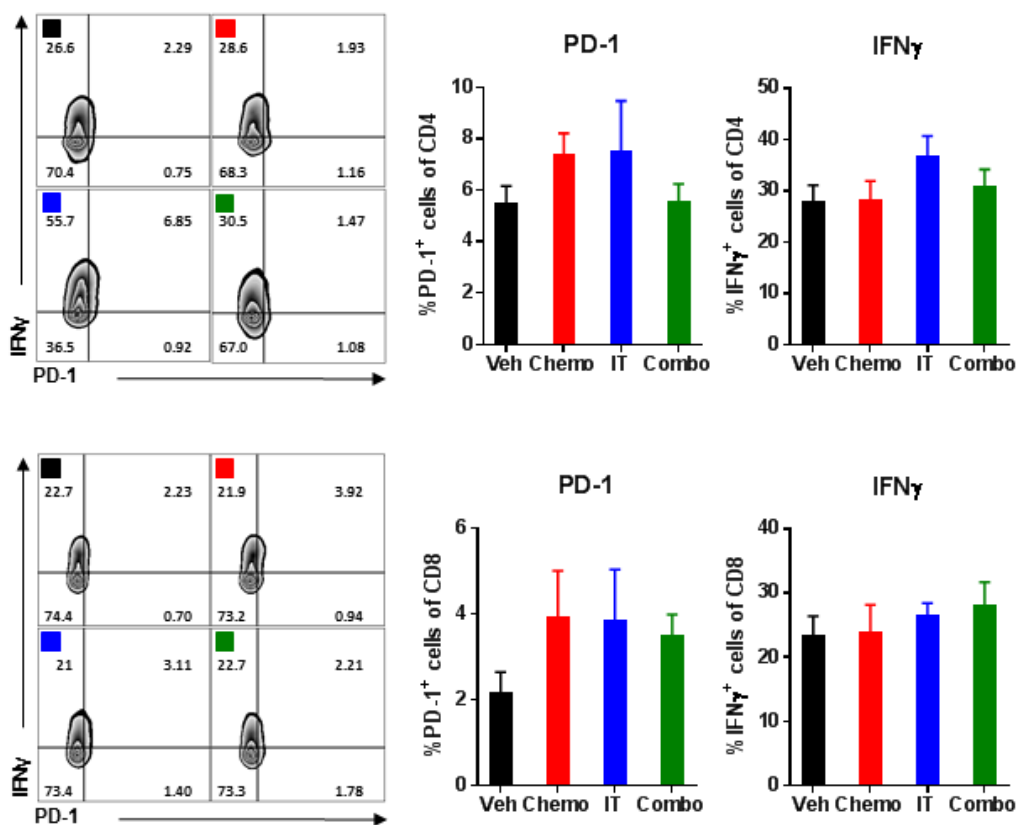
Supplementary Figure 7. Expression of IFNγ or PD-1 on T cells is not affected shortly after treatment. Peritoneal cells harvested from mice treated with vehicle (Veh); chemotherapy (Chemo); anti-IL-10, 2'3'-cGAMP, and anti-PD-L1 immunotherapy (IT); or both Chemo and IT (Combo) were assessed by flow cytometry four days after initiation of treatment. Flow cytometry gating of subsets of PD-1^{+} and IFNγ^{+} g CD4^{+} and CD8^{+} T cells are shown as scatter plots and quantified at right. Experiment was performed twice with n=4 biological replicates. Statistics were calculated using one-way ANOVA with Tukey's multiple comparisons test. Data are presented as mean ± SEM.
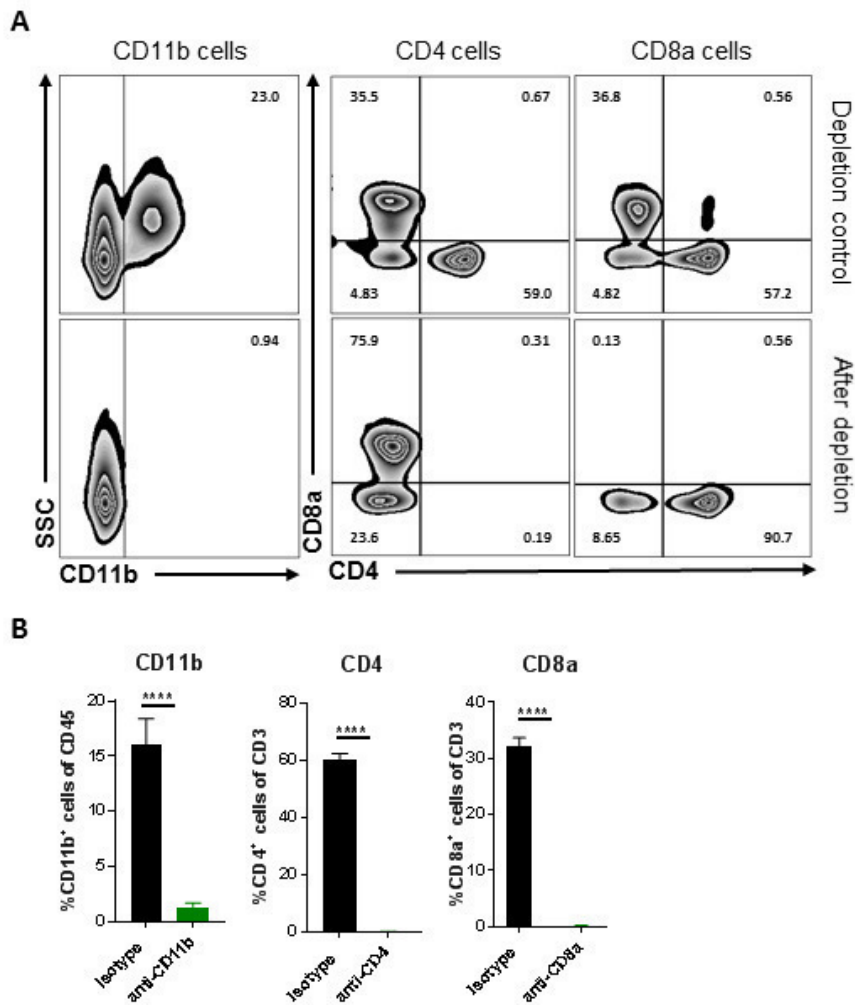
**Supplementary Figure 8. Flow cytometry analysis confirms that CD11b⁺ myeloid cells, CD8a⁺ T cells, and CD4⁺ T cells are depleted following administration of appropriate antibodies.** (**A**) Plots are shown for leukocytes isolated from blood after initiation of treatment. (**B**) Quantification of depletion is representative of n=6 mice, and the experiment was performed twice. Statistics were calculated using a two-sided unpaired t-test. Data are presented as mean ± SEM **** p≤0.0001.
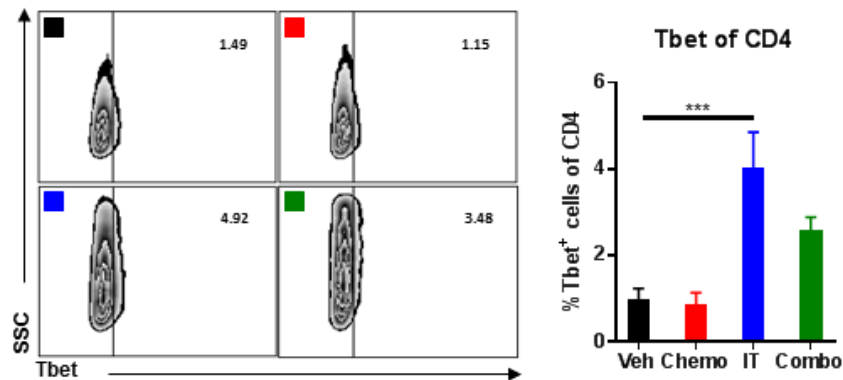
Supplementary Figure 9. Tbet transcription factor is upregulated after immunotherapy. Peritoneal cells harvested from mice treated with vehicle (Veh); chemotherapy (Chemo); anti-IL-10, 2'3'-cGAMP, and anti-PD-L1 immunotherapy (IT); or both Chemo and IT (Combo) were assessed by flow cytometry 13 days after initiation of treatment. Bar graph shows quantification of flow cytometry gating of Tbet expression on CD4$^+$ T cells. Experiment was performed twice with n=4 biological replicates. Statistics were calculated using one-way ANOVA with Tukey's multiple comparisons test. Data are presented as mean ± SEM *** p≤0.001.
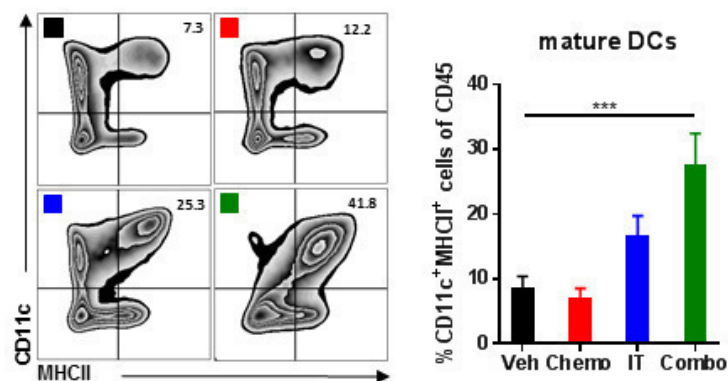
Supplementary Figure 10. Combination therapy increases the proportion of mature dendritic cells. Peritoneal cells harvested from mice treated with vehicle (Veh); chemotherapy (Chemo); anti-IL-10, 2'3'-cGAMP, and anti-PD-L1 immunotherapy (IT); or both Chemo and IT (Combo) were assessed by flow cytometry 13 days after initiation of treatment. Bar graph shows quantification of flow cytometry gating of MHCII/CD11c expression on CD45$^+$ T cells. Experiment was performed twice with n=4 biological replicates. Statistics were calculated using one-way ANOVA with Tukey's multiple comparisons test. Data are presented as mean ± SEM *** p≤0.001.

8. Abbreviations and definitions

%	percentage	cGAS	cyclic GMP-AMP synthase
#	number	Chemo	chemotherapy
°C	degree Celsius	cm^2	square centimeter
4-1BB	tumor necrosis factor receptor superfamily, member 9	CO_2	carbon dioxide
5-FU	fluorouracil	Combo	combination therapy
A	area	CST	Cell Signaling Technology
ACK	ammonium-chloride-potassium	CTL(s)	cytotoxic T cell(s)
ACT	adoptive cell transfer	CTLA-4	cytotoxic T lymphocyte associated antigen 4
adj	adjusted	Ctr	control
ADU	Aduro Biotech	CXCL	C-X-C motif chemokine
AE	adverse event	Cy	cychrome
AF	Alexa Fluor	d	day(s)
AMP	adenosine monophosphate	DC	dendritic cell
ANOVA	analysis of variance	dd	double distilled
APC	allophycocyanin	ddH2O	double distilled water
APC	antigen presenting cell	DDX41	DEAD-box helicase 41
Arg	arginase	Defb29	β-defensin 29
BD	Becton Dickinson	Dep	depletion
BMS	Bristol-Myers Squibb	DEPC	diethyl pyrocarbonate
Brca	breast cancer	DFCI	Dana-Farber Cancer Institute
btw	between	di-GMP	cyclic diguanylate
BV	brilliant violet	DMEM	Dulbecco's modified Eagle's medium
Ca^{2+}	calcium ion	DMSO	dimethyl sulfoxide
cat	catalogue	DNA	deoxyribonucleic acid
CCL	chemokine (C-C motif) ligand	DPBS	Dulbecco's phosphate-buffered saline
CCR	C-C chemokine receptor type	dsDNA	double-stranded DNA
CD	cluster of differentiation	DTR	diphtheria toxin receptor
CDN	cyclic dinucleotide	EDTA	ethylenediaminetetraacetic acid
cGAMP	cyclic guanosine monophosphate–adenosine monophosphate	EOMES	eomesodermin
		ER	endoplasmic reticulum

et al.	latin "*et alii*", - "and others"		IRF	interferon regulatory transcription factor
FACS	fluorescence activated cell sorting		ISRE	interferon-sensitive response element
Fas	apoptosis antigen 1		IT	immunotherapy
FBS	fetal bovine serum		iTreg	induced Treg
FFPE	formalin-fixed paraffin-embedded		IVC	individually ventilated cages
FC	flow cytometry		IVIS	*in vivo* imaging system
Fig	figure		kg	kilogram
FITC	fluorescein isothiocyanate		L	length
FoxP3	forkhead box P3		LLC	Lewis Lung Carcinoma
FSC	forward scatter		log	logarithm
G	gauge		LPS	lipopolysaccharide
Gal	galectin		Lys	lysine
GEMM	genetically engineered mouse model		M	macrophage
GFP	green fluorescent protein		MDSC	myeloid derived suppressor cell
GMP	guanosine monophosphate		Met	methionine
GZMB	granzyme B		mg	milligram
H	height		Mg^{2+}	magnesium ion
H_2O	water		MHC	major histocompatibility complex
HCl	hydrogen chloride		min	minute(s)
HGSOC	high-grade serous ovarian carcinomas		MIP1α	macrophage inflammatory protein-1α
hrs	hours		MK	Merck
HSPG	heparin sulfate proteoglycan		ml	milliliter
IACUC	Institutional Animal Care and Use Committee		mm	millimeter
ICAM	intercellular adhesion molecule		mm^3	cubic millimeter
ICOS	inducible T-cell costimulator		MMP	matrix metalloproteinase
IDO	indoleamine-2,3-dioxygenase		MOSEC	murine ovarian surface epithelial cell
IFI16	interferon gamma inducible protein 16		mRNA	messenger RNA
IFN	interferon		ms	medium survival
IgG	immunoglobulin G		mtDNA	mitochondrial DNA
IL	interleukin		n	number
i.p.	intraperitoneal		NCT	national clinical trial
			Neut	neutralization

NF-κB	nuclear factor kappa-light-chain-enhancer of activated B cells		TGF-β	transforming growth factor beta
ng	nanogram		Th	T helper
NK	natural killer		TIL	tumor infiltrating lymphocyte
ns	not significant		TLR	toll-like-receptors
NSCLS	non-small cell lung cancer		TNF	tumor necrosis factor
p	probability value		Treg	regulatory T cell
P/S	penicillin/streptomycin		tx	treatment
PARP	poly (ADP-ribose) polymerase		Veh	vehicle
PBS	phosphate buffered saline		Vegf	vascular endothelial growth factor
PEG	polyethylene glycol		W	width
PD-1	programmed cell death-1		α	alpha
PDGF	platelet derived growth factor		β	beta
PD-L1	programmed cell death-1 ligand 1		γ	gamma
PE	phycoerythin		μg	microgram
PerCP	peridinin chlorophyll protein complex		μm	micrometer
R&D	research and development		μl	microliter
RNA	ribonucleic acid			
RORγt	RAR-related orphan receptor gamma			
rpm	rounds per minute			
RPMI	Roswell park memorial institute			
RT	room temperature			
s.c.	subcutaneous			
sec	seconds			
SEM	standard error of the mean			
Ser	serine			
SSC	side scatter			
STING	stimulator of interferon genes			
TAM	tumor associated macrophage			
Tbet	T-box transcription factor TBX21			
TBK1	TANK-binding kinase 1			
TCR	T cell receptor			